

Dissertation
submitted to the
Combined Faculty of Natural Sciences and Mathematics
of the Ruperto Carola University Heidelberg, Germany
for the degree of
Doctor of Natural Sciences

Presented by

M. Sc. Michael Kilian

Born in: Heidelberg, Germany

Oral examination: 16th of April 2021

Major Histocompatibility Complex Class II Antigen Responses as Drivers of Brain Tumor Immunity

Referees: Prof. Dr. Michael Platten
Dr. Haikun Liu

Acknowledgements

First, I want to thank Michael Platten for giving me the opportunity to work in his team. Thank you for all the advice, scientific input and the unlimited freedom to pursue my interests.

I want to thank Heidi Cerwenka for fruitful (NK) discussions during my TAC meetings, Haikun Liu for being a valuable TAC member and agreeing of being my second examiner as well as Marc Freichel who accepted to join my examination committee. A special thanks goes to Walter Mier, who (with some interruptions) joined my way from Bachelor to PhD and always gave support whenever needed.

Thanks to all the people who helped performing the experiments, described in this thesis, Stefan Pusch for helping with all the cloning questions, Daisuke Kawauchi for introducing me into fancy electroporation techniques, my former Offringa lab who helped out whenever an antibody was missing. Thanks to the people in the DKFZ core facilities, especially the boys at the flow cytometry core and a special thanks to the animal caretakers and the Centre for Preclinical Studies, for always supporting me with the experiments.

Thanks a lot, to all the current and former members of D170. Thanks for helping in big experiments, answering questions, fruitful discussions, coffees, cakes and the great times. Thanks to the senior PhDs Jana and Katrin for all the advice when I joined the team. Thanks to Ed and Isabel for the scientific support.

Thanks to the MDs, Master students and new PhDs, Christopher for joining the MHCII team, Verena for providing and distributing relevant information, Kyle for being patient with my single cell analysis and everyone for the support.

Thanks to the technicians Anna, Kristine and Steffi, who helped a lot during the past 3.5 years and tried to keep the lab chaos to a minimum.

Thanks to Vera for all the support, for being tolerant all the time and for being a great fourth floor buddy.

Thanks to Frederik and Khwab, my PhD fellows. It was great to grow up with you.

Thanks to Kevin. For all the fun, the friendship and for awakening the love for NK cells.

A special thanks goes to Lukas, for the great support from beginning on, the scientific discussions and your indestructible positivity and motivation.

Thanks to all my friends and my family for the support. Now I am actually done.

Finally, a big thank you to Mirco. For all the discussions with you, your patience, motivation, your unlimited support, and for serendipitously stepping into my life.

Zusammenfassung

Die Präsentation von Antigenen ist ein relevanter Teil der Tumorummunologie. Zusätzlich zur Präsentation auf Haupthistokompatibilitätskomplex (Major Histocompatibility Complex, MHC) Klasse I, erringt die Antigenpräsentation auf MHC Klasse II mehr und mehr Bedeutung. Präklinische und klinische Studien konnten zeigen, dass eine erfolgreiche Immuntherapie insbesondere von der Präsenz MHC Klasse II präsentierter Neoantigene abhängt. Der genaue Mechanismus, der zur Induktion einer Tumorantwort über MHC Klasse II in Gliomen führt, ist jedoch nicht bekannt, ebenso wenig, in wie weit die Antigenpräsentation auf Tumordinfiltrierenden Makrophagen eine Rolle bei der tumorspezifischen T Zellantwort spielt. Gliome sind grundsätzlich durch eine geringe Präsenz von Neoantigenen charakterisiert. Für einige Tumor-treibende Mutationen konnte bereits eine Immunogenität gezeigt werden, trotzdem bleibt die Zahl angreifbarer Neoantigene und Effektivität einer antigenspezifischen Immuntherapie in Gliomen gering.

In der vorliegenden Arbeit wurden zuerst häufig vorkommende Mutationen in niedriggradigen Gliomen auf ihre Immunogenität hin untersucht. Die Mutation R215W im Gen *capicua* transcriptional repressor (CIC) induzierte eine mutationsspezifische Immunantwort in MHC-humanisierten Mäusen. Nachfolgende Analysen konnten zeigen, dass dieses Epitop auf MHC Klasse II präsentiert wird und eine CD4⁺ T Zell-getriebene-Immunantwort auslöst. Mittels Einzelzellsequenzierung Antigen-spezifischer T Zellen konnten reaktive T Zell Rezeptoren (TCRs) gegen CICR215W identifiziert werden. Des Weiteren wurde in dieser Arbeit die virale Transduktion von T Zellen mit dem TCR Konstrukt etabliert und die Funktionalität TCR transgener T Zellen validiert. Zur *in vivo* Validierung wurde ein neues Gehirntumormodell in MHC-humanisierten Mäusen entwickelt. Mittels lokalem adoptivem Transfer von TCR transgenen T Zellen konnte dann ein Tumorwachstum-verlangsamender Effekt beobachtet werden. Es konnte somit ein neues Target in Gliomen etabliert werden, das mittels adoptivem Transfer von TCR transgenen T Zellen zur Auslösung einer anti-Tumor Immunantwort beitragen kann.

Des Weiteren wurde in dieser Arbeit die Rolle von stromalem MHC Klasse II in Gehirntumoren untersucht. Mittels einem neuartigen Mausmodell, das die spezifische Depletion von MHC Klasse II auf myeloiden Zellen erlaubt, konnte gezeigt werden, dass MHC Klasse II für das Ansprechen einer Immuntherapie unabdingbar ist. Dies beruht auf der Aktivierung tumordinfiltrierender CD4⁺ T Zellen. Mittels antigenspezifischer Tumormodelle und Einzelzellsequenzierung konnte gezeigt werden, dass das Fehlen aktivierter CD4⁺ T Zellen zu einer schnelleren Erschöpfung Tumor-reaktiver CD8⁺ T Zellen führt. Bei Fehlen von MHC Klasse II waren die zytotoxischen T Zellen nicht mehr in der Lage, Tumorzellen effizient zu lysieren. Dieser Effekt war aber nur bei einer

initialen Tumorantwort vorhanden, eine spätere Depletion von MHC Klasse II hatte keinen Einfluss auf das Tumorwachstum.

Zusammenfassend konnten in dieser Arbeit sowohl neue Angriffspunkte für die Therapie von Gliomen gefunden werden, als auch die Relevanz der Antigenpräsentation auf MHC Klasse II auf Tumor-assoziierten myeloiden Zellen für die Aktivität zytotoxischer CD8⁺ T Zellen gezeigt werden.

Abstract

Antigen presentation on major histocompatibility complex (MHC) plays an important role in anti-tumor immunity. In addition to epitope presentation on MHC class I that activates cytolytic T cells, antigen presentation on MHC class II and a resulting CD4⁺ T cell immune response have gained increasing relevance. Preclinical and clinical studies have shown that a successful immunotherapeutic intervention depends on the presentation of neoantigens on MHC class II. However, the exact mechanisms that drive an MHC class II-restricted immune response as well as the relevance of different antigen-presenting cell subsets are not fully understood. Brain tumors such as glioma are characterized by a low mutational load and therefore a reduced abundance of potential neoepitopes. For some glioma associated tumor-driver mutations immunogenicity has been shown; however, the number of targetable epitopes and efficacy of neoantigen specific immunotherapies remains low.

In the present thesis several mutations frequently present in low grade gliomas have been screened for immunogenicity. The point mutation CICR215W has been shown to elicit mutation specific immune responses in an MHC-humanized mouse model. This neoepitope was shown to be presented on MHC class II and to lead to a CD4⁺ T cell-driven immune response. Using single cell T cell receptor sequencing, CICR215W-specific TCRs could be retrieved and functionality was validated *in vitro*. For *in vivo* validation, a novel brain tumor model was established using CRISPR-Cas9 mediated genetic manipulations. Locoregionally adoptive transfer of T cell receptor-transgenic T cells led to a reduced tumor growth in CICR215W-mutant brain tumor-bearing mice. Overall, a novel shared therapeutic target in gliomas could be established, that can be targeted via adoptive transfer of T cell receptor transgenic T cells in order to elicit anti-tumor immune responses.

Furthermore, the relevance of MHC class II presentation in gliomas has been investigated. Using a novel mouse model allowing for depletion of MHC class II on tumor infiltrating macrophages, it could be shown that prevalence of MHC class II is essential for the response to immunotherapy due to necessary activation of CD4⁺ T cells. Using antigen-specific tumor models and single-cell transcriptomics it could be shown that the lack of activated CD4⁺ T cells leads to an exhausted phenotype of tumor-reactive CD8⁺ T cells that thereupon lose their ability to lyse tumor cells. This effect was only apparent during early stages of T cell activation. A late depletion of MHC class II did not result in any differences in CD8⁺ T cell activation. In summary, the present thesis describes a novel target for T cell mediated immunotherapy and demonstrates the necessity of MHC class II-restricted antigen presentation on tumor-infiltrating macrophages for successful anti-tumor activity of cytotoxic CD8⁺ T cells.

List of publications not related to this work

Tomek, P. *et al.* Imprinted and ancient gene: A potential mediator of cancer cell survival during tryptophan deprivation. *Cell Commun. Signal.* (2018) doi:10.1186/s12964-018-0301-7.

Bunse, L. *et al.* Suppression of antitumor T cell immunity by the oncometabolite (R)-2-hydroxyglutarate. *Nat. Med.* (2018) doi:10.1038/s41591-018-0095-6.

Aslan, K. *et al.* Heterogeneity of response to immune checkpoint blockade in hypermutated experimental gliomas. *Nat. Commun.* (2020) doi:10.1038/s41467-020-14642-0.

Contents

<i>List of Abbreviations</i>	X
<i>List of figures</i>	XIII
<i>List of tables</i>	XV
1 Introduction	1
1.1 Brain tumors	1
1.2 The immunosuppressive tumor microenvironment in glioma	2
1.3 T cell exhaustion and immunotherapy.....	5
1.4 Immunotherapy approaches in glioma	7
1.5 Cellular therapies in brain tumors.....	8
1.6 Brain tumor models.....	9
1.7 Objectives of this study	12
2 Materials and methods	13
2.1 Reagents	13
2.2.1 Chemicals.....	13
2.1.2 Kits.....	14
2.1.3 Cytokines.....	15
2.1.4 Primary antibodies, unconjugated.....	15
2.1.5 Secondary antibodies	15
2.1.6 <i>In vivo</i> antibodies.....	15
2.1.7 Antibodies used for flow cytometry	16
2.1.8 Peptides	17
2.1.9 Buffer	18
2.2 Plasmids and primers	18
2.3 Methods	19
2.3.1 Mice.....	19
2.3.2 Cell lines and cell culture	20
2.3.3 Isolation and culturing of primary murine immune cells.....	20
2.3.4 Vaccination of mice	21
2.3.5 ELISpot	21

2.3.6	Flow cytometry.....	21
2.3.7	Generation of A2.DR1 gliomas	22
2.3.8	Mutation detection and copy number alteration.....	22
2.3.9	Histology	23
2.3.10	Western blot.....	23
2.3.11	Quantitative real-time PCR.....	23
2.3.12	Generation of T cell lines and TCR sequencing	23
2.3.13	Cloning of CIC-reactive TCRs.....	24
2.3.14	TCR transduction.....	25
2.3.15	Co-culture assays with TCR-transduced T cells	26
2.3.16	<i>In vivo</i> proliferation assay.....	26
2.3.17	Intracranial tumor cell inoculation.....	26
2.3.18	Therapeutic adoptive T cell transfer	27
2.3.19	Isolation of tumor infiltrating immune cells	27
2.3.20	MRI imaging.....	27
2.3.21	Mutation specific PCR	28
2.3.22	Co-culture assays using OT-I/OT-II T cells.....	28
2.3.23	Treatment of mice	28
2.3.24	Single-cell RNA sequencing.....	28
2.3.25	Graphical data representation and statistics.....	29
3	Results.....	30
3.1	CICR215W as a novel target for adoptive TCR therapy.....	30
3.1.1	CICR215W induces mutation specific immune response in HLA humanized mice.....	30
3.1.2	CICR215W is an MHC class II restricted neoepitope and a mutational hotspot in oligodendroglioma.....	32
3.1.3	Generation of an HLA humanized A2.DR1 glioma tumor model	33
3.1.4	Phenotyping of the A2.DR1 glioma model	35
3.1.5	Single-cell VDJ sequencing of CICR215W reactive T cell lines reveals high heterogeneity between mice	36
3.1.6	Retrieval of CICR215W reactive TCRs	38
3.1.7	TCR transduced T cells remain reactive to peptide stimuli <i>in vitro</i> and <i>in vivo</i>	40
3.1.8	Intraventricular adoptive transfer of anti-CICR215W TCR-transduced T cells leads to delayed tumor growth.....	41
3.1.9	Detection of CICR215W-mutated patient tissue	42
3.2	Relevance of MHC class II antigen presentation in the glioma tumor microenvironment .	43
3.2.1	Macrophages induce an MHC class II dependent CD4 ⁺ T cell activation.....	43
3.2.2	Continuous <i>in vivo</i> depletion of MHC class II does not alter myeloid infiltration.....	44

3.2.3	Depletion of myeloid but not microglial MHC class II leads to a decrease of CD4 T cell abundance and activation.....	45
3.2.4	Myeloid but not microglial MHC class II is required for response to immune checkpoint blockade	46
3.2.5	Myeloid MHC class II is required for CD8 ⁺ T cell response	47
3.2.6	Tumor-reactive T cells are only found in the tumor microenvironment.....	49
3.2.7	MHC class II expression shapes immune cell infiltration in experimental gliomas.....	50
3.2.8	MHC class II expression alters the phenotype of tumor infiltrating myeloid cells	51
3.2.9	Myeloid MHC class II expression shapes CD4 ⁺ T cell and bystander CD8 ⁺ T cell phenotype.....	52
3.2.10	Myeloid MHCII expression shapes tumor-reactive CD8 ⁺ T cell phenotype.....	54
3.2.11	Depletion of MHC class II leads to an exhausted CD8 ⁺ T cell phenotype and diminishes cytotoxic capacity.....	56
3.2.12	Late depletion of myeloid MHC class II leads to delayed tumor immune escape.....	57
4	<i>Discussion</i>	58
4.1	Identification and therapeutic usage of CIC as a glioma specific antigen	58
4.2	Using T cell receptor-transgenic T cells for the treatment of glioma.....	59
4.3	Enhancing T cell therapy for glioma	60
4.4	Relevant cell type for MHC class II antigen presentation.....	61
4.5	CD4 is help required for CD8 ⁺ T cell response	62
4.6	Conclusion and implication for future therapies	64
5	<i>Literature</i>	65

List of Abbreviations

ACK	Ammonium-Chloride-Potassium
ANOVA	analysis of variance
APC	Antigen-presenting cell
TP53	Tumor Protein P53
TCGA	The Cancer Genome Atlas
HSC	hematopoietic stem cells
BMDM	Bone marrow-derived macrophages
VEGF	Vascular Endothelial Growth Factor
MAPK	mitogen-activated protein kinase
CAR	Chimeric antigen receptor
CCL	CC chemokine ligand
CCR	C-C Motif Chemokine Receptor
CD	Cluster of differentiation
cDNA	complementary DNA
TIL	Tumor infiltrating lymphocyte
CNS	Central nervous system
PDX	patient derived xenografts
CSF1R	Colony stimulating factor 1 receptor
CRISPR	Clustered Regularly Interspaced Short Palindromic Repeats
CTA	Cancer testis antigen
GEM	Genetically engineered mouse
CTLA-4	Cytotoxic T-lymphocyte-associated protein 4
CXCL	Chemokine (C-X-C motif) ligand
DAPI	4',6-Diamidin-2-phenylindol
DC	Dendritic cell
CIC	capicua transcriptional repressor
DMEM	Dulbecco's modified eagle medium
DMSO	Dimethyl sulfoxide
DNA	Deoxyribonucleic acid
LGG	Low-grade glioma
Nf1	Neurofibromin 1
Pten	Phosphatase and tensin homolog
NSG	immunodeficient non-obese diabetic scid gamma
EGFR	Epidermal growth factor receptor
ELISA	Enzyme-linked immunosorbent assay
RT-qPCR	Real-Time quantitative PCR
ERK	Extracellular signal-regulated kinase
FACS	Fluorescence-activated cell sorting
CT	Clonotype
FasL	First apoptosis signal ligand
FBS	Fetal bovine serum
FcR	Fc receptor

FDA	Food and drug administration
<i>Gapdh</i>	Glyceraldehyde-3-phosphate dehydrogenase
IRES	internal ribosomal entry site
GBM	Glioblastoma
SNP	single nucleotide polymorphism
GI261	Glioma 261
KLRG1	killer-cell lectin like receptor G1
TOX	Thymocyte Selection Associated High Mobility Group Box
ISO	Isotype
H2-Db	Histocompatibility 2, D region, B alpha chain
H2-Kb	Histocompatibility 2, K1, K region
HBSS	Hanks balanced salt solution
HLA	Human major histocompatibility complex
i.c.	Intracranial
ICB	Immune checkpoint blockade
MOG	Myelin Oligodendrocyten Glykoprotein
IDH1	Isocitrate dehydrogenase 1
KO	Knockout
WT	Wildtype
Ifn	Interferon
IDO	Indoleamine 2,3-dioxygenase
Ig	Immunglobulin
LN	lymph node
UMAP	Uniform Manifold Approximation and Projection
TIGIT	T Cell Immunoreceptor With Ig And ITIM Domains
IL	Interleukin
IMDM	Iscove's modified dulbecco's media
iNOS	Inducible nitric oxide synthase
i.p.	Intraperitoneal
MAST	Model-based Analysis of Single-cell Transcriptomics
TLR	Toll-like Receptors
EAE	experimental autoimmune encephalomyelitis
LAG-3	Lymphocyte-activation gene-3
LDH	Lactate dehydrogenase
LPS	Lipopolysaccharide
MACS	Magnetic-activated cell sorting
LCMV	lymphocytic choriome-ningitis virus
MFI	Median fluorescence intensity
MHC	Major histocompatibility complex
MDSC	Myeloid derived suppressor cells
M-CSF	Monocyte-colony stimulating facto
MRI	Magnetic resonance imaging
mTOR	Mechanistic target of rapamycin
NEAA	Non-essential amino acids

NFAT	Nuclear factor of activated T-cells
NF- κ B	Nuclear factor kappa-light-chain-enhancer of activated B cells
NK cells	Natural killer cells
NR	Non-responder
PBMC	Peripheral blood monocytic cells
GFP	green fluorescent protein
CTFR	Cell Trace Far Red
ITGA	Integrin alpha
Tmem	Transmembrane
G-CSF	Granulocyte
PD-L1	Programmed death ligand 1
PD-1	Programmed death protein 1
PCR	Polymerase chain reaction
PBS	Phosphate-buffered saline
PI3K	Phosphoinositide 3-kinase
TCF1	T cell factor 1
TME	tumor microenvironment
RNA	Ribonucleic acid
RPMI	Roswell park memorial institute
RT	Room temperature
RT-qPCR	Reverse transcription-quantitative PCR
s.c.	Subcutaneously
SEM	Standard error of the mean
TCR	T cell receptor
TGF	Transforming growth factor
TIL	Tumor infiltrating lymphocyte
TIM-3	T-cell immunoglobulin and mucin-domain containing-3
Treg	Regulatory T cell
TNF	Tumor necrosis factor
WHO	World health organization

List of figures

Figure 1: Classification and grading of gliomas according to 2016 WHO classification of gliomas.	2
Figure 2: Composition of the glioma tumor microenvironment.....	5
Figure 3: Mechanisms of T cell exhaustion.....	6
Figure 4 Overview about cellular therapies.....	9
Figure 5: Overview about different mouse modes used in tumor research.....	11
Figure 6 Exemplary plasmids for TCR expression and gene/minigene expression.....	19
Figure 7: Overview for TCR cloning strategy.....	25
Figure 8: Identification of CICR215W/Q point mutations as potential target for targeted immunotherapy.....	31
Figure 9. CICR215W triggers an MCHII restricted CD4 ⁺ T cell driven immune response and is frequently mutated in oligodendroglioma.	32
Figure 10: Generation of the A2.DR1 glioma cell line.....	34
Figure 11: A2.DR1 glioma is MHC class II negative and overexpression of CicR215W.....	35
Figure 12: Retrieval of functional TCRs by single VDJ sequencing.....	37
Figure 13: Identification of CICR215W reactive TCRs.....	38
Figure 14: TCR transduced T cells maintain activity after transduction and expansion.....	40
Figure 15: Adoptive transfer of α -CICR215W-TCR T cells targeting CicR215W mutated A2.DR1 gliomas.....	41
Figure 16: Establishment of a mutation-specific PCR and development of a mutation-specific antibody.....	42
Figure 17: Macrophages can antigen-specifically activate CD4 ⁺ T cells.....	43
Figure 18: MHC class II is efficiently depleted on myeloid cells and does not alter the intratumoral myeloid cell composition.....	44
Figure 19: Depletion of MHC class II leads to a decrease of intratumoral CD4 ⁺ T cell abundance.	45
Figure 20: Depletion of MHC class II on myeloid cells leads to abrogation of response to immune checkpoint blockade.....	46
Figure 21: Depletion of MHC class II leads to abrogation of MHCI driven tumor control.	48
Figure 22: MHC class II is depleted in all lymphatic organs but tumor-reactive T cells are only found in the tumor environment.....	49
Figure 23: Single cell sequencing of tumor infiltrating immune cells.....	50
Figure 24: MHC class II knockout leads to an altered abundance and activation state of tumor associated myeloid cells.....	51

Figure 25: Depletion of MHC class II abrogates the presence of activated CD4⁺ T cells in the tumor microenvironment. 53

Figure 26 Depletion of MHC class II leads to an exhausted phenotype in tumor-reactive CD8⁺ T cells..... 55

Figure 27: Activated CD4⁺ T cells are required for the formation of functional CD8⁺ T cells..... 56

Figure 28: Late depletion of MHC class II does not lead to an exhausted CD8⁺ T cell phenotype. 57

List of tables

Table 1: Chemicals.....	13
Table 2: Kits.....	14
Table 3: Cytokines.....	15
Table 4: Unconjugated antibodies.....	15
Table 5: Secondary antibodies.....	15
Table 6: <i>In vivo</i> antibodies.....	15
Table 7: Flow cytometry antibodies.....	16
Table 8: Peptides.....	17
Table 9: Buffer.....	18
Table 10: Primers.....	18

1 Introduction

1.1 Brain tumors

Gliomas represent the most common brain tumors with an incidence of approximately six cases per 100,000 individuals^{1,2}. The classification and diagnosis of brain tumors has recently undergone significant revision with the introduction of molecular parameters in addition to histological features^{3,4}. Histologically, gliomas are graded into grade I-VI, including oligodendroglioma, astrocytoma, glioblastoma and diffuse midline glioma. Grade II-III represent a group of slow growing brain neoplasia that eventually progress to more malignant grade IV glioblastomas³. Diagnostic biomarkers according to the 2016 WHO classification are IDH1/2 mutations, 1p/19q co-deletions, H3.3-K27M mutations, ATRX loss and C11orf95-RELA fusions (Figure 1). Additionally, MGMT-promotor methylation serves as a predictive biomarker for alkylating chemotherapy as for example temozolomide⁵. Approximately 50% of all gliomas are diagnosed as glioblastoma (GBM), the most aggressive subtype of brain tumors, with an median survival of only 14-17 month^{5,6}. Improvements in standard therapy including surgery, radiation and chemotherapy has not led to significant improved outcome for patients so far^{7,8}. GBMs are characterized by a highly heterogenous nature, between patients and within a single patient⁹, that are driven by distinct chromosomal aberrations and driver mutations¹⁰⁻¹². This heterogeneity can lead to fast adaption to -and escape from- therapeutic interventions making it particularly difficult to find widely applicable therapeutic approaches targeting glioblastomas or brain tumors^{9,13}.

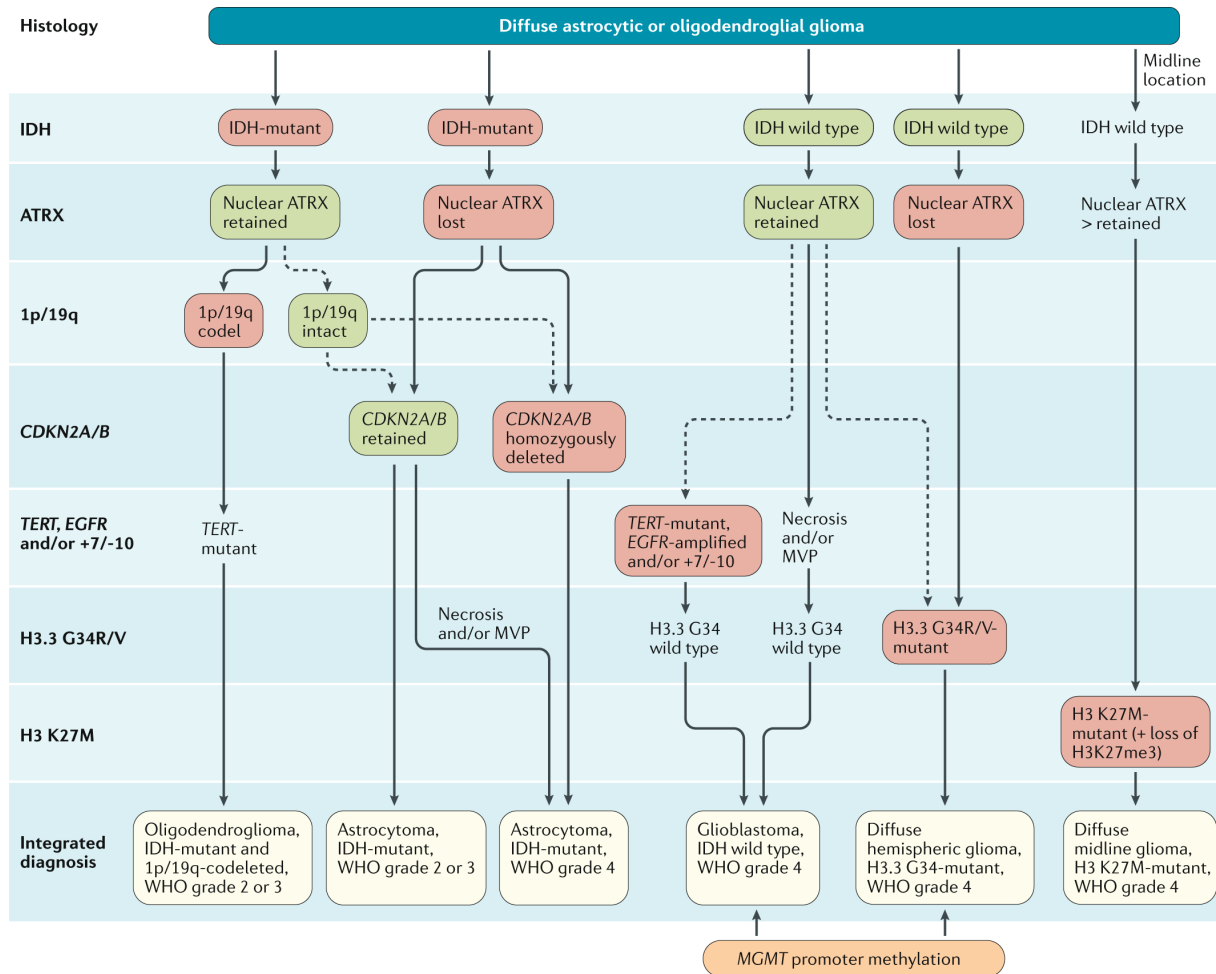


Figure 1: Classification and grading of gliomas according to 2016 WHO classification of gliomas. From Weller *et al.*⁷

1.2 The immunosuppressive tumor microenvironment in glioma

Tumor immune surveillance in gliomas has long been described as being hampered by the immune-privileged characterization of brain tumors due to the blood brain barrier that prevents immune cell infiltration into the central nervous system (CNS)^{14–18}. This view was mainly built on the observation that T cell responses against xenogeneic grafts are not as effectively initiated as compared to the periphery and adoptively transferred CNS autoreactive T cells do not infiltrate into the antigen expressing brain regions^{18–20}. However, despite this immune privilege, there has been evidence that immune cells such as monocytes constantly infiltrate the healthy CNS²¹. T cells, however, have been found to remain located in the perivascular and meningeal spaces with mainly CD4⁺ T cells patrolling the parenchymal borders^{22–24}. Recently, the discovery of CNS-draining lymphatic vessels shed new light into the concept of the immune-privileged characteristics of the brain^{25,26}. Furthermore, it has been shown that tumor antigens drain to the cervical lymph nodes via the meningeal lymphatic vessel and activate tumor-reactive T cells, which then traffic to the

inflammation site^{27,28}. Elevating lymphatic drainage by VEGF-C was shown to elevate tumor vulnerability to immune checkpoint inhibition.

Nonetheless, despite the fact that tumor-reactive T cells are able to infiltrate CNS tumors, brain tumors have been described to harbor a particular immune suppressive microenvironment²⁹. In addition to classical cell types such as immune cells, fibroblasts and endothelial cells constituting the tumor microenvironment (TME)³⁰, brain tumors are defined by a distinguished cellular composition. Brain-resident cell types including microglia, astrocytes and neurons together with blood-derived macrophages can make up to 30-50% of the total mass of brain tumors^{31,32} (Figure 2A). Brain-resident microglia and bone-marrow-derived macrophages make up the majority of immune cells within the brain TME^{33,34}. Microglia are the long-living tissue-resident macrophages of the brain, developing from yolk-sac-derived erythro-myeloid progenitors and seeding the brain early in embryonic development and are not renewed by hematopoietic stem cells (HSCs)^{35,36}. In contrast, bone marrow monocyte-derived macrophages are recruited to the brain parenchyma during inflammation³⁷. The discrimination between the two cell types without genetic models has been a matter of debate especially in the human setting. Recently, several novel surface markers have been proposed, discriminating microglia and monocyte derived macrophages, including Tmem119 exclusively expressed on microglia and CD49D/ITGA4 overexpressed in monocyte derived macrophages³⁸. The role of macrophages in brain tumor development, progression and immune surveillance is still not fully understood. Several studies have shown that macrophages are important for sustained tumor growth^{39,40}. Furthermore, they are a major source of inhibitory cytokines like transforming growth factor beta (TGF β) and Interleukin-10 (IL10) and can be re-programmed by glioma cancer stem cells^{31,41,42}. Additionally, macrophages have been shown to facilitate tumor angiogenesis^{35,43} and potentially contribute to brain metastasis formation⁴⁴. Consequently, targeting macrophages by depletion or repolarization with colony-stimulating factor-1 receptor (CSF-1R) inhibitors leads to decelerated tumor growth^{45,46}.

Dendritic cells (DCs) have long been neglected due to a minor prevalence in the brain TME²⁹ (Figure 2B). However, as DCs are defined as professional antigen presenting cells (APCs) they play an important role in T cell driven anti-tumor immunity and have gained attention for brain tumor immunotherapeutic approaches⁴⁷.

Astrocytes are also specific to the brain TME and have shown to interact closely with neighboring tumor cells (Figure 2E). They have shown to form functional gap junctions with tumor cells to support tumor growth^{48,49}. Recently, reactive astrocytes have been reported to support the immunosuppressive TME in glioma via release of anti-inflammatory cytokines like TGF β , IL10 or Granulocyte colony-stimulating factor (G-CSF)⁵⁰.

T cells together with B cells pose the adaptive immune cell compartment and upon antigen recognition can adopt a complex variety of distinct phenotypes and effector functions⁵¹ (Figure 2D). T cells are activated through antigen specific T cell receptor (TCR) stimulation through binding to an MHC-epitope complex. However, the mutational burden in brain tumors is comparably low, making it difficult for the immune system to launch a strong T cell driven immune response^{52,53}. The brain tumor microenvironment has been shown to be particularly immunosuppressive for T cells^{54,55}. Tumor-infiltrating T cells show strong upregulation of immune checkpoints like PD-1, CTLA-4 and LAG-3, reduced cytokine production and an increased exhaustion signature⁵⁵. Additionally, shared driver mutations like IDH1 can - by oncometabolic reprogramming of the TME - enhance T cell dysfunction⁵⁶. Additionally, the high activity of indolamine 2,3-dioxygenase (IDO) depletes tryptophan from the TME, which in turn suppresses T cell activity⁵⁷.

Natural Killer Cells (NK cells) represent the innate immunity arm of the lymphoid compartment and are considered the first line of innate anti-tumor immune response and as such strongly shape the tumor environment. Different immunotherapeutic approaches can lead to NK cell recruitment, enhanced activation and cytotoxicity towards tumor cells in murine brain tumor models^{58,59}. However, interestingly, NK cells can develop a regulatory phenotype in experimental auto-immune disease by direct killing of activated, antigen-specific T cells^{60,61}. Few studies have found limited indications that suggest a similar role for NK cells in a tumor setting^{62,63}. Further investigations are needed to dissect this previously unrecognized, counterintuitive, paradigm-shifting role of NK cells in the glioma TME.

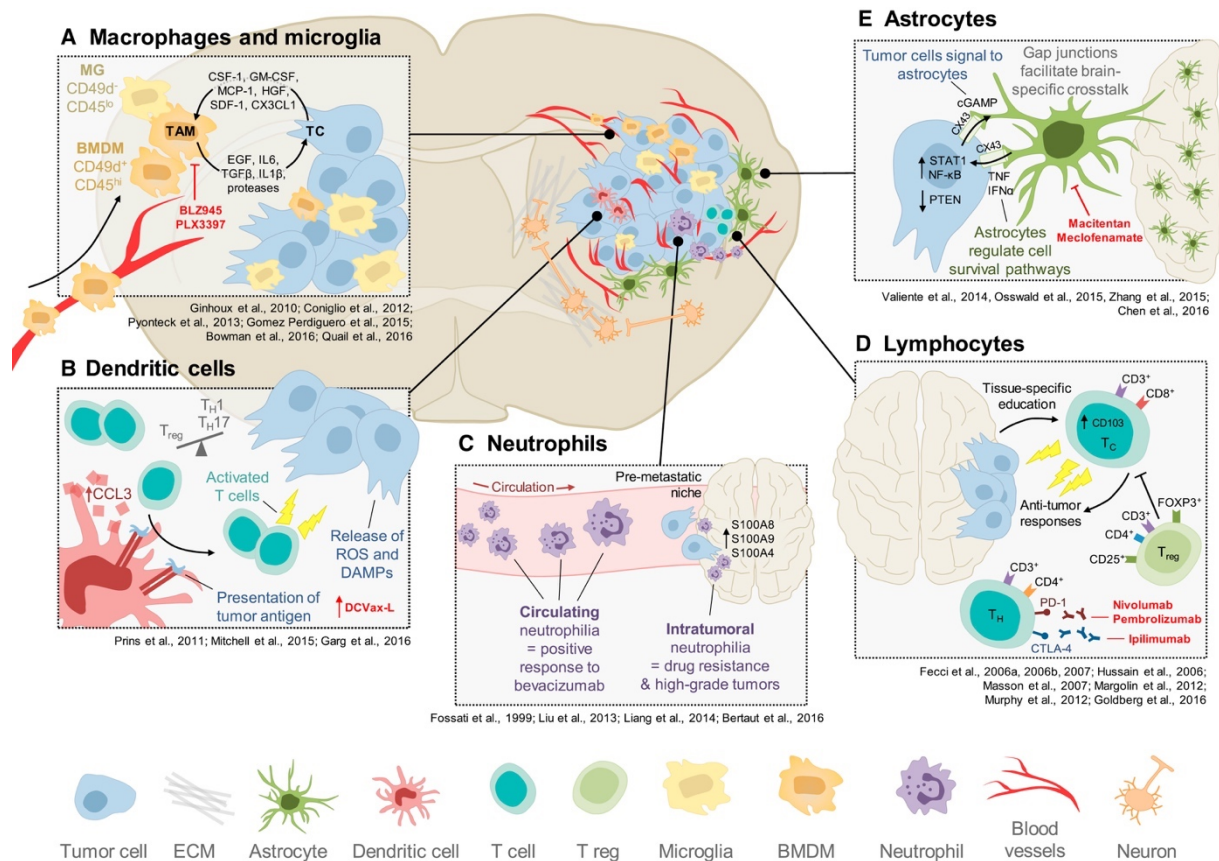
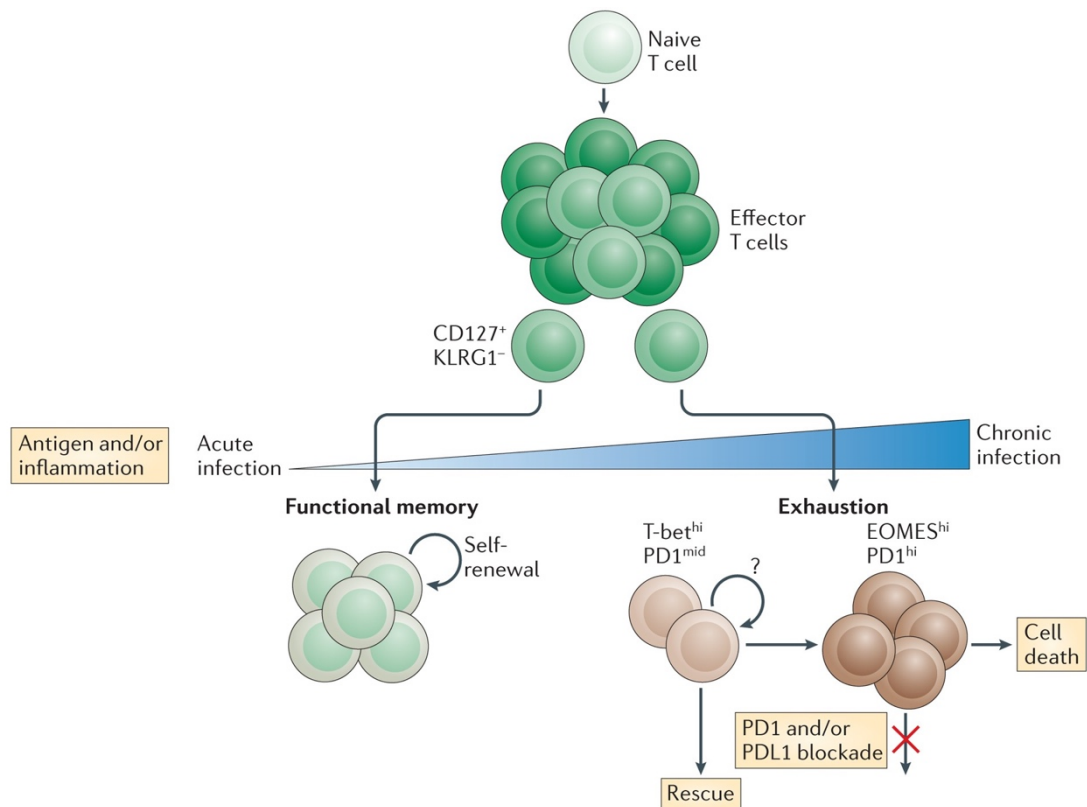


Figure 2: Composition of the glioma tumor microenvironment. From Quail and Joyce²⁹

1.3 T cell exhaustion and immunotherapy

One of the most promising treatment strategies for cancer established recently has been immunotherapy, which has revolutionized oncology for distinct cancer entities^{64–66}. Early studies in mice have shown that mice can develop memory and resistance to tumors^{67,68}. These observations led to the “immunosurveillance” hypothesis by Thomas and Burnet, stating that tumors are constantly controlled by immune cells targeting potential neoantigens presented on tumor cells⁶⁹. Further studies linked the immunosurveillance concept to primarily T cells that elicit tumor-specific immune responses⁷⁰. However, antigen-specific anti-tumor immune responses are often not durable, which led to the concept of immunoeediting, which describes the adaption of tumor cells to attacks by the immune system: after an early elimination phase, tumor cells escaping the immune system by downregulation of antigen expression or expression of inhibitory molecules are selected, eventually leading to immune escape and uncontrolled growth of tumors^{71,72}. Recently, the concept of T cell exhaustion has gained increasing interest in cancer research. This concept was first described in viral infection and has been adapted to tumor immunology. Constant antigen experience and chronic TCR stimulation leads to the upregulation of checkpoint molecules on T cells like PD-1, CTLA-4, TIM-3, LAG3 and KLRG1 (Figure 3)⁷³. Depending on a numerous

internal and external factors, the following differentiation process can result in either effector memory T cells or dysfunctional, exhausted T cells unresponsive to stimulation⁷⁴. Exhausted T cells are characterized by a loss of effector functions, such as proliferation and cytokine production, and changes in transcriptional and metabolic activity. T cell dysfunction has been shown to take place very early after T cells enter the tumor⁷⁵. Recently, T cell exhaustion has been shown to be epigenetically imprinted in early phases of T cell activation^{76,77}. In particular, the transcription factor TOX has been linked to states of exhausted T cells in cancer and viral infections^{78–80}. The current view is that TOX mediates the long-term maintenance of a dysfunctional T cell state. TCF-1 and TIM3 have recently been shown to be the counteracting parts in terminal T cell exhaustion. TCF-1 expressing T cells mark the progenitor exhausted population that can be targeted with immunotherapeutic interventions whereas TIM3 positive T cells mark the terminally exhausted population that fail to be reinvigorated^{81–84}.



Feature	Functional memory T cell	Exhausted T cell
Proliferative potential	+++	+/-
Cytokine production	+++	+/-
Memory markers (e.g. CD44, CD62L, CD127 or CXCR3)	+++	+/-
Inhibitory receptors (e.g. PD1, LAG3, CD160 or 2B4)	-	+++
IL-7- and/or IL-15-driven self-renewal	++	-
Antigen dependency	-	+

Figure 3: Mechanisms of T cell exhaustion. From Wherry *et al.*⁷³

In brain tumors like GBM, T cell exhaustion has been described to be more severe than in other tumor entities, and exhausted T cells display a unique transcriptional signature⁸⁵.

In recent years, targeting these tumor-reactive but dysfunctional T cells has become an emerging field in oncology. In particular, the usage of immune checkpoint-inhibiting antibodies targeting T cell checkpoint molecules like PD-1 and CTLA-4 or their ligands has led to tremendous results in cancer therapy^{86,87}. These checkpoint inhibitors can elicit a durable tumor regression by elevating endogenous immune responses⁸⁸⁻⁹⁰. Checkpoint inhibitors aim to reinvigorate dysfunctional cells in the tumor microenvironment. To date, there are more than 3000 active clinical trials listed investigating T cell immunity modulating agents⁹¹. However, a favorable outcome of checkpoint inhibition is limited to a minority of patients in cancer types like melanoma or lung cancer and response-predictive biomarkers are required^{92,93}. Cancers like melanoma - that are known to harbor a high mutational load - have frequently been reported to be responsive to immunotherapy^{94,95}. A higher mutational load increases the likelihood of inducing an anti-tumor T cell response via targetable antigens presented on MHC molecules on the cancer cell surface⁹⁶. Consequently, tumors with low mutational load as, for example, gliomas, are less likely to respond to immunotherapy^{52,96}.

1.4 Immunotherapy approaches in glioma

Immunotherapeutic approaches have not been able to show robust clinical effects in brain tumors so far. This fact has been associated with a distinct low mutational burden in glioma^{52,53} and the distinct immunological phenotype determined by the privileged location in the CNS and low numbers of tumor infiltrating lymphocytes^{97,98}. Additionally, as described above, the TME of gliomas produces high amounts of immunosuppressive cytokines and T cell activity can be suppressed by tumoral depletion of tryptophan from the microenvironment.

Several immunotherapeutic strategies have been exploited in brain tumors. Targeting TGF β or IDO in order to prevent their immunosuppressive effects has failed to show survival benefits in phase II and III clinical trials^{99,100}. A number of clinical trials and preclinical studies have investigated the activity of mutated IDH1 inhibition^{101,102}. In a preclinical model, IDH inhibition has been shown to synergize with checkpoint inhibition by remodeling the tumor microenvironment¹⁰³.

Targeting potentially immunosuppressive tumor associated macrophages using inhibition of the cytokine colony-stimulating factor 1 receptor (CSF-1R) has shown to elicit durable responses in preclinical models of glioma^{45,104}. However, a clinical phase II trial did not show responses in patients with recurrent GBM¹⁰⁵.

Checkpoint inhibition in preclinical studies has shown to induce durable responses in murine models of GBM^{106,107}. However, most of the clinical trials using checkpoint-inhibiting molecules in gliomas till now failed to show a beneficial clinical outcome for patients^{108,109} (Checkmate 143, 498). Though, recently, three independent trials showed response of neoadjuvant PD-1 therapy in recurrent and resectable GBM^{110–112}. The response to PD-1 resulted in enhanced cytokine and chemokine expression, increased T cell clonality and was correlated with an enrichment in the MAPK pathway.

1.5 Cellular therapies in brain tumors

Cellular therapies have become an emerging field in preclinical and clinical research. In 1980 Rosenberg *et al.* conducted a clinical trial treating 157 patients with lymphokine-activated killer cells and interleukin-2 (IL2, Figure 4a)¹¹³. This strategy was further developed and resulted in several clinical trials using heavily expanded tumor-infiltrating lymphocytes (TILs) and high dose IL2^{114,115}. However TIL therapy showed little activity in any cancer entity except melanoma¹¹⁶. In brain tumors, TIL therapy has shown effects in some patients with GBM and melanoma brain metastasis^{117–119}. Nonetheless, the overall clinical outcome of these trials was not positive even though TIL cultures from GBM patients have been shown to be potentially tumor-reactive¹²⁰. Recently, the usage of genetically modified T cells has become more relevant in tumor immunotherapy. Chimeric antigen receptor (CAR) T cell therapy has already been approved for B cell lymphoma or acute lymphoblastic leukemia (Figure 4c)¹²¹. CARs are composed of an extracellular antigen recognition domain, a hinging transmembrane domain and an intracellular signaling domain. The antigen recognition domain is composed of antibody-derived variable regions and can therefore bypass MHC presentation of the antigen. Modifying the intracellular signaling domain and the addition of co-stimulatory signals has led to the development of second, third, and fourth-generation CARs¹²². Several CARs have been developed against glioma-associated antigens such as IL13R α 2, EGFRvIII, B7-H3, chlorotoxin and GD2^{123–127}. In preclinical brain tumor models CAR T cell therapy has proven to lead to profound anti-tumor effects using human derived orthotopic xenograft GBM models^{126,128,129}. A case report reported regression in a patient with GBM after CAR T cell therapy against IL13R α 2¹³⁰.

Since CAR T cells are only able to target extracellular, mostly non-tumor-specific targets, TCR transgenic T cells provide the possibility to also target intracellular targets that are presented on MHC class I and II. TCRs for TCR therapy are selected from patient's TILs based on tumor recognition. Due to MHC restriction, TCR based treatments are patient-specific therapies targeting

tumor-specific neoantigens. For tumors with low mutational load like brain tumors, detection of targetable neoantigens remains challenging.

Dendritic cell vaccination has also gained increasing clinical interest, especially in brain tumors. DC vaccinations are used to enhance T cell responses by delivering antigen-presenting cells pulsed with tumor lysate¹³¹. Preclinical studies have shown promising results in tumor regression,^{132–134} which led to the conduction of several clinical trials^{135,136}. These results demonstrate the potential of DC vaccination and phase III clinical trials have been initiated.

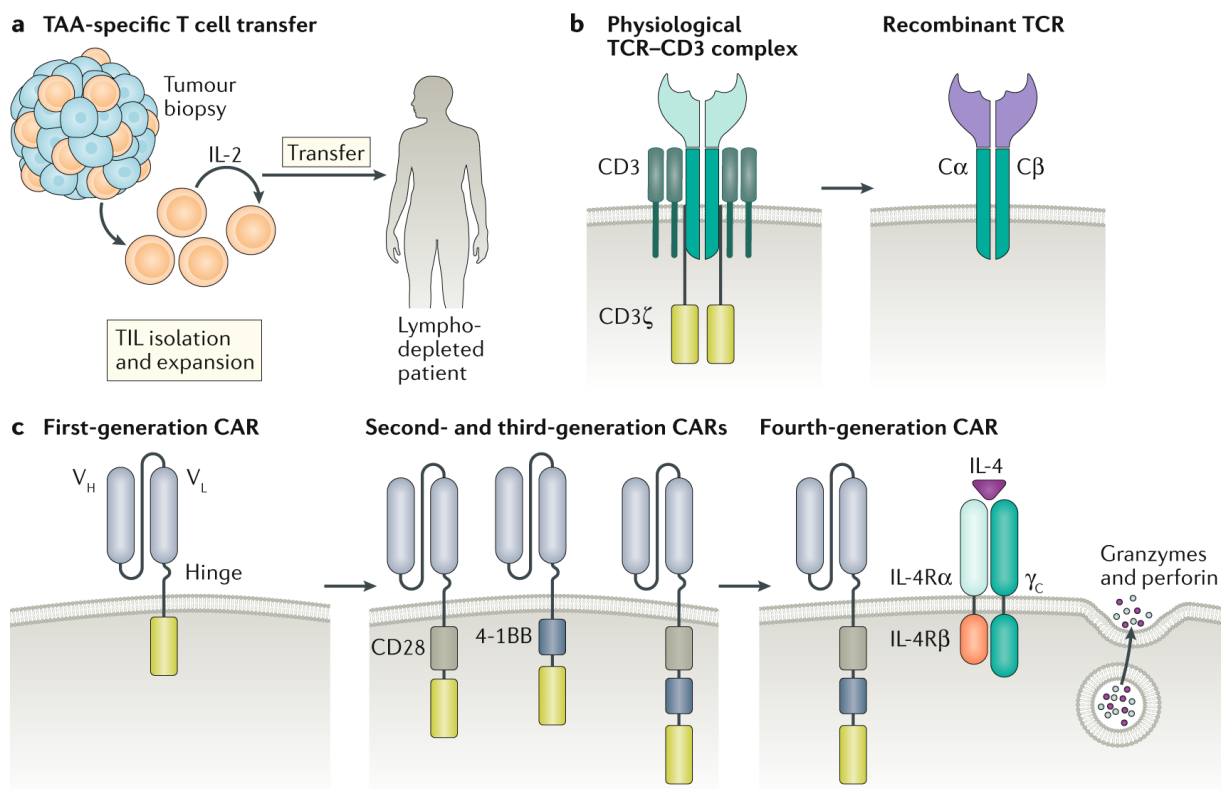


Figure 4 Overview about cellular therapies. From Waldman *et al.*⁶⁴

1.6 Brain tumor models

Dissection of fundamental mechanisms in tumor immunology and investigation of novel treatment strategies has the indispensable need for adequate tumor models. Brain tumor models have long been restricted to only a few syngeneic models like GL261 or CT-2A (Figure 5a)¹³⁷. Even though these models have led to relevant novel insights in brain tumor biology, they harbor some inherent limitations and the choice for the right tumor model needs to be carefully evaluated. Syngeneic models like GL261 that are also being used in this thesis have been established by injecting carcinogens into the brain and cell lines were established from these spontaneous tumors (Figure 5a, c)¹³⁸. These cell lines typically harbor an unphysiological mutational load and are missing defined driver genes or neoantigens¹³⁹. However, they are still widely used, as they can mimic the aggressive

growth of glioblastoma and are a valuable tool for immunotherapeutic studies due to their immunogenicity^{106,107,140,141}. Additionally, they grow in immunocompetent mice with a complete immune system present, which enables the investigation of endogenous immune responses as well as physiological immune cell infiltration^{139,142}.

A lot of effort has been put into the establishment of patient-derived xenografts (PDX) in immunodeficient mice (Figure 5b). Usually, fresh tumor pieces or single cell suspensions are directly injected into the flank or orthotopically injected into the brain of different kinds of immune deficient mice¹⁴³. Grown tumors often retain their heterogenous histological and genetic phenotypes^{143–145}. Success rates, however, heavily depend on the aggressiveness of the original tumor and the chosen mouse strain¹⁴⁶. Brain tumors and especially low-grade gliomas are difficult to grow as PDX¹⁴⁷. Once established, these tumors can be further passaged *in vitro* or *in vivo* and can be used for assessing the effectiveness of therapeutic interventions in a human tumor setting¹⁴⁸. PDX are usually limited to agents directly targeting the tumor cells as a competent immune system is missing. Still, there have also been novel insights into tumor biology and tumor evolution^{49,149,150}. However, with the lack of the immune system, these models are missing a relevant part which might be circumvented by the usage of humanized mouse models in the future. Whereas these models are usually achieved by injecting human immune or stem cells into immunodeficient mice, there are also genetically engineered mouse models that are only partially humanized. An important model is the A2.DR1 mouse model that carries fully humanized HLA alleles and a knockout of murine MHC molecules¹⁵¹. This model has been successfully used for the discovery and investigation of neo-epitopes in brain tumors^{152,153}. In recent years, novel gene targeting techniques like CRISPR-Cas have enabled researchers to specifically target genes relevant for tumorigenesis (Figure 5d)^{154,155}. For example, knocking out specific tumor suppressor genes can lead to very defined tumors in immunocompetent mice useful for the investigation of brain tumor development as well as brain tumor immunology¹⁵⁶.

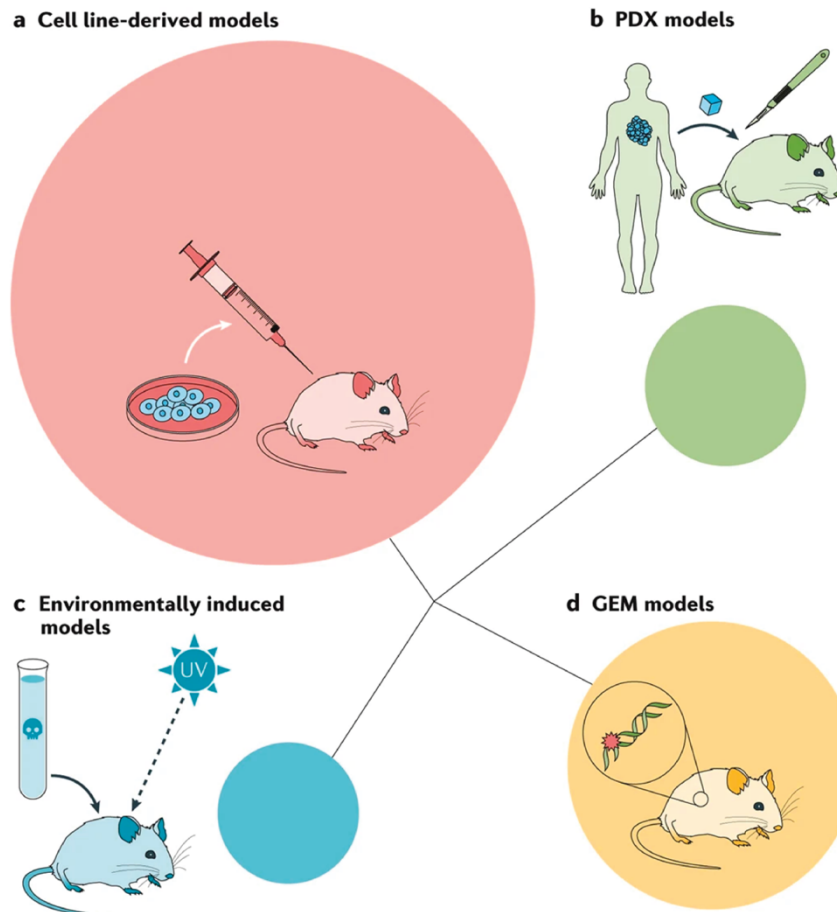


Figure 5: Overview of different mouse modes used in tumor research. Adapted from Gengenbacher *et al.*¹⁵⁷

1.7 Objectives of this study

Within this study, the role and relevance of MHC class II restricted antigen presentation in the glioma context was investigated.

The effectiveness of tumor-targeting immunotherapy relies on the activation of tumor-specific T cells via neoantigen presentation on MHC class I and II. Whereas cytolytic CD8⁺ T cells are activated via MHC class I on tumor cells, activation of CD4⁺ helper T cells takes place via MHC class II on tumor cells or antigen-presenting cells. The mechanisms through which CD4⁺ T cell activation drive response to immunotherapy is not yet fully understood. First, the aim of this study was to find novel targets that can be used for off-the-shelf treatment concepts. Therefore, frequently mutated glioma-associated potential epitopes were screened for immunogenicity in an MHC-humanized mouse model to obtain tumor-reactive T cell receptor sequences that can be used for therapeutic adoptive transfer of genetically modified T cells.

Second, using an inducible knockout mouse system, the relevance of MHC class II presentation on tumor-infiltrating macrophages was investigated. Using timed knockouts, an antigen-specific tumor model, multi-color flow cytometry and high dimensional single cell sequencing the relationship between MHC class II presentation and CD8⁺ T cell driven immune responses was dissected.

2 Materials and methods

2.1 Reagents

2.2.1 Chemicals

Table 1: Chemicals.

Item	Manufacturer
2,3,7,8-Tetrachlorodibenzo- <i>p</i> -dioxin (TCDD)	Sigma-Aldrich
4-(2-hydroxyethyl)-1-piperazineethanesulfonic acid (HEPES)	Invitrogen
Accutase	Gibco Life Technologies
ACK Lysing Buffer	Gibco Life Technologies
Albumin Fraktion V	Carl Roth
Aldara Cream	Meda Pharma
Bepanthen	Bayer
Bio-Rad protein assay	Bio-Rad
Blasticidin	Sigma-Aldrich
Carprofen	Pfizer
Ciprofloxacin	Sigma-Aldrich
CloneAmp HiFi PCR Premix	Takara
ConA supplement	Eichmüller group, DKFZ
Dimethyl sulfoxide (DMSO)	Carl Roth
DMEM	Sigma-Aldrich
DMEM/F12	Sigma-Aldrich
ECL prime	Amersham, GE Healthcare
Enhanced chemoluminescence (ECL) solution	Amersham, GE Healthcare
Ethylenediaminetetraacetic acid (EDTA)	Sigma Aldrich
FACS flow	BD Biosciences
Fetal bovine serum (FBS)	Sigma-Aldrich
Fixable viability dye eFluor780	eBioscience
FuGene HD transfection reagent	Promega
GlutaMAX supplement	Gibco Life Technologies
Hank's Buffered Salt Solution (HBSS)	Sigma-Aldrich
Human serum AB	Sigma-Aldrich
Imiquimod creme	MEDA Pharma
Ionomycin	Sigma-Aldrich
Ketamine	Zoetis

L-Glutamine	Sigma-Aldrich
Lipopolysaccharides (E. coli)	Sigma-Aldrich
Low-melting agarose	Sigma-Aldrich
Matrigel	Gibco Life Technologies
Methyl α -D-mannopyranoside	Sigma-Aldrich
Montanide	Seppic
Non-essential amino acids (NEAA)	Gibco Life Technologies
Penicillin	Invitrogen
Phorbol 12-myristate 13-acetate (PMA)	Sigma-Aldrich
Sodium chloride	Carl Roth
Sodium pyruvate	Sigma-Aldrich
Staphylococcus enterotoxin B (SEB)	Sigma-Aldrich
Streptomycin	Invitrogen
SYBR Green qPCR master mix (ROX)	Applied Biosystems
Tamoxifen	Sigma-Aldrich
Thymidine, [Methyl- 3 H]	PerkinElmer
Tris hydrochloride	Carl Roth
Triton X-100	Biochemica
Trypan blue	Gibco Life Technologies
Xylazine	Bayer
β -Mercaptoethanol	Sigma-Aldrich

2.1.2 Kits

Table 2: Kits.

Kit	Manufacturer
High-Capacity cDNA Reverse Transcription Kit	Applied Biosystems
RNeasy Mini Kit	Qiagen
CD4 T Cell Isolation Kit	Miltenyi
CD8a T Cell Isolation Kit	Miltenyi
MagniSort™ Mouse T cell Enrichment Kit	Thermo Fisher
Cytofix/Cytoperm™ Fixation/Permeabilization Kit	BD
Intracellular Fixation & Permeabilization Buffer Set	Thermo Fisher
DNeasy Blood & Tissue Kit	Qiagen
Chromium Single Cell 5' Reagent Kit	10x Genomics
rhAmp SNP Genotyping System	IDT

2.1.3 Cytokines

Table 3: Cytokines.

Item	Manufacturer
rm-GM-CSF	PeprōTech
rm-IFN γ	PeprōTech
rh-IL2	Novartis
rm-IL4	PeprōTech
rm-MCSF	PeprōTech

2.1.4 Primary antibodies, unconjugated

Table 4: Unconjugated antibodies.

Antigen	Host	Clone	Manufacturer	Method
murine CD28	mouse	Polyclonal	eBioscience	in vitro
murine CD3	mouse	Polyclonal	BioLegend	in vitro
murine GAPDH	goat	Polyclonal	Linaris	WB
murine CD16/CD32	rat	Polyclonal	BioLegend	FC
murine F4/80-FITC	rat	BM8	BioLegend	IF
CIC	rabbit	Polyclonal	Abcam	WB
murine MHCII	rat	M5/114.15.2	eBioscience	IF
TotalSeqC Hashtag 1-10	Rat	M1/42; 30- F11;	Biolegend	10x
DRB1.01	mouse	L243	Biolegend	IF

2.1.5 Secondary antibodies

Table 5: Secondary antibodies.

Antigen	Host	Clone	Conjugate	Manufacturer	Method
goat IgG	donkey	ab97110	HRP	Abcam	WB
rabbit IgG	goat	sc-2004	HRP	Santa Cruz	WB
mouse IgG	goat	polyclonal	AF488	Thermo Fisher	IF
mouse IgG	goat	polyclonal	HRP	Bethyl	WB

2.1.6 *In vivo* antibodies

Table 6: *In vivo* antibodies.

Antigen	Clone	Manufacturer
---------	-------	--------------

mPD-L1	10F.9G2	BioXCell
mPD-1	RMP1-14	BioXCell
mCTLA-4	9D9	BioXCell
InVivoMAb mouse IgG2b isotype control	MPC-11	BioXCell
InVivoMAb rat IgG2a isotype control	2A3	BioXCell
InVivoMAb rat IgG2b isotype control	LTF-2	BioXCell

2.1.7 Antibodies used for flow cytometry

Table 7: Flow cytometry antibodies.

Antigen	Conjugate	Clone	Manufacturer
mCD11b	APC	M1/70	BioLegend
mCD11b	PE-Dazzle	M1/70	BioLegend
mIFN γ	PE	XMG1.2	BioLegend
HLA-A2	APC	BB7.2	BioLegend
HLA-DR	PerCp eF1710	L243	BioLegend
mIFN γ	APC	XMG1.2	BioLegend
mCD69	PE Cy7	H1.2F3	BioLegend
mCD3	APC	17A2	BioLegend
mCD3	BV421	17A2	BioLegend
mCD3	BV711	17A2	BioLegend
mCD3	FITC	17A2	BioLegend
mCD3	PE	17A2	BioLegend
mCD4	APC	RM4-5	BioLegend
mCD4	PB	RM4-5	BioLegend
mCD4	PE Texas Red	RM4-5	Invitrogen
mCD45	BV510	30-F11	BioLegend
mCD8	AF700	53-6.7	BioLegend
mCD4	BV510	RM4-5	BioLegend
mCD8	PerCP-Cy5.5	3-6.7	eBioscience
mCD8	BV510	53-6.7	BioLegend
mPD-1	PerCP-Cy5.5	J43	eBioscience
mTim3	BV 421	RMT3-23	BioLegend
mTim3	BV605	RMT3-23	BioLegend
MHC II (I-A/I-E)	AF700	M5/114.15.2	BioLegend
mFOXP3	APC	FJK-16s	eBioscience
mCD25	PE Cy7	PC61	BioLegend

mNK1.1	Vio Bright B515	REAffinity	Miltenyi
mGranzyme B	PE Cy7	NGZB	eBioscience
mCD4	PE Cy7	RM4-5	Invitrogen
mLy6C	APC	HK1.4	BioLegend
mCD19	BV605	6D5	BioLegend
mKi67	BV605	16A8	BioLegend
mTNFa	BV421	MP6-XT22	eBioscience
SIINFEKL-H2-Kb	PE	n.a.	Immudex
mPD-L1	BV711	10F.9G2	BioLegend
mCD11c	BV786	N418	BioLegend
mF4/80	BV421	BM8	BioLegend
CTFR		n.a.	Invitrogen
SIINFEKL-H2-Kb	APC	n.a.	Immudex
fixable viability dye eFluor780		n.a.	eBioscience

2.1.8 Peptides

Table 8: Peptides.

Name	Sequence
p53 Y88C	DDRNTFRHSVVVP C EPPEVGS DCT* T HY
p53 R141C	SSGNLLGRNSFEV C VCACPGRDRRTEE
p53 R116Q	NYMCNSSCMGGMN Q RPILTIITLEDSS
CIC R215W	RPMNAFMIFSKRH W ALVHQRHPNQDNR
CIC R215Q	RPMNAFMIFSKRH Q ALVHQRHPNQDNR
p53 wt88	DDRNTFRHSVVVPYEPPEVGS DCT* T HY
p53 wt141	SSGNLLGRNSFEV R VCACPGRDRRTEE
p53 wt116	NYMCNSSCMGGMN R RPILTIITLEDSS
CIC wt215	RPMNAFMIFSKRH R ALVHQRHPNQDNR
CICR215W 15 mers	
1	RRPMNAFMIFSKRH W
2	RPMNAFMIFSKRH W A
3	PMNAFMIFSKRH W AL
4	MNAFMIFSKRH W ALV
5	NAFMIFSKRH W ALVH
6	AFMIFSKRH W ALVHQ
7	FMIFSKRH W ALVHQR

8	MIFSKRHWALVHQRH
9	IFSKRHWALVHQRHP
10	FSKRHWALVHQRHPN
11	SKRHWALVHQRHPNQ
12	KRHWALVHQRHPNQD
13	RHWALVHQRHPNQDN
14	HWALVHQRHPNQDNR
15	WALVHQRHPNQDNRT
OT-I Epitope	SIINFEKL
OT-II Epitope	ISQAVHAAHAEINEAGR
MOG	MEVGWYRSPFSRVVHLYRNGK
Flu	PKYVKQNTLKLAT

2.1.9 Buffer

Table 9: Buffer.

Buffer	Ingredient	Specification
CellTrace FarRed staining buffer	1X PBS	Sigma-Aldrich; D8537
	0.1% BSA	Roth; 8076.4
FACS buffer	1X PBS	Sigma-Aldrich; D8537
	3% FBS	Sigma-Aldrich; S0615
	2mM EDTA	AppliChem; A3562.1000
	1X PBS	Sigma-Aldrich; D8537
MACS buffer	3% FBS	Sigma-Aldrich; S0615
	10 mM EDTA	AppliChem; A3562.1000
	1X PBS	Sigma-Aldrich; D8537

2.2 Plasmids and primers

Table 10: Primers.

Primer	Sequence
Cic_RT_01_f	GGCCTCCAACCAGAGCAAAG

Cx3Cr1^{CreERT2} mice that were used for breeding. For experiments, Cx3Cr1^{CreERT2}-MHCII^{flox/flox} and MHCII^{flox/flox} littermates were used. Rosa^{CreERT2} mice were provided DKFZ internally. OT-I, OT-II and immunodeficient non-obese diabetic (NOD) scid gamma mice (NOD.Cg-Prkdc^{scid} Il2rg^{tm1Wjl}/SzJ, NSG) mice were bred at the DKFZ animal facility.

All animal procedures followed the institutional laboratory animal research guidelines and were approved by the governmental authorities (Regional Administrative Authority Karlsruhe, Germany). 8–16-week old mice were assigned to age-matched and sex-matched experimental groups.

2.3.2 Cell lines and cell culture

Hek Phoenix Eco cells were provided by S. Pusch and cultured in DMEM supplemented with 10% FBS, 100 U/ml penicillin, and 100 µg/ml streptomycin (P/S, Sigma Aldrich) and selected for transgene expression with hygromycin (Sigma Aldrich).

A2.DR1 Glioma cell lines were generated as described below and cultured in DMEM supplemented with 10% FBS, P/S. Transfected cell lines were selected with 9 µg/ml blasticidine (Gibco). Cells were tested for mycoplasma contamination before inoculation.

GL261 cells were purchased from the National Cancer Institute. Cell lines were cultured in Dulbecco's modified Eagle's medium (DMEM) supplemented with 10% fetal bovine serum (FBSP), P/S, at 37 °C, 5% CO₂. Cells were routinely tested for mycoplasma contamination. GL216-OVA cell lines were generated by transfecting GL261 cells with the pMXS-OVA-IRES-blasticidine or pMXS-OVA-SIINFEKL-IRES-Blasticidine and cultured in DMEM supplemented with 10% FBS, P/S. Transfected cell lines were selected with 9 µg/ml blasticidine (Gibco).

2.3.3 Isolation and culturing of primary murine immune cells

Spleen and lymph nodes from mice sacrificed by cervical dislocation were mashed through a 70 µm strainer. Erythrocytes were lysed using ACK lysis buffer (Thermo). CD4⁺ or CD8⁺ T cells were magnetically separated using MACS negative isolation kits (Miltenyi). In brief, splenocytes were incubated with biotin-labeled antibodies to label unwanted populations. Anti-biotin magnetic beads were added and cells were separated through a column in the magnetic field of a MACS separator (Miltenyi). Pan T cells were isolated using the MagniSort™ Mouse T cell Enrichment Kit (Thermo Fischer). Splenocytes or isolated T cells were cultured in DMEM, 10% FCS, P/S, 0.1% β-mercaptoethanol (Sigma Aldrich), 1% sodium-pyruvate (Sigma Aldrich), 5 mM HEPES (Invitrogen), Non-essential amino acids (NEAA, Gibco) (T cell medium, TCM) or used for subsequent experiments.

For bone marrow-derived macrophages, bone and hip from mice sacrificed by cervical dislocation were isolated and grinded using a mortar and pestle in IMDM (Thermo Fischer). Cells were flushed through a 40 μ M strainer and contaminating erythrocytes were lysed using ACK lysis buffer. For the generation of BMDMs, cells were cultured in IMDM, supplemented with 10% FBS and P/S containing 20 ng/ml M-CSF (PeproTech) at 37°C and 5% CO₂. Medium was changed after 72 h. Cells were used for assays after 7 days.

2.3.4 Vaccination of mice

A2.DR1 or C57B/6J mice were vaccinated with 100 μ g respective peptide emulsified in 100 μ l 1:1 PBS:Montanide-ISA51 (Seppic). Mice received 50 μ l each in the lateral pectoral regions. rmGM-CSF (300 ng, Immunotools) in PBS was injected subcutaneously between injection sites, and Aldara cream containing 5% imiquimod (Meda Pharma) was applied on shaved injection site. Mice were boosted at day 10 with peptide and Aldara cream. Mice were terminated at day 21.

2.3.5 ELISpot

ELISpot was performed as previously described¹⁵². Briefly, wetted ELISpot plates (MAIPSWU10, Millipore) were incubated with 100 μ l 15 μ g/ml IFN γ coating antibody (AN-18, Mabtech) and incubated over night at 4 °C. Cells from spleen and lymph nodes from vaccinated mice were extracted at day 21 after vaccination and resuspended in TCM. IFN γ coating antibody was removed and ELISpot plates were blocked with TCM. 300.000 to 600.000 cells were plated, and peptides were added at 10 μ g/ml concentration. For positive control, 20 ng/ml PMA and 1 μ g/ml ionomycin was used. Plates were incubated for 40 h. Cells were removed and the plate was incubated with 1 μ g/ml biotinylated IFN γ detection antibody (R4-6A2, Mabtech) in PBS with 0.5% FBS for 2 h at room temperature. The detection antibody was removed and plates were incubated with 1 μ g/ml streptavidin-ALP (Mabtech) in PBS with 0.5% FBS for 1 h. Streptavidin-ALP was removed and plate was incubated with APL development buffer (Bio-Rad) until distinct spots emerge. Spots were quantified with an ImmunoSpot Analyzer (Cellular Technology Ltd).

2.3.6 Flow cytometry

According to the experiment settings, approximately 1 million cells were placed into v-bottom wells of a 96 well plate. All incubation and centrifugation steps were performed at 4 °C. Murine cells were blocked with rat anti-mouse CD16/32 (0.5 μ g per well, eBioscience) and stained with respective antibodies (Table 7) for 30 min. eFluor 780 fixable viability dye (eBioscience) was used to exclude dead cells.

For intracellular staining of cytokines, cells were incubated with 5 µg/ml Brefeldin A (Sigma Aldrich) and respective stimulus (10 µg/ml for peptides, see also ELISpot) for 5-6 h. Intracellular staining was performed using the eBioscience™ Intracellular Fixation & Permeabilization Buffer Set (Thermo Fisher) or the Cytotfix/Cytoperm™ Fixation/Permeabilization Kit (BD) according to manufacturer's protocol. Non-fixed samples were acquired within 4 h, fixed samples within 48 h on a BD FACS Canto II, a BD LSR Fortessa or a Attune NxT (Thermo Fisher). Data was analyzed using FlowJo V10.

2.3.7 Generation of A2.DR1 gliomas

A2.DR1 gliomas were generated as previously described¹⁵⁹ in new-born A2.DR1 pups. P0 pups were electroporated with guide RNAs for p53, Pten and Nf1 cloned into pX330 plasmid together with DNA encoding for Cas9. P0 mice were anaesthetized with 2% isoflurane and medially injected at lambda: -3.6 and D/V: -0.7 with 1 µg DNA in 1 µl. After injection, electric square pulses were delivered laterally using forceps-like electrodes (35 mV (VZ), 50ms-on, 950ms-off, 5 pulses). Successful electroporation was confirmed by co-electroporation of the plasmid pT2K IRES-luciferase and imaging of bioluminescence signal of luciferase seven days after electroporation (IVIS, Perkin Elmer). When mice showed symptoms of neurological deficit, mice were sacrificed via heart perfusion with PBS and tumors were excised (between 90 and 120 days). Tumors were digested with 50 µg/ml liberase (Sigma) for 30 minutes and subsequently mashed through a 100 µm strainer. Tumor cells were immediately re-injected into the flank of NSG mice for *in vivo* passage. After tumors reached 1cm in diameter, tumor cells were isolated as described and tumor cells were cultured in DMEM/F12 (Thermo Fisher) supplemented with 10% FBS and P/S for at least three passages to ensure removal of contaminating stromal cells.

2.3.8 Mutation detection and copy number alteration

DNA and RNA were isolated from tumors from the *in vivo* passage or from cells grown as monolayer after six passages using RNeasy Mini Kit or DNeasy Blood & Tissue Kit (Qiagen) according to manufacturers' instructions. Libraries were sequenced on an Illumina NovaSeq (2 x 50 nt). DNA- and RNA-derived sequence reads were aligned to the mm9 genome as described previously¹⁶⁰. Detection of mutations and copy number calling was performed as described previously¹⁶⁰. Genes exhibiting copy number alterations were annotated with their respective chromosomal location and transcript length by accessing the Biomart database in R (www.biomart.org) and using the Ensembl mouse genome (GRCm38.p6) as reference. Analysis was performed by Martin Löwer (TRON - Translational Oncology at the University Medical Center of Johannes Gutenberg University, Mainz, Germany).

2.3.9 Histology

Brains from PBS-perfused A2.DR1 glioma or GL261-bearing mice were stored in Tissue-Tek OCT compound (Sakura) at -80 °C and cut into 6-8 µm slices using a cryotome (Leika).

For HE staining, slices were fixed with Roti-Histofix 4.5% (Carl Roth) and haematoxylin and eosin staining was performed using haematoxylin and bluing reagent for 4 min.

For immunofluorescence staining, slides were air dried, incubated with cold methanol (Sigma Aldrich) and blocked for 2 h with 10% new goat serum (Sigma Aldrich). Slides were incubated with the primary antibodies overnight in blocking buffer. Secondary antibodies were incubated for 2 h and slides were mounted in mounting medium containing DAPI (Invitrogen). Images were acquired within 6 h on a Cellobserver (Zeiss) or LSM700 confocal microscope (Zeiss).

2.3.10 Western blot

Frozen cell pellets were lysed using RIPA buffer (Thermo Fisher) and protein supernatant was used for analysis. Protein concentration was quantified using BCA Protein Assay Kit according to manufacturer's protocol and absorbance was measured using an iMark™ Microplate Absorbance Reader plate reader (Bio-Rad). 25 µg of protein lysate was boiled in loading buffer containing 10% β-mercaptoethanol at 95 °C for 5 minutes and separated on an 8% SDS polyacrylamide gel for 90 minutes (15 mA). Gels were plotted on methanol activated PVDF membranes using a Bio-Rad Trans-Blot Turbo Transfer System. Membranes were blocked with 5% Milk dissolved in TBST and incubated with the primary antibody overnight. Secondary antibodies were incubated for 1 h and membranes were developed with ECL prime and imaged on a Bio-Rad ChemiDoc Imaging System.

2.3.11 Quantitative real-time PCR

For qPCR, RNA was isolated using RNeasy Mini kit (Qiagen) and cDNA was obtained from 1 µg RNA using the High-Capacity cDNA Reverse Transcription Kit (Applied Biosystems). qPCR was run on a QuantStudio 3 (Applied Biosystems). Primers are indicated in Table 10.

2.3.12 Generation of T cell lines and TCR sequencing

CICR215W reactive T cell lines were obtained as previously described¹⁶¹. Briefly, splenocytes from CICR215W vaccinated A2.DR1 mice were isolated and cultured for 7 days in TCM containing 10 µg/ml CICR215W peptide. Medium was exchanged weekly after 7 days and supplemented with 3% ConA supplement (kindly provided by W Osen) and 15 mM α-methylmonopyranoside (α-

MM, Sigma-Aldrich). T cells were re-stimulated with irradiated (30 Gy) autologous splenocytes from A2.DR1 mice loaded with 2 µg/ml peptide every 4 weeks.

After two re-stimulations T cell lines were subjected to an IFN γ secretion assay (Miltenyi). IFN γ ⁺ CD4⁺ T cells were sorted on a BD Aria II. Sorted T cells were used for 10x VDJ sequencing using customized primers. The generated library was sequenced on a NextSeq 550 system and subsequently analyzed through the cell ranger pipeline 1.1 (10x Genomics). For TCR deep sequencing, DNA was isolated (QIAmp DNA Mini Kit, Qiagen) and submitted for murine ImmunoSEQ[®] (Adaptive). Data was analyzed using the adaptive immunoSEQ analyzer (Adaptive).

2.3.13 Cloning of CIC-reactive TCRs

A retroviral construct was used for TCR transduction of primary T cells. First, the variable chain of respective TCRs was synthesized by Eurofins and subsequently cloned in a vector containing the murine constant alpha and beta chains. Subsequently, the full length TCR was cloned into pMXS-TCR-IRES-GFP via pDONR (Thermo Fisher) using the Gateway cloning system (Thermo Fisher). The pMXS-IRES-GFP was kindly provided by Stefan Pusch (DKTK Clinical Cooperation Unit Neuropathology, German Cancer Research Center (DKFZ), Heidelberg, Germany).

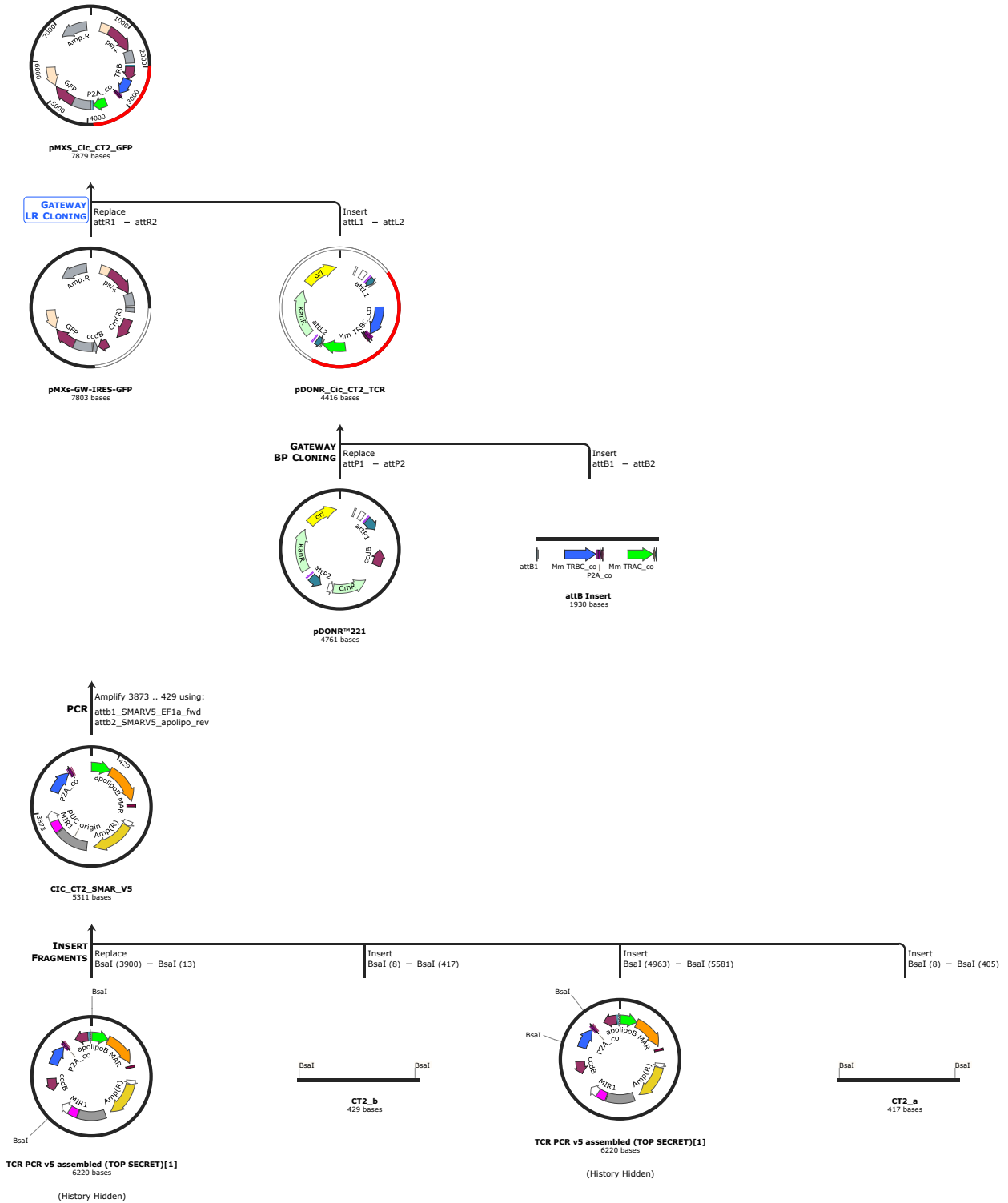


Figure 7: Overview for TCR cloning strategy.

2.3.14 TCR transduction

A2.DR1 T cells were isolated as described above. Plates for T cell activation were coated with anti-hamster IgG (MPBio) for 3 h at 37 °C at 8 µg/ml and subsequently incubated with 0.1 µg/ml αCD3e (eBioscience) at 4 °C for 45 min. T cells were incubated on activation plates in TCM with

1*10⁴ IU/ml hIL2, 1 µg/ml α CD28 (Biolegend) for 24 h. For virus production, HEK Phoenix Eco cells were seeded at a density of 3.5*10⁵ cells/ml and transfected the next day with 12 µg DNA per 10 ml using Fugene (Promega) according to manufacturer's protocol at a ratio of 1:4 DNA:Fugene. Medium was changed after 24 h and virus was harvested 48 h after transfection. The virus particle containing supernatant was filtered through a 0.45 µm filter and added to retronectin (Takara, 16 µg/ml, 2h, 37°C) coated cell culture plates. The virus-containing plates were centrifuged at 4000 rpm for 1 h at room temperature (RT) and T cells were added at a density of 6*10⁶ cells/ml and subsequently centrifuged at 2300 rpm for 1 h at RT. T cells were incubated for 5 h at 37°C and resuspended in fresh TCM containing 20IU hIL2. T cells were used for subsequent assays after 36-40 h.

2.3.15 Co-culture assays with TCR-transduced T cells

T cells were transduced as described above. Splenocytes from A2.DR1 mice were isolated, irradiated (30 Gy) and loaded with 10 µg/ml peptide. Transduced T cells were added in a 1:1 ratio and incubated overnight and subsequently stained for IFN γ and CD69 expression as described above.

For the NFAT-reporter assay, T cells were co-transduced with an NFAT reporter cloned into pDONR (kindly provided by Edward Green, DKTK Clinical Cooperation Unit Neuroimmunology and Brain Tumor Immunology, German Cancer Research Center (DKFZ), Heidelberg, Germany) and incubated with peptide-loaded splenocytes as described above. Nano-Glo (Promega) reagents were used according to manufacturer's instructions. Luciferase activity was measured using a Pherastar plate reader (BMG Labtech).

2.3.16 *In vivo* proliferation assay

T cells were transduced as described above. After 40 h, T cells were sorted on a BD Aria II for CD3⁺ GFP⁺ T cells. Sorted T cells were expanded using αCD3e/αCD28 as described above. 5 days after expansion, T cells were rested for 24 h and labeled with 1 µM Cell Trace Far Red (CTFR, Thermo Fisher) and intravenously injected into A2.DR1 mice. 24 h after injection mice were intravenously injected with 50 µg aCD40 antibody (Bioxcell) and 50 µg CICR215W or MOG peptide. 4 days after T cell transfer, spleens were extracted and analyzed by flow cytometry.

2.3.17 Intracranial tumor cell inoculation

For A2.DR1 gliomas, 2*10⁴ tumor cells were resuspended in 2 µl PBS. For GL261 tumors, 10⁵ tumor cells were resuspended in 2 µl PBS. Tumor cells were stereotactically implanted into the

right hemisphere of 7–14-week-old male A2.DR1 mice using following coordinates: 2 mm right lateral of the bregma and 1 mm anterior to the coronal suture with an injection depth of 3 mm below the dural surface. A 10 μ l Hamilton micro-syringe driven by a fine step stereotactic device (Stoelting) was used. The surgery was performed under anesthesia (Ketamin, 100 mg/kg i.p. und Xylazin, 10 mg/kg i.p) and mice received analgesics for 2 days post-surgery. Mice were checked daily for tumor-related symptoms and mice were sacrificed when stop criteria were met or mice showed signs of neurological deficit.

2.3.18 Therapeutic adoptive T cell transfer

A2.DR1 T cells were transduced with the CICR215W reactive CT2 or control (Flu) TCR as described above. After 40 h T cells were sorted for GFP expression as described above. Sorted T cells were expanded for 3 days as described above. Before injection, T cells were incubated with 20 μ g/ml PD-1 and CTLA-4 blocking antibodies (both Bioxcell) for 1 h. 400.00 T cells were stereotactically injected in 4 μ l PBS into the left ventricle of A2.DR1 glioma bearing mice at a speed of 1 μ l/s (coordinates: 0.5 mm left lateral of the with an injection depth of 1.8 mm below the dural surface). The syringe was allowed to stay at the injection side for 3 minutes. T cell inoculation was performed under anesthesia and mice received analgesics for 3 days post operation.

2.3.19 Isolation of tumor infiltrating immune cells

After perfusion with PBS, brains of tumor-bearing mice were extracted and tumors were digested with liberase as described above and mashed through 100 μ m and 70 μ m strainer (Miltenyi). Myelin was removed using a 30% continuous Percoll (GE Healthcare) gradient.

2.3.20 MRI imaging

MRI was carried out by the small animal imaging core facility at DKFZ using a Bruker BioSpec 3Tesla (Ettlingen, Germany) with ParaVision software 360 V1.1 or at the Radiology Department, University Clinic Heidelberg using a BioSpec 94/20 USR, Bruker BioSpin GmbH, with a four-channel phased-array surface receiver coil.

For imaging, mice were anesthetized with 3.5% sevoflurane in air. For lesion detection, T2 weighted imaging were performed using a T2_TurboRARE sequence: TE = 48 ms, TR = 3350 ms, FOV 20x20 mm, slice thickness 1,0mm, averages = 3, Scan Time 3m21s, echo spacing 12 ms, rare factor 8, slices 20, image size 192x192. Tumor volume was determined by manual segmentation using Bruker ParaVision software 6.0.1.

2.3.21 Mutation specific PCR

Mutation-specific primers were designed using the rhAmp Genotyping Design Tool (IDT). PCR was performed using the rhAmp SNP Genotyping System (IDT) according to manufacturer's protocol using a 2 color (FAM, VIC) reference system. PCR was run and analyzed on a QuantStudio 3.

2.3.22 Co-culture assays using OT-I/OT-II T cells

For CD4⁺ T cell activation assays, splenocytes were isolated from OT-II mice as described above and incubated with 100 IU hIL2 and 0.1 µg/ml OVA(329-337) for 72 h in TCM at a density of 10⁶ cells/ml. CD4⁺ T cells were subsequently isolated as described above and rested for 48 h in TCM supplemented with 20 IU hIL2. For re-stimulation, BMDMs were loaded with 10 µg/ml OVA(329-337) and OT-II T cells were added at a 1:1 ratio. FACS staining was performed after 12 h after 5 h of BrefeldinA incubation.

OT-I T cells were isolated as described above and co-cultured in TCM supplemented with 20 IU hIL2 with BMDMs loaded with 25 nM SIINFEKL for 48 h. CD8⁺ T cells were subsequently isolated as described above and rested for 48 h. T cells were then co-cultured with GL261-SIINFEKL at a ratio of 1:1 and after 12 h 5 µg/ml BrefeldinA were added. FACS staining was performed after 5 h as described above.

2.3.23 Treatment of mice

Cx3Cr1^{CreERT2}-MHCII^{flox/flox} mice or littermates received tamoxifen via oral gavage. For targeting all myeloid cells, 4 days before tumor inoculation, mice were treated with 5 mg tamoxifen (Sigma Aldrich) dissolved in 100 µl corn oil/ethanol (90%/10%, Sigma Aldrich) for 4 consecutive days. Tamoxifen application was repeated every 4-5 days. For a microglia-specific KO, mice were treated with tamoxifen on 5 consecutive days 5-6 weeks before tumor inoculation.

Immune checkpoint blockade was composed of 250 µg PD-1, 100 µg CTLA-4 and 200 µg PD-L1 blocking antibodies and were intraperitoneally injected starting from day 13 every 3 days for 4 doses.

2.3.24 Single-cell RNA sequencing

For single cell RNA sequencing of GL261 tumors infiltrating immune cells, mice were sacrificed on day 20 after tumor inoculation and tumors were processed as described above. Cells were hashed for individual mice using TotalSeqC antibodies (Biolegend) stained for dead cells, CD45, CD3, CD11b, SIINFEKL-H2-kb, CD8 and sorted for CD3 negative, tetramer double positive and

tetramer negative cell populations on a BD Aria II or BD Aria Fusion. 10x library preparation was performed according to manufacturer's protocol (10x genomics) and libraries were sequenced on a NovaSeq lane (Illumina). Data processing was performed using the 10x cell ranger platform V3.1.0 by Kyle Tan (DKTK Clinical Cooperation Unit Neuroimmunology and Brain Tumor Immunology, German Cancer Research Center (DKFZ), Heidelberg, Germany). The resulting count files were analyzed using Seurat v3 dataset integration workflow¹⁶². The data was filtered for features that are expressed in at least 3 cells and cells with at least 200 and maximum 6000 features and a maximum percentage of mitochondrial genes of 10% (Arguments min.cells = 3, min.features = 200, percent.mt < 10%). Mitochondrial genes were regressed out and data was normalized using a scale factor of 10,000 (scale.factor = 10.000). Datasets were combined using the integration function with expected dimensions set to 30.

Differential gene expression was performed using the FindMarkers function, using the MAST test¹⁶³.

2.3.25 Graphical data representation and statistics

All data are presented as individual values or as means with standard error of the mean (\pm SEM) as indicated in the figure legend. Sample sizes (n) and statistical tests are indicated in the figure or figure legends and were performed with GraphPadPrism 9.0 with unpaired, two-tailed t test or one-way ANOVA with Holm-Šidák multiple comparison test or Tukey's multiple comparisons test. The Kaplan-Meier method was used to assess survival patterns and survival statistics were performed by log-rank Mantel-Cox test. $P < 0.05$ was considered significant (* $p < 0.05$, ** $p < 0.01$, *** $p < 0.001$). High dimensional single cell plots were generated using R v3.6.2. Experimental overview figures were generated using BioRender.

3 Results

3.1 CICR215W as a novel target for adoptive TCR therapy

3.1.1 CICR215W induces mutation specific immune response in HLA humanized mice

In an effort to screen for novel shared immune therapeutic targets in low grade gliomas, five different epitopes were screened that have been described to be frequently mutated in low grade gliomas¹⁶⁴ by using peptide vaccination of A2.DR1 HLA-humanized mice (Figure 8a). Potential targets were first screened by predicting HLA-A2 and HLA-DR1-binding affinities using NetMHC4.0 and NetMHCIIpan4.0. Five neoantigens encompassing point mutations were predicted to strongly bind to HLA-A2, including two point mutations at position 215 in capicua transcriptional repressor (CIC) and three point mutations in tumor protein 53 (TP53). All 5 neoepitopes were predicted to bind considerably stronger to the mutated form than the wildtype form (Figure 8b). Peptides carrying the amino acid exchange R to W or Q at position 215 in the CIC gene showed point mutation-specific Interferon-gamma (IFN γ) responses in spleen and lymph nodes (Figure 8c, d, e). In contrast, peptides encompassing p53 point mutations did not elicit an antigen-specific immune response (Figure 8f).

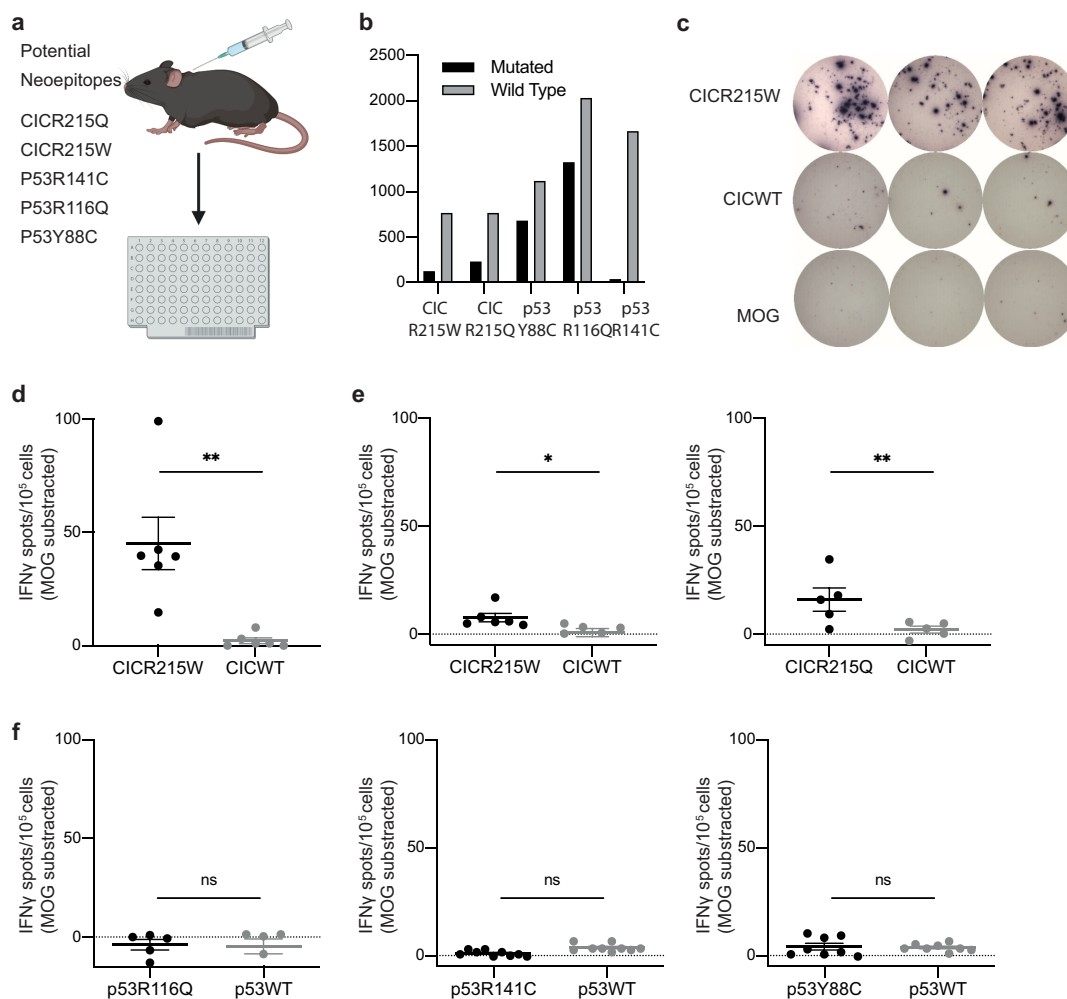


Figure 8: Identification of CICR215W/Q point mutations as potential target for targeted immunotherapy. a. Experimental overview. Peptides harboring potential glioma-related neopeptides were used for vaccination of A2.DR1 MHC-transgenic mice. B. Binding affinity for selected amino acid alterations for HLA-A*0201 determined by NetMHC 4.0. c. Representative IFN γ ELISpot assay of splenocytes isolated from CICR215W vaccinated mice restimulated for 48 h with the indicated peptide. d. Quantification of data shown in b, n = 6 mice. e, f. Quantification of IFN γ ELISpot using cells isolated from lymph nodes from vaccinated A2.DR1 mice restimulated with the indicated peptides. d-f. Data are represented as mean \pm SEM. Statistical significance was determined by paired two-tailed Student's t-test.

3.1.2 CICR215W is an MHC class II restricted neopeptide and a mutational hotspot in oligodendroglioma

IFN γ immune responses can be induced by both, CD4⁺ and CD8⁺ T cells. To address the question which cell type is accountable for the immune response against CICR215W, intracellular staining of splenocytes of vaccinated mice was performed. IFN γ expression was clearly restricted to CD4⁺ T cells (Figure 9a, b), leading to the hypothesis that CICR215W is a MHC class II-restricted neopeptide. Analysis of the TCGA LGG cohort revealed that the position 215 in the CIC gene is a mutational hotspot resulting in either CICR215W or CICR215Q, with approximately 2% of all WHO grade 2 gliomas carrying this mutation with an enrichment (3.5-6.0%) in oligodendrogliomas, which was shown in two independent cohorts (Figure 9c, d).

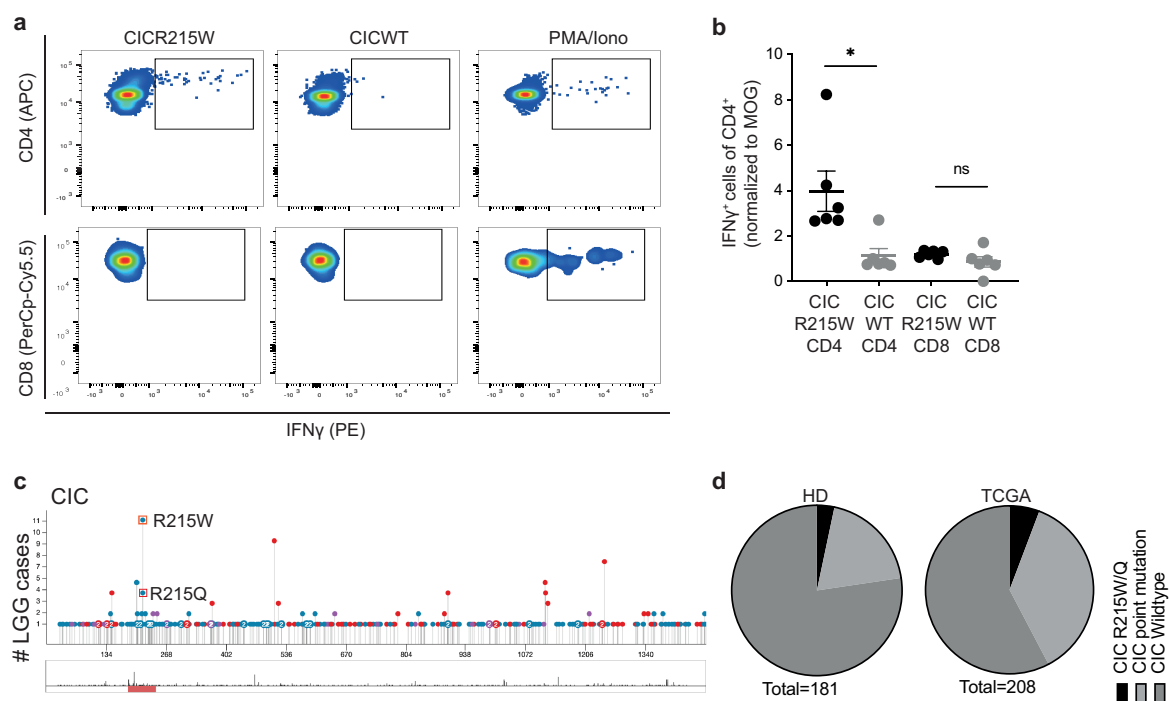
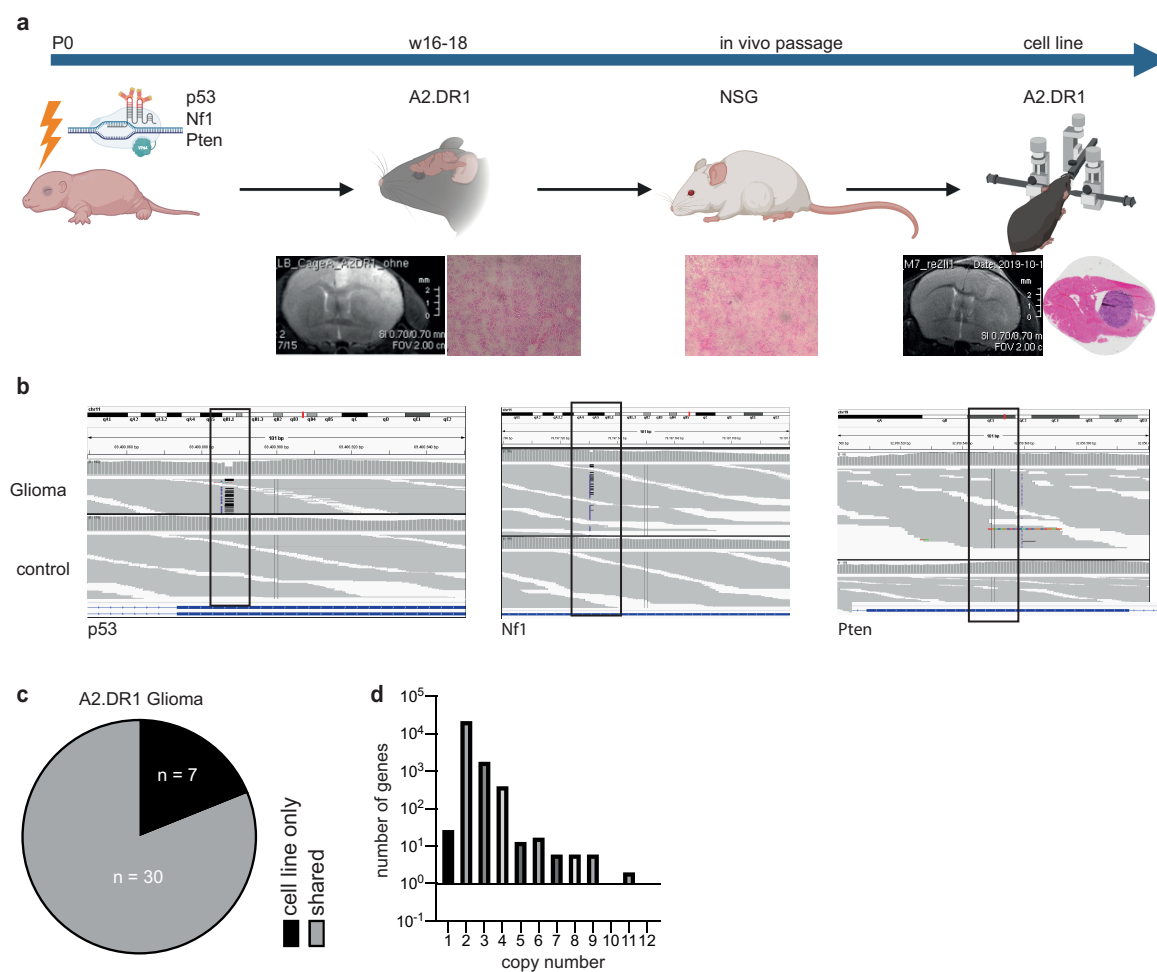


Figure 9. CICR215W triggers an MHC class II-restricted CD4⁺ T cell driven immune response and is frequently mutated in oligodendroglioma. a. Representative flow cytometric analysis of splenocytes from CICR215W vaccinated mice re-stimulated for 24 h with the indicated peptide and intracellularly stained for IFN γ production. b. Quantification of data shown in a, n = 6 mice. c. TCGA analysis of the TCGA LGG dataset (n = 516), frequent mutations at protein position 215 are shown. d. Proportion of CIC point mutated and CIC215-mutated patients in the TCGA and Heidelberg oligodendroglioma cohort. b. Data are represented as mean \pm SEM. Statistical significance was determined by paired two-tailed Student's t-test.

3.1.3 Generation of an HLA humanized A2.DR1 glioma tumor model

Preclinical assessment of immunotherapeutic interventions in brain tumors has always been hampered by the lack of adequate tumor models. Thus, A2.DR1 gliomas were generated using a previously described CRISPR-Cas9-based genetic approach, enabling somatic deletion of tumor suppressors Neurofibromin 1 (Nf1), Phosphatase and tensin homolog (Pten) and Tp53¹⁵⁹ in newborn pups (Figure 10a). The triple knockout led to the formation of brain tumors after three months and to lethal tumor growth after four to five months. Grown tumors were subsequently excised and directly injected into the flank of immunodeficient non-obese diabetic (NOD) scid gamma (NSG) mice. After *in vivo* passage, tumors were dissociated and *ex vivo* cultured for three passages before being defined as cell line. Generated tumors maintained their histological integrity and were histopathologically defined as oligosarcoma (Figure 10a). Using RNA and exome sequencing, the triple knockout in the cell line could be verified (Figure 10b). Interestingly, exome sequencing revealed a low mutational load with 37 mutations, only seven of which were acquired during six *in vitro* passages (Figure 10c). The observed low mutational load was similar to human oligodendrogliomas,¹⁶⁵ although different driver mutations were used. Copy number analysis showed a diploid chromosomal set, with only minor (10%) copy number alterations (Figure 10d).



3.1.4 Phenotyping of the A2.DR1 glioma model

Next, the antigen-presenting capacity of the generated A2.DR1 glioma cell line was investigated. Flow cytometric analysis and immunofluorescence staining revealed that the tumor cell line is positive for HLA-A2 MHC class I but negative for DRB1.01 MHC class II, even when treated with IFN γ (Figure 11a, b). For *in vivo* testing of CicR215W reactive TCRs, the full CicR215W protein was overexpressed in the A2.DR1 cell line. The overexpression was verified using immunofluorescence staining, western blot and RT-qPCR (Figure 11c, d, e).

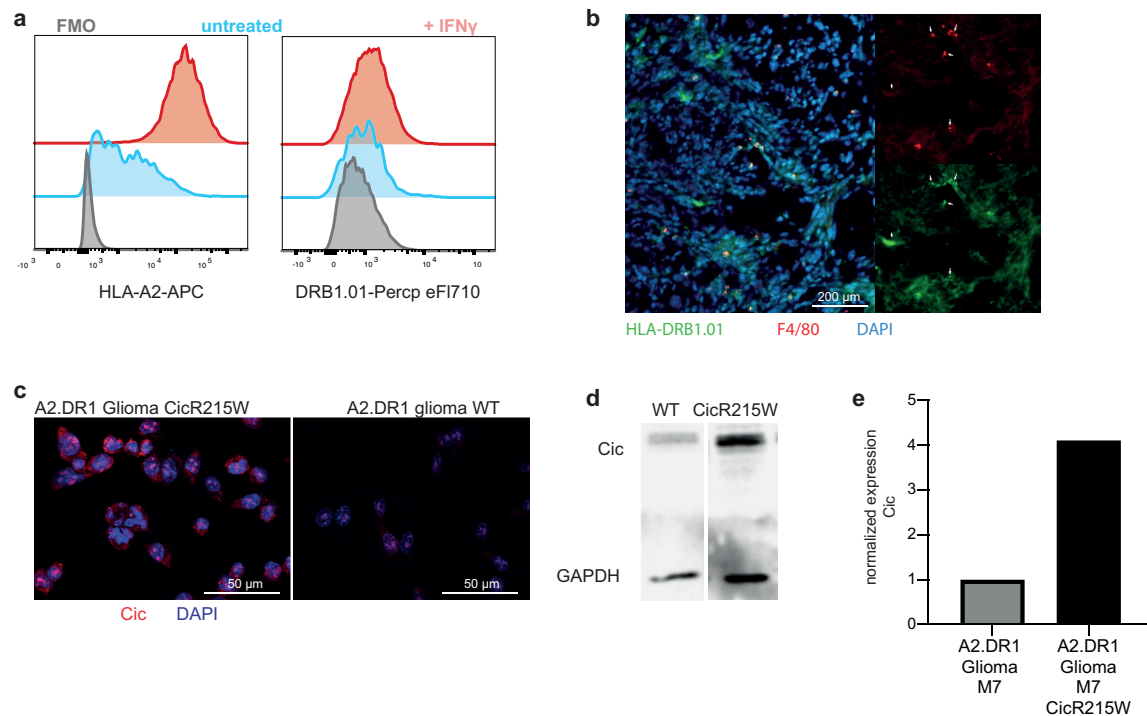


Figure 11: A2.DR1 glioma is MHC class II negative and overexpression of CicR215W. a. MHC expression on A2.DR1 glioma cell line incubated with recombinant murine IFN γ for 24 hours. b. Immunofluorescence image for MHCII and F4/80 of A2.DR1 glioma orthotopically injected into the brain of adult A2.DR1 mice, 20 days after injection. c. Immunofluorescence image of CicR215W transfected cells and the parental cell line, stained with an anti-Cic antibody. d. Immunoblot depicting overexpression of the Cic protein in the CicR215W transfected A2.DR1 cell line compared to the parental line (WT). e. RT-qPCR of relative Cic expression in the CicR215W transfected A2.DR1 cell line compared to the parental line.

3.1.5 Single-cell VDJ sequencing of CICR215W reactive T cell lines reveals high heterogeneity between mice

Therapeutic peptide vaccination has shown to induce tumor regression in subcutaneous tumor models. However, brain tumor-targeting vaccination strategies have not shown adequate preclinical or clinical anti-tumor effects^{152,166}. Vaccination strategies rely on trafficking and homing of peripheral T cells into the immune-privileged CNS. In contrast, local delivery of Chimeric Antigen Receptor (CAR)-transgenic T cells into the contralateral ventricle has demonstrated profound preclinical efficacy against human glioma cells in immunodeficient mouse models^{128,129,167}. Applying this strategy of adoptive T cell therapy to our MHC-humanized glioma model in immunocompetent A2.DR1 mice, peptide-specific expanded T cell lines from splenocytes isolated from CICR215W vaccinated A2.DR1 mice were generated. These T cell lines were subjected to an IFN γ secretion assay and peptide specific IFN γ -producing T cells were sorted and droplet-based single cell VDJ sequencing was performed using the 10x Genomics single-cell sequencing platform (Figure 12b). For specific enrichment of TCR specific RNA templates, primers encompassing the VDJ regions of murine TCRs in accordance to the 10x genomics human TCR enrichment protocol were designed (Figure 12a). Deep TCR- β sequencing for each mouse enabled us to map back each TCR pair to the respective individual mouse it originated from (Figure 12b). High heterogeneity was observed between different mice, with one to two clones being highly prevalent in each mouse (13-78%, Figure 12c). Strikingly, VDJ CT2 was found in 4 out of 5 mice with a frequency of 0.002% to 48.781% (Figure 12d).

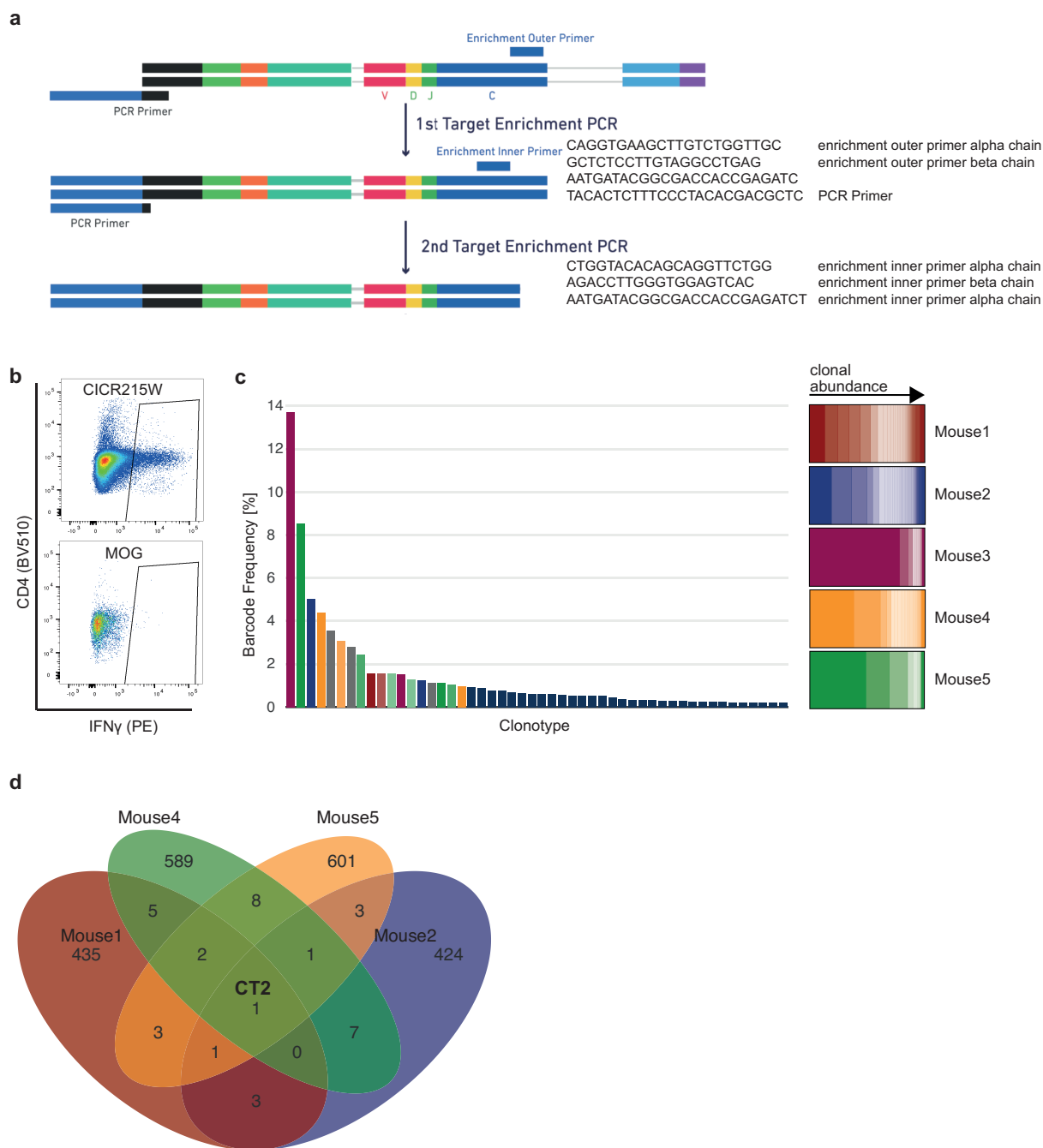


Figure 12: Retrieval of functional TCRs by single-cell VDJ sequencing. a. Overview showing the TCR enrichment PCR strategy. PCR primers for murine VDJ enrichment designed to be compatible with the 10x Genomics systems are depicted. b. IFN γ -secretion assay of pooled T cell lines from five individual mice vaccinated with CICR215W peptide. IFN γ ⁺ T cells were sorted and subsequently subjected to single-cell VDJ sequencing using the 10x Genomics platform. c. left: clonotype distribution of pooled single cell library, color-coded for individual mice retrieved by deep TCR sequencing (right), with respective abundance. d. Venn diagram of shared TCR- β sequences in T cell lines generated from 4 CICR215W vaccinated mice from c.

3.1.6 Retrieval of CICR215W reactive TCRs

Using retroviral transduction of murine primary T cells, a TCR testing strategy was established (see also methods). An internal ribosomal entry site (IRES) allowed for the detection of transduced T cells via the co-expression of GFP. Flow cytometric analysis of IFN γ and CD69 protein expression was used to screen for reactive TCRs (Figure 13a). The system was benchmarked using a known TCR against influenza-virus (Flu) peptide (Figure 13b). All top 3 TCR clones (CT1-3) showed a stable mutation-specific IFN γ and CD69 expression upon recall with CICR215W 27-mer peptide that was comparable to the Flu TCR response (Figure 13b, c). CT2 showed the highest IFN γ release which was validated in three independent assays (Figure 13d) as well as by NFAT activation as determined by an NFAT-reporter assay that induces a luciferase signal upon stimulation (Figure 13e). Of note, re-stimulation with all possible 20-mers encompassing the CICR1215W mutation did not lead to activation of the CT2 TCR (Figure 13bf).

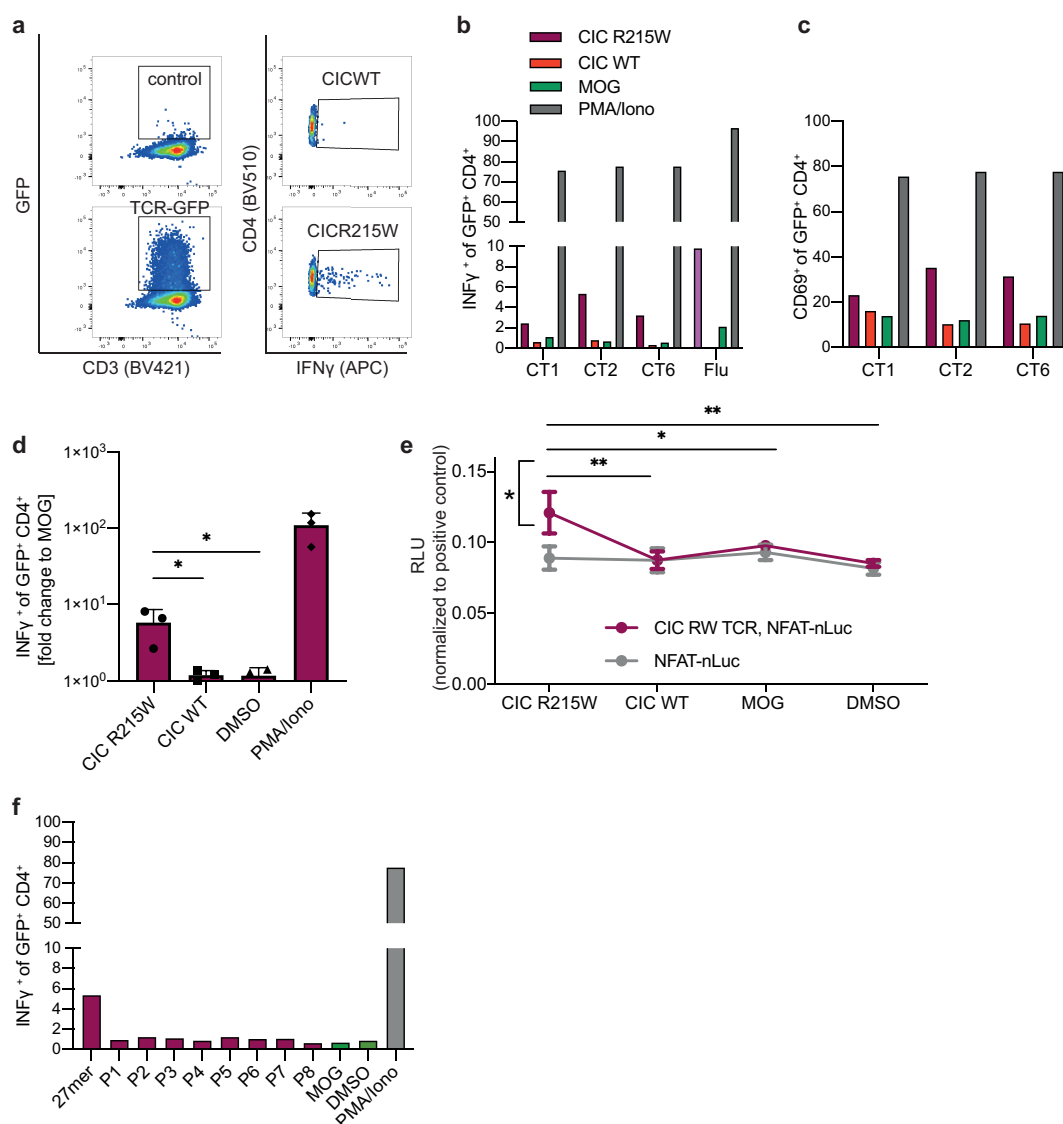


Figure 13: Identification of CICR215W reactive TCRs. a. Exemplary gating strategy for the validation of α -CICR215W-TCR-transduced (CT2) CD4⁺ T cells. Left: Co-expression of GFP after an IRES site as reporter for TCR expression in α -CICR215W-TCR-transduced T cells, determined by flow cytometry. Right: IFN γ production of GFP⁺

α -CICR215W-TCR-transduced T cells after re-stimulation with irradiated splenocytes pulsed with CICR215W. b. quantification of a, re-stimulated with the indicated peptides. c. CD69 expression of α -CICR215W-TCR-transduced T cells after re-stimulation with irradiated splenocytes pulsed with the respective peptide. d. Repeated measurements of CT2. e. NFAT-reporter assay of TCR and NFAT reporter transduced A2.DR1 T cells, re-stimulated for 4 hours with the indicated peptide, measured by luciferase signal. f. IFN γ production of GFP $^+$ α -CICR215W-TCR-transduced T cells after re-stimulation with irradiated splenocytes pulsed with CICR215W 19(P1) to 26-mers (P8). d, e: Statistical significance was assessed by one two-way ANOVA with Tukey's multiple comparisons test.

3.1.7 TCR transduced T cells remain reactive to peptide stimuli *in vitro* and *in vivo*

As T cells need to be strongly activated before viral transduction, it was checked if transduced T cell remain functional. For benchmarking, we used the MHC class II-restricted OT-II TCR transduced into wildtype C57B6/J T cells. Transduced T cells retained their antigen-induced proliferation capacity even after enrichment sort and 5 days of expansion (Figure 14a). Similar results were obtained using CT2 transduced into A2.DR1 T cells (Figure 14b, c). Strong T cell activation via α CD3/ α CD28 combined with high doses of Interleukin-2 (IL2) induces the upregulation of checkpoint molecules like PD-1 and CTLA-4. In order to attenuate intratumoral exhaustion of adoptively transferred T cells, we reinvigorated the transduced T cells with immune checkpoint-blocking antibodies α -mPD-1, α -mCTLA-4. The pre-treatment of checkpoint antibodies led to an increase of IFN γ production upon re-stimulation (Figure 14d).

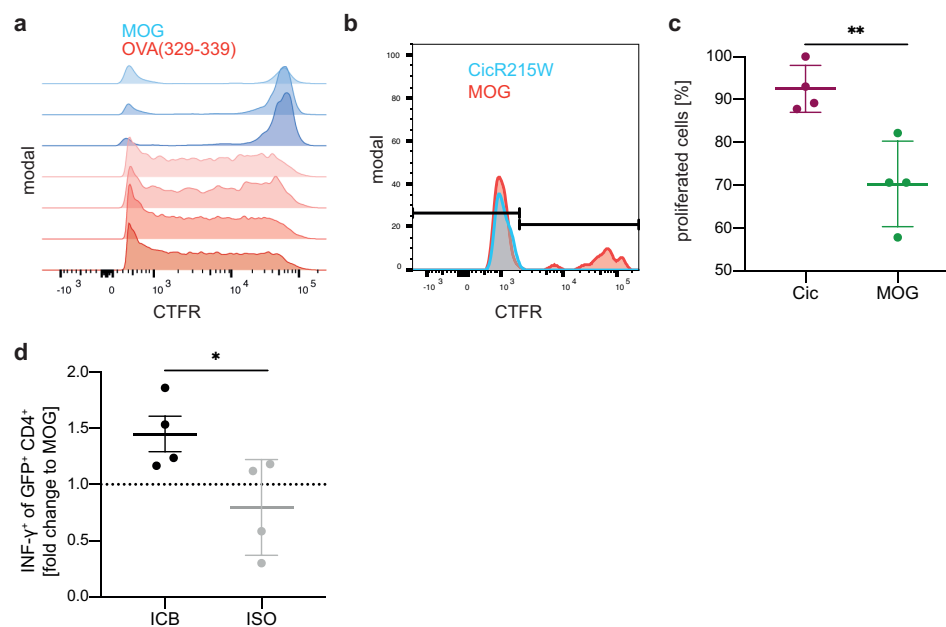


Figure 14: TCR transduced T cells maintain activity after transduction and expansion. a. C57B6/J T cells were transduced with the OT-II TCR, sorted for GFP expression and subsequently expanded with α CD3/ α CD28 antibodies for 5 days. After labeling, cells were injected *i.v.* into WT recipient mice and 24 hours later injected with the indicated peptide and α CD40 antibody. Cell proliferation was assessed by CTFR dilution by flow cytometry after 4 days. b. A2.DR1 T cells were treated as in a and transduced with CICR215W reactive CT2. c. Quantification of b. d. Normalized IFN γ production of expanded CT2 TCR-transduced T cells incubated with 20 μ g/ml α PD-1 and α CTLA-4 or isotypes and re-stimulated with CICR215W 27-mer peptide. c, d. Data are represented as mean \pm SEM. Statistical significance was determined by two-tailed student's t tests. a. Experiment was performed together with Khwab Sanghvi, DKTK Clinical Cooperation Unit Neuroimmunology and Brain Tumor Immunology, German Cancer Research Center (DKFZ), Heidelberg, Germany. ICB, immune checkpoint blockade; ISO, isotype.

3.1.8 Intraventricular adoptive transfer of anti-CICR215W TCR-transduced T cells leads to delayed tumor growth

As described before, locoregional injection of transgenic CAR-T cells has been shown to be superior to systemic intraventricular injection^{128,129}. Therefore, CT2 and control (Flu) transduced T cells were stereotactically injected into the contralateral ventricle of CicR215W A2.DR1 glioma-bearing mice as shown in Figure 15a. Two doses of CT2 transgenic T cells increased median survival from 29 days (Flu) to 33 days (Figure 15b). No neurological symptoms could be observed, suggesting that TCR transduced T cells did not lead to neurotoxicity due to off-target effects. Treatment with CT2 also had a slight but not significant effect on tumor volume (Figure 15c). Endpoint analysis of tumor and control tissue by flow cytometry demonstrated a high prevalence of TCR-transduced T cells in the tumor and the contralateral hemisphere, but no enrichment of transgenic T cells in the cervical lymph nodes (Figure 15c). This leads to the assumption that intracranially injected T cells do not traffic back through lymphatic vessels and are restricted to the CNS.

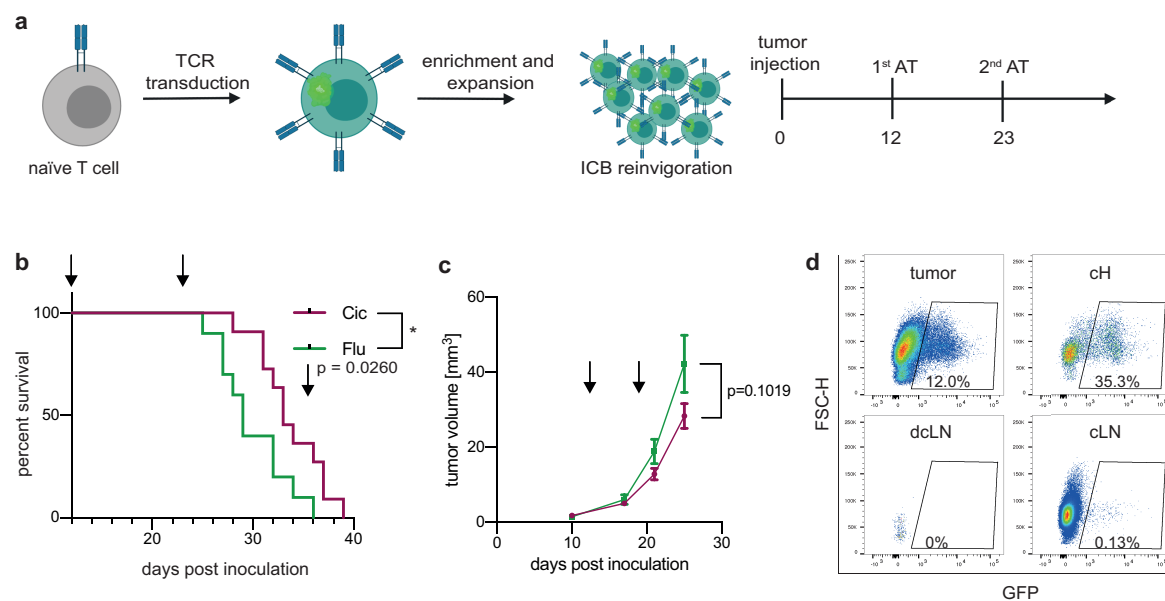


Figure 15: Adoptive transfer of α -CICR215W-TCR T cells targeting CicR215W mutated A2.DR1 gliomas. a. Experimental overview. Activated T cells were transduced with the CICR215W reactive TCR CT2 or Flu TCR, enriched for GFP expression and subsequently expanded with α CD3/ α CD28 antibodies for 5 days. After reinvigoration with 20 μ g/ml α PD-1 and α CTLA-4, T cells were adoptively transferred (AT) into the contralateral ventricle of A2.DR1 CicR215W glioma bearing mice. b. Kaplan-Meier curve of A2.DR1 glioma-bearing mice treated with 2 intraventricular adoptive transfers of α -CICR215W-TCR CT2 T cells and α -Flu-TCR T cells. $n = 10$ for Flu and $n = 11$ for CIC. Statistical significance was determined by log-rank Mantel-Cox test. c. Tumor volumes of mice from b measured by MRI. d. Representative GFP expression in CD3⁺ T cells isolated from tumor, contralateral hemisphere (cH), cervical lymph node (cLN) or deep cervical lymph node (dcLN) of A2.DR1 CicR215W glioma-bearing mice adoptively transferred with CT2 α -CICR215W TCR-transduced T cells. Experiment was performed with the help of Mirco Friedrich, DKTK Clinical Cooperation Unit Neuroimmunology and Brain Tumor Immunology, German Cancer Research Center (DKFZ), Heidelberg, Germany

3.1.9 Detection of CICR215W-mutated patient tissue

The detection of CICR215W-mutated patients is not yet established in clinical routine. Therefore, a mutation-specific PCR was developed, using the rhAmp SNP Genotyping System and a dual reporter approach. In a cohort of 45 patients, the PCR detected 4 patients as clearly CICR215W-mutated (Figure 16a). For 2 out of 4 patients, this point mutation was verified by panel sequencing. In a second approach, mice were vaccinated with a CICR215W 10-mer and serum was tested against lysate from A2.DR1 glioma-overexpressing CicWT or CicR215W (Figure 16b). In three murine sera, a mutation specific band could be detected. B cells from respective mice were then transformed into hybridomas and will be tested for potentially mutation-specific antibody-expressing clones.

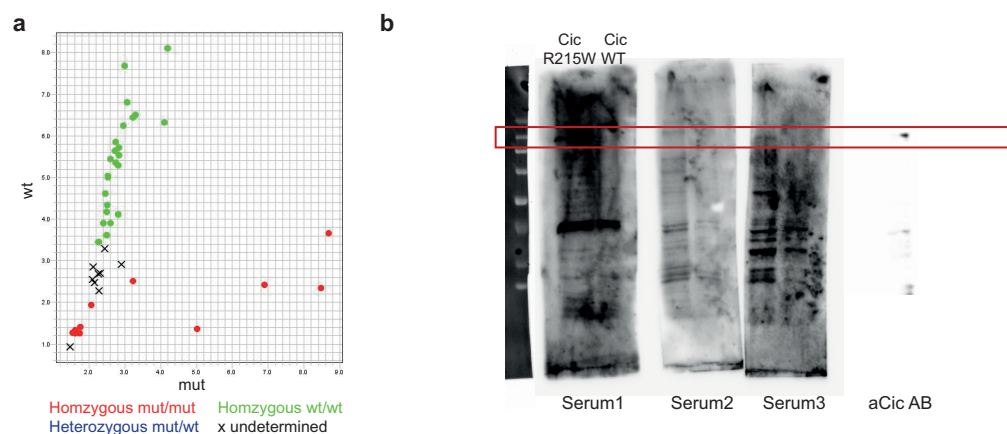


Figure 16: Establishment of a mutation-specific PCR and development of a mutation-specific antibody. a. Allelic discrimination plot of $n = 45$ oligodendroglioma patients after mutation specific PCR. b. Western blot with serum of CicR215W vaccinated mice or an α CIC antibody against lysate from A2.DR1 glioma overexpressing CicWT or CicR215W. Vaccination of mice was performed together with the Antibody Unit of the Genomics and Proteomics Core Facility DKFZ.

To this point, it was shown that MHC class II-restricted (neo-)epitopes can elicit profound anti-tumor responses. However, the exact mechanisms how MHC class II-restricted epitopes drive these effects are still elusive, as well as the relevant antigen-presenting cellular subset. To shed light on the mechanisms involved in MHC class II-induced immune responses in brain tumor immunity, a newly developed mouse model was used.

3.2 Relevance of MHC class II antigen presentation in the glioma tumor microenvironment

3.2.1 Macrophages induce an MHC class II dependent CD4⁺ T cell activation

In order to elucidate the role of MHC class II in brain tumors, we used a MHCII^{flox/flox}-mouse, crossed to different Cre^{ERT2} promotor lines. As the infiltrating myeloid compartment in brain tumors is mainly composed of monocyte-derived macrophages, we first aimed to show that macrophages can be a relevant-antigen presenting immune cell compartment. In bone marrow derived macrophages from Rosa^{CreERT2}-MHCII^{flox/flox} mice MHC class II could efficiently be depleted after tamoxifen treatment. Tamoxifen treatment was most efficient directly after bone marrow isolation and did not affect MHC class II expression on wildtype MHCII^{flox/flox} littermates (Figure 17a). Antigen primed OT-II CD4⁺ T cells showed an antigen-specific Interleukin 2 (IL2) and IFN γ release after co-culture with peptide loaded MHCII WT but not MHCII KO BMDMs (Figure 17b).

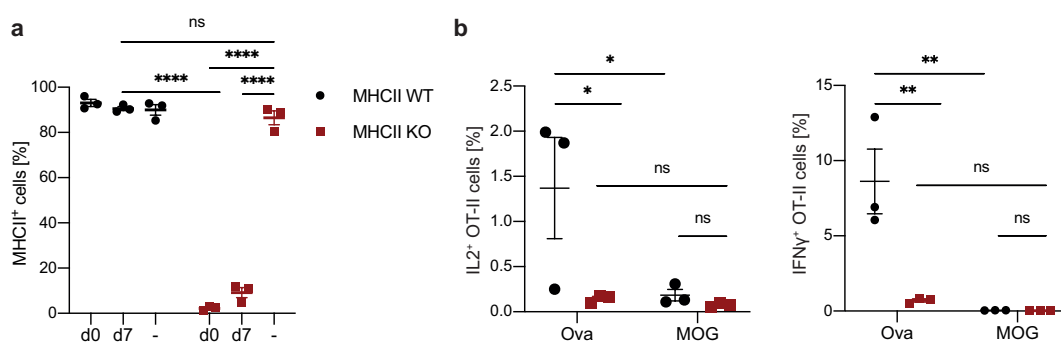


Figure 17: Macrophages activate CD4⁺ T cells antigen-specifically. BMDMs were generated from Rosa^{CreERT2}-MHCII^{flox/flox} mice or MHCII^{flox/flox} littermates, treated with Tamoxifen-OH and co-cultured with CD4⁺ OT-II T cells with the respective peptide. a. MHC class II expression after addition of IFN γ and LPS. BMDMs were treated with tamoxifen from day 0 (before differentiation) or day 7 (after differentiation) on. b. Frequency of IL2 positive OT-II T cells after stimulation with OVA(329-337) or MOG. c. IFN γ positive OT-II T cells after stimulation with OVA(329-337) or MOG. a, b. As determined by flow cytometry. a, b. Statistical significance was assessed by one-way ANOVA with Tukey's multiple comparisons test.

3.2.2 Continuous *in vivo* depletion of MHC class II does not alter myeloid infiltration

Next, the relevance of MHC class II in an *in vivo* tumor setting was investigated. For *in vivo* experiments, the myeloid specific promoter Cx3Cr1 was used to create Cx3Cr1^{CreERT2}-MHCII^{fllox/fllox} mice (MHCII KO). Cx3Cr1 is expressed in all myeloid cells. Dosing of tamoxifen therefore results in a knockout of MHC class II in all myeloid cells. However, monocyte-derived cells are replenished after several weeks. Tissue-resident microglia, in contrast, are long-living cells, that are replaced over time. Continuous dosing of tamoxifen therefore leads to a complete knockout of MHCII in all myeloid cells, whereas a single dose of tamoxifen leads to a microglia specific knockout after several weeks (Figure 18a). Immunofluorescence staining verified the MHC class II knockout in all F4/80-expressing myeloid cells in syngeneic GL261 murine brain tumors, whereas MHCII^{fllox/fllox} littermates (MHCII WT) showed a profound expression of MHC class II in the tumor (Figure 18b, c). Flow cytometric analysis of tumor-infiltrating immune cells showed a specific ablation of MHC class II on different myeloid subsets, but not on B cells or NK cells (Figure 18d). As expected, the MHC class II knockout did not lead to changes in myeloid, B or NK cell frequencies in the tumor microenvironment (Figure 18e).

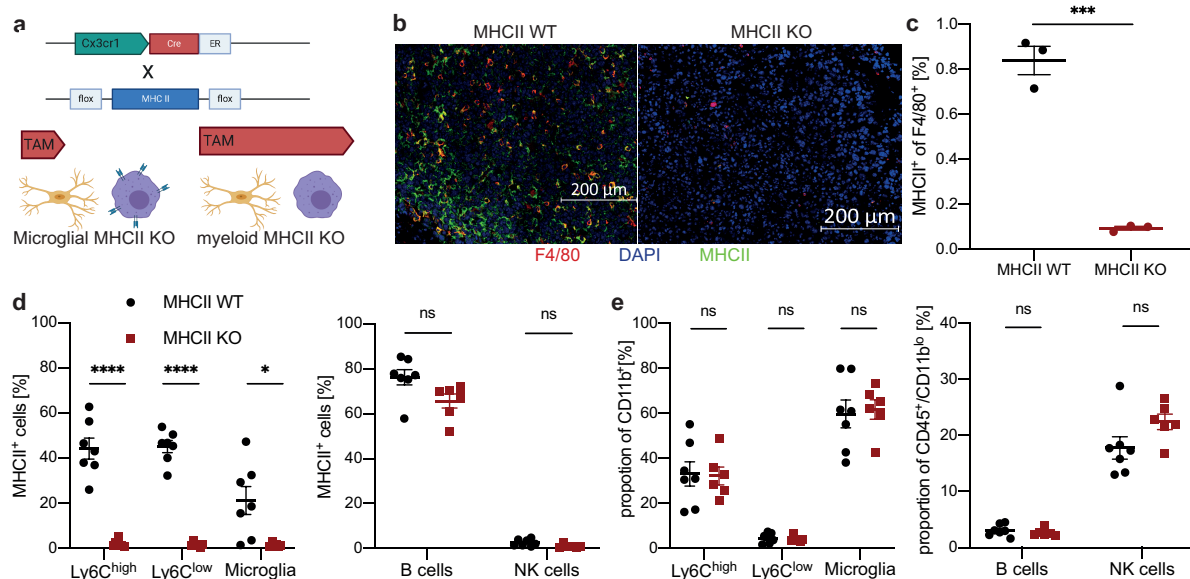


Figure 18: MHC class II is efficiently depleted on myeloid cells and does not alter the intratumoral myeloid cell composition. a Schematic overview of the Cx3Cr1^{CreERT2}-MHCII^{fllox/fllox} genotype. By timed dosages of tamoxifen, a MHCII knockout can either be achieved in all myeloid cells or in tissue resident microglia only. b. Immunofluorescence imaging of GL261 tumors from MHCII KO or WT mice. Green: MHCII, red: F4/80, blue: DAPI. c. Quantification of b. d. MHCII expression on myeloid cells and NK and B cells from GL261 tumors from MHCII KO or WT mice. e. Frequencies of indicated cell populations, gated for living CD45⁺ cells. c-d. Data are represented as mean \pm SEM. Statistical significance was determined by two-tailed student's t tests corrected for multiple testing using the Holm-Šidák method. b, c. Immunofluorescence images were taken and analyzed by Christopher Krämer (CCU Neuroimmunology and Brain Tumor Immunology, DKFZ Heidelberg, Germany).

3.2.3 Depletion of myeloid but not microglial MHC class II leads to a decrease of CD4 T cell abundance and activation

Depletion of MHC class II on all myeloid cells was sufficient to strongly decrease the frequency of tumor-infiltrating CD4⁺ T cells, which in turn leads to a relative increase of CD8⁺ T cells (Figure 19a). An effect on CD8⁺ T cell activation could not be observed, however, CD4⁺ T cells showed a mild, but not significant increase in programmed-death ligand 1 (PD-1) expression and a strong decrease in proliferation measured by Ki67 staining (Figure 19b). In contrast to these observations, a microglia-specific knockout of MHC class II achieved by single dosing of tamoxifen did not lead to alterations in T cell frequencies or CD4⁺ T cell activation (Figure 19c, d). Collectively, this data suggests that CD4⁺ T cells are being activated and proliferate in the tumor microenvironment via interaction with the antigen-MHCII-complex on monocyte-derived myeloid cells.

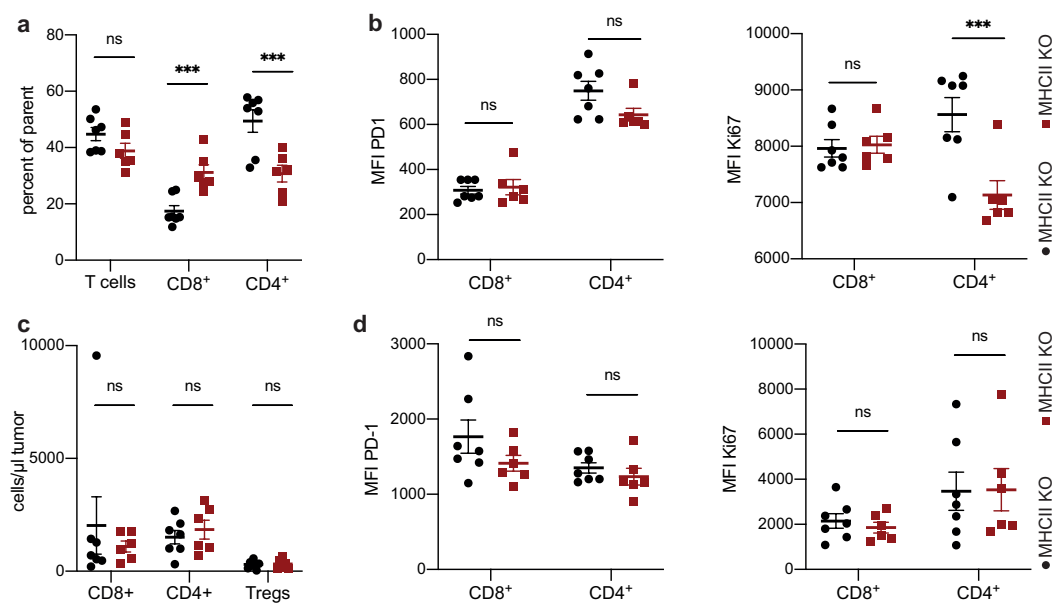


Figure 19: Depletion of MHC class II leads to a decrease of intratumoral CD4⁺ T cell abundance. CD45⁺ CD3⁺ T cells from GL261 tumors from MHCII KO or WT mice were analyzed by flow cytometry. a, b. Continuous tamoxifen application. a. Frequencies of intratumoral T cell populations. b. Median expression of the exhaustion marker PD-1 and the proliferation marker Ki67 on T cells. c, d. Single tamoxifen doses 6 weeks before tumor inoculation. c. Frequencies of intratumoral T cell populations. d. Median expression of the exhaustion marker PD-1 and the proliferation marker Ki67 on T cells. a-d. Data are represented as mean \pm SEM. Statistical significance was determined by two-tailed student's t tests and corrected for multiple testing using the Holm-Šidák method. Experiment was performed together with Christopher Krämer.

3.2.4 Myeloid but not microglial MHC class II is required for response to immune checkpoint blockade

Based on these observations, the relevance of MHC class II expression for immune checkpoint inhibition was assessed. The GL261 tumor model has been shown to respond to immune checkpoint blockade in about 40-60% of all mice^{42,107}. To this end, GL261 tumor-bearing MHCII KO and MHCII WT mice were treated with five doses of combined immune checkpoint blockade composed of PD-1, CTLA-4 and PD-L1-blocking antibodies (ICB). The continuous depletion of MHC class II on all myeloid cells led to a complete abrogation of the effect of ICB. While 33% of all MHCII WT mice in the treatment group showed a decrease of tumor volume after the 2 weeks with 25% long term survivors, none of the MHCII KO mice showed response to ICB and mice performed similar to isotype-treated control mice (Figure 20a, b, c). As expected from previous results, a microglia-specific knockout of MHC class II did not lead to any decrease in response to ICB (Figure 20d, e, f).

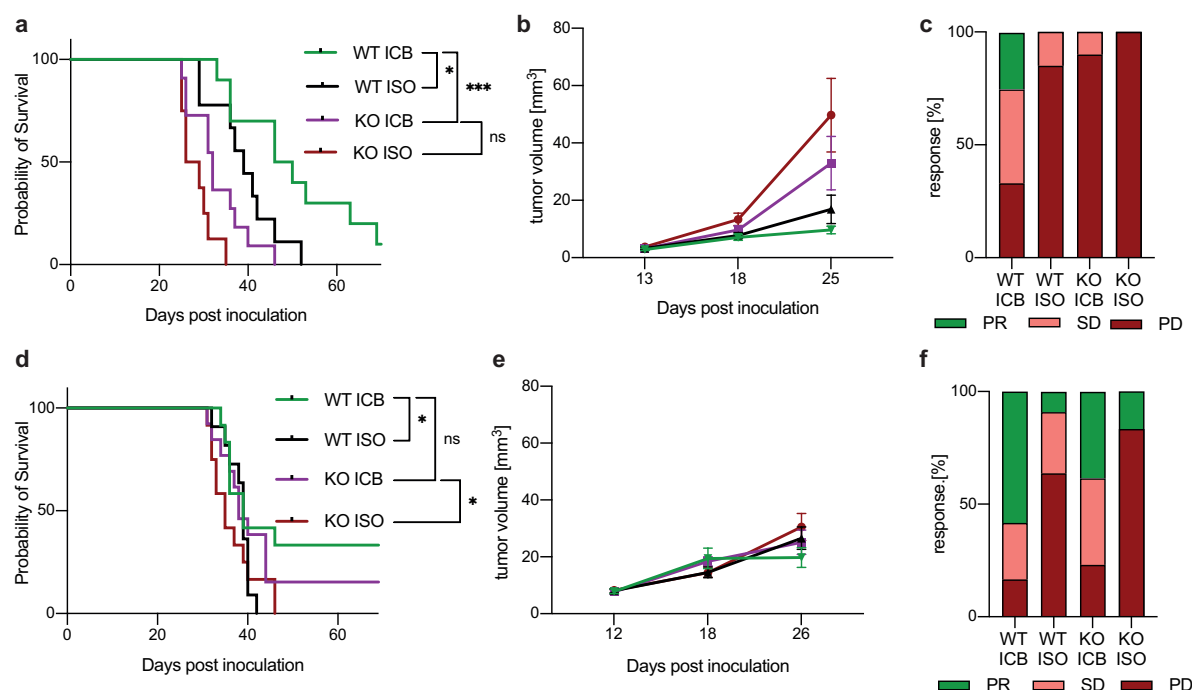


Figure 20: Depletion of MHC class II on myeloid cells leads to abrogation of response to immune checkpoint blockade. MHCII KO and WT littermates were inoculated with GL261 and treated with 250 μ g PD-1, 100 μ g CTLA-4 and 200 μ g aPD-L1 every 3 days for 5 treatments from day 13. a-c. Continuous Tamoxifen application. WT ICB: n = 10, WT ISO n = 9, KO ICB = 11, KO ISO n = 8. d-f. Single tamoxifen doses 6 weeks before tumor inoculation. WT ICB: n = 12, WT ISO n = 11, KO ICB = 13, KO ISO n = 12. a, d. Survival curve Log-rank Mantel-Cox test was used to assess significant differences between survival curves. b, e. Tumor growth curves measured by MRI. Data are represented as mean \pm SEM. c, f. PR partial responder (fold increase tumor volume 2nd to 3rd MRI < 0), SD stable disease (fold increase tumor volume 2nd to 3rd MRI < 0.5), PD progressive disease (fold increase tumor volume 2nd to 3rd MRI > 0.5).

3.2.5 Myeloid MHC class II is required for CD8⁺ T cell response

In order to identify the mechanism that drives loss of response to ICB after MHC class II depletion, the model antigen ovalbumin (OVA) was used, stably overexpressed in GL261. Ovalbumin harbors a strong MHC class I-restricted epitope that is recognized by CD8⁺ T cells. A minigene approach was used to only express the MHC class I epitope SIINFEKL in GL261. When injected into mice, the tumors were controlled in MHCII WT mice, whereas tumor control was abolished in MHCII KO mice (Figure 21a). As has been observed in GL261 WT tumors, CD8⁺ T cell infiltration was not changed whereas a strong decrease in CD4⁺ T cell infiltration could be observed (Figure 21b, c). Interestingly, no change in (T regulatory cell) Treg infiltration was observed (Figure 21d). The SIINFEKL antigen allows for flow-cytometric detection of tumor-reactive T cells using a dextramer specific for H2-Kb SIINFEKL-binding TCRs. Surprisingly, even though SIINFEKL is an immunogenic CD8⁺ T cell antigen, no difference in tumor-reactive T cell infiltration was observed (Figure 21e). This observation was confirmed by re-stimulating TILs with SIINFEKL peptide, where there were no differences in IFN γ production of CD8⁺ T cells (Figure 21f). Using single cell VDJ sequencing of TILs positive or negative for SIINFEKL tetramer confirmed an increase in clonality for both populations in the MHCII KO mice (Figure 21g). These results show that tumor-reactive CD8⁺ T cells home to the tumor site irrespective of MHC class II expression. However, their anti-tumor function seems to be hampered when MHC class II is removed from the myeloid compartment.

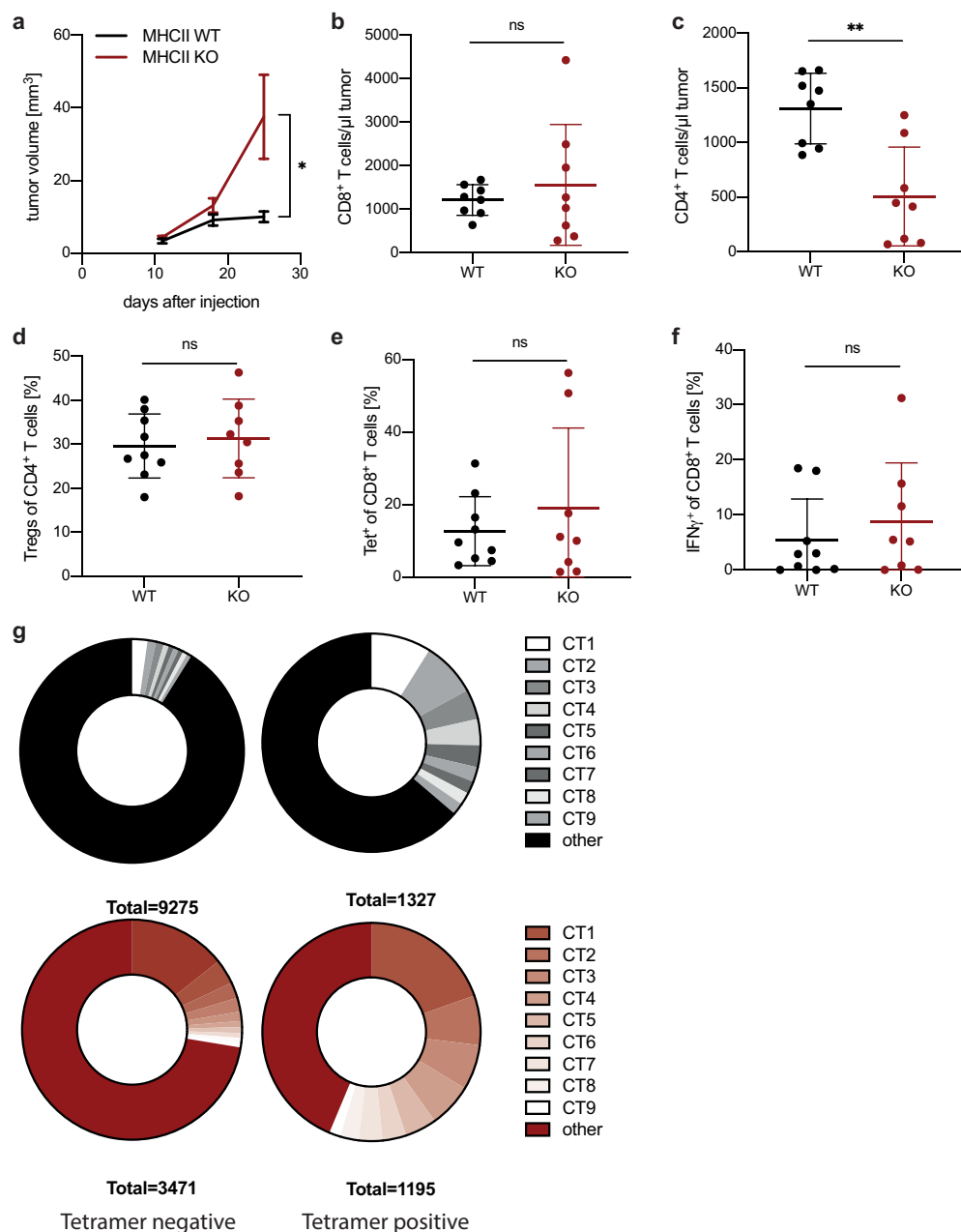


Figure 21: Depletion of MHC class II leads to abrogation of MHC I driven tumor control. a-f GL261 SIINFEKL tumors were orthotopically injected into MHCII KO and WT mice and analyzed by flow cytometry at day 20. n = 8 for each genotype. a. tumor volumes measured by MRI. b, c. Cells/ μ l tumor of indicated CD4⁺, CD3⁺ T cell population. d, e. Foxp3 CD4⁺ or SIINFEKL-dextramer positive cells of CD8⁺ T cells. f. TILs were *ex vivo* stimulated with SIINFEKL or MOG peptide. IFN γ positive CD8⁺ T cells. g. Clonality of the top 9 clones recovered by 10x VDJ single cell sequencing at day 20 after GL261 SIINFEKL tumor inoculation. Pooled from n = 6 (KO) and 8 (WT) mice. a-f Data are represented as mean \pm SEM. Statistical significance was determined by two-tailed student's t tests.

3.2.6 Tumor-reactive T cells are only found in the tumor microenvironment

Using flow cytometric phenotyping of different lymphatic compartments and cell populations, it could be shown that the MHC class II knockout takes place in the spleen, lymph nodes (LN) and tumor in all myeloid compartments in MHCII KO mice (Figure 22a). To identify the relevant compartment for MHC class II restricted antigen presentation, we checked for antigen-reactive T cells in the cervical LN. First, a difference in CD4⁺ or CD8⁺ T cell frequencies could not be observed in the cervical LN (Figure 22b). Second, in contrast to the tumor microenvironment (Figure 21e), no IFN γ producing CD8⁺ T cells could be detected in the cervical lymph nodes (Figure 22c). Using a full OVA-expressing GL261 tumor cell line harboring a well-described MHC class II restricted antigen, there was only minor increase in IFN γ production compared to MOG control, whereas there was a more prominent reactivity in the tumor (Figure 22d). Of note, there was no difference in MHCII WT vs KO mice. Taken together, these results indicate that the relevant MHC class II antigen presentation and T cell activation takes place in the tumor microenvironment.

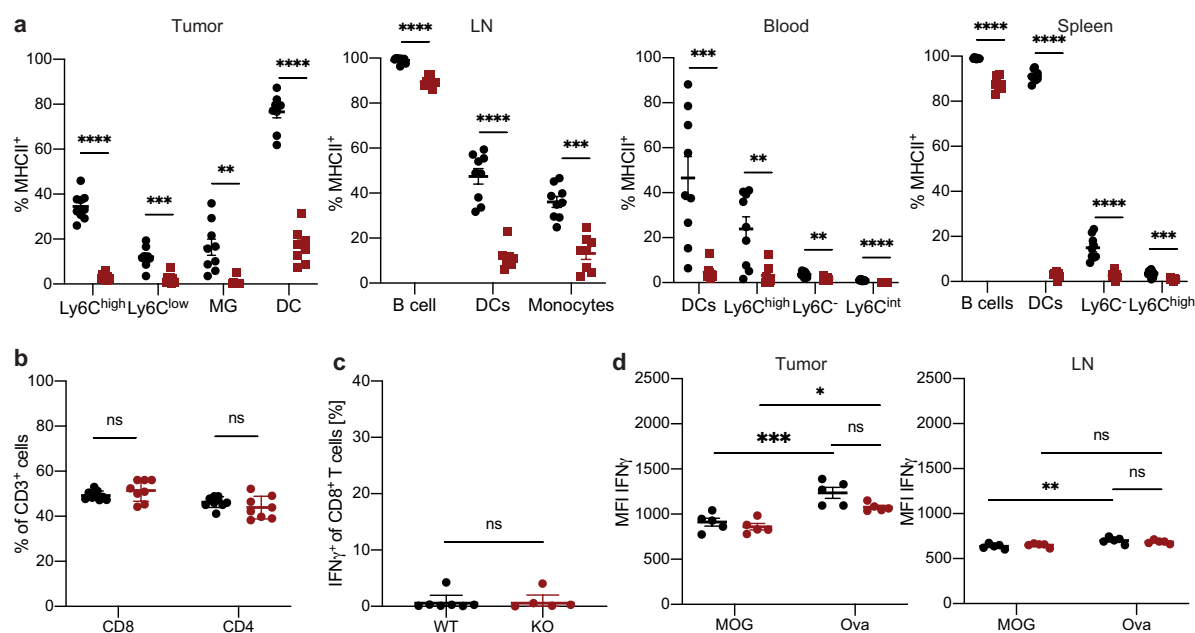


Figure 22: MHC class II is depleted in all lymphatic organs but tumor-reactive T cells are only found in the tumor environment. a-c. GL261 SIINFEKL tumors were analyzed at day 20 after tumor inoculation. a. MHCII positive CD45⁺ cells in tumor, cervical lymph nodes, blood and spleen. b. indicated CD3⁺ T cell population in cervical lymph nodes. c. IFN γ positive CD8⁺ T cells in cervical lymph nodes after *ex vivo* re-stimulation with SIINFEKL or MOG peptide. d. CD45⁺, CD3⁺, CD4⁺ T cells from GL261 OVA tumors or cervical lymph nodes were isolated at day 20 after tumor inoculation and *ex vivo* stimulated with OVA(323-339) or MOG. IFN γ positive CD4⁺ T cells. a-d. Analyzed by flow cytometry. Data are represented as mean \pm SEM. a-c. Statistical significance was determined by two-tailed student's t tests and corrected for multiple testing using the Holm-Šidák method. d. Statistical significance was assessed by one-way ANOVA with Tukey's multiple comparisons test.

3.2.7 MHC class II expression shapes immune cell infiltration in experimental gliomas

In an attempt to decipher how the MHCII KO shapes the tumor microenvironment and abolishes CD8⁺ T cell immune responses, single cell transcriptomic analysis of tumor infiltrating immune cells of SIINFEKL-expressing GL261 tumors was performed. As described, tumor-reactive CD8⁺ T cells could be detected by tetramer staining. Specificity of the tetramer stain was confirmed as all tetramer positive T cells were positive for CD8⁺ (Figure 23a). As expected, single cell analysis of all recovered cells showed the two dominating clusters to be lymphocytes and myeloid cells (Figure 23b). The MHC class II knockout led to altered immune cell abundances in some clusters, e.g. T cells (cluster 0, 1) and macrophages and microglia (cluster 2, 3) (Figure 23c).

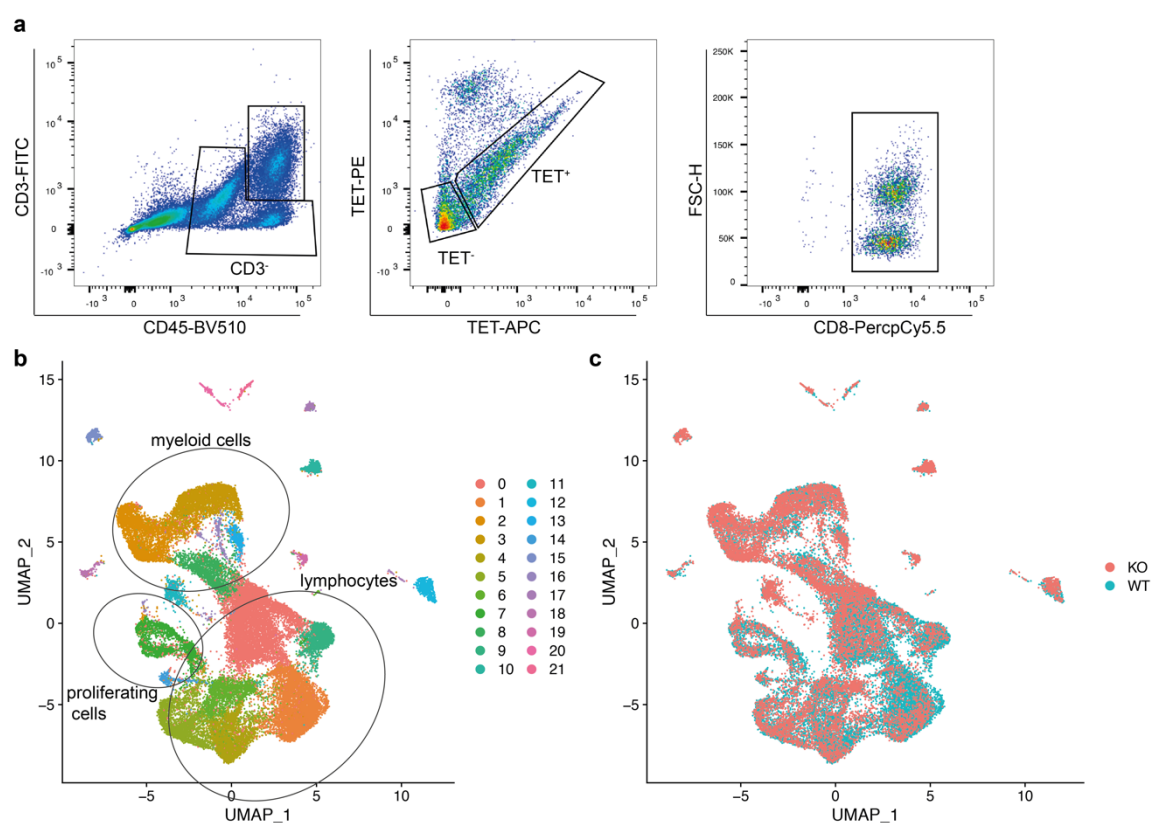


Figure 23: Single cell sequencing of tumor infiltrating immune cells. GL261 SIINFEKL tumors were isolated 20 days after tumor inoculation and sorted for CD45⁺, CD3⁻/CD3⁺/Tetramer⁺ cells. a. gating strategy. b. Single cell transcriptomic data was obtained using the 10x technology and analyzed using the Seurat package. Color coded K-means clustering. Myeloid cells, T cells and proliferating cells are marked as dominant clusters. c. UMAP of single cells split by genotype.

3.2.8 MHC class II expression alters the phenotype of tumor infiltrating myeloid cells

More detailed analysis of the myeloid compartment revealed that in MHCII WT mice, the myeloid compartment is dominantly composed of monocyte-derived macrophages whereas the dominant cell type in MHC KO mice is the microglia cluster. As shown before, there was no difference in DC or NK cell abundance in the tumor microenvironment (Figure 24a). Applying an antigen presentation signature or homeostatic signature showed a clear decrease of antigen presentation and strong increase in homeostasis in MHCII KO mice (Figure 24b)¹⁶⁸. As the monocyte-derived macrophage cluster (1) was significantly enriched in MHCII WT mice, differential gene expression analysis of cluster (1) was performed. 239 genes were significantly differentially expressed between MHCII KO and WT mice (Figure 24c). Interestingly, the T cell-attracting chemokines Cxcl9 and Ccl5 were overexpressed in MHCII WT mice, suggesting a T cell-attracting microenvironment in tumors with an intact MHC class II⁺ myeloid compartment (Figure 24d).

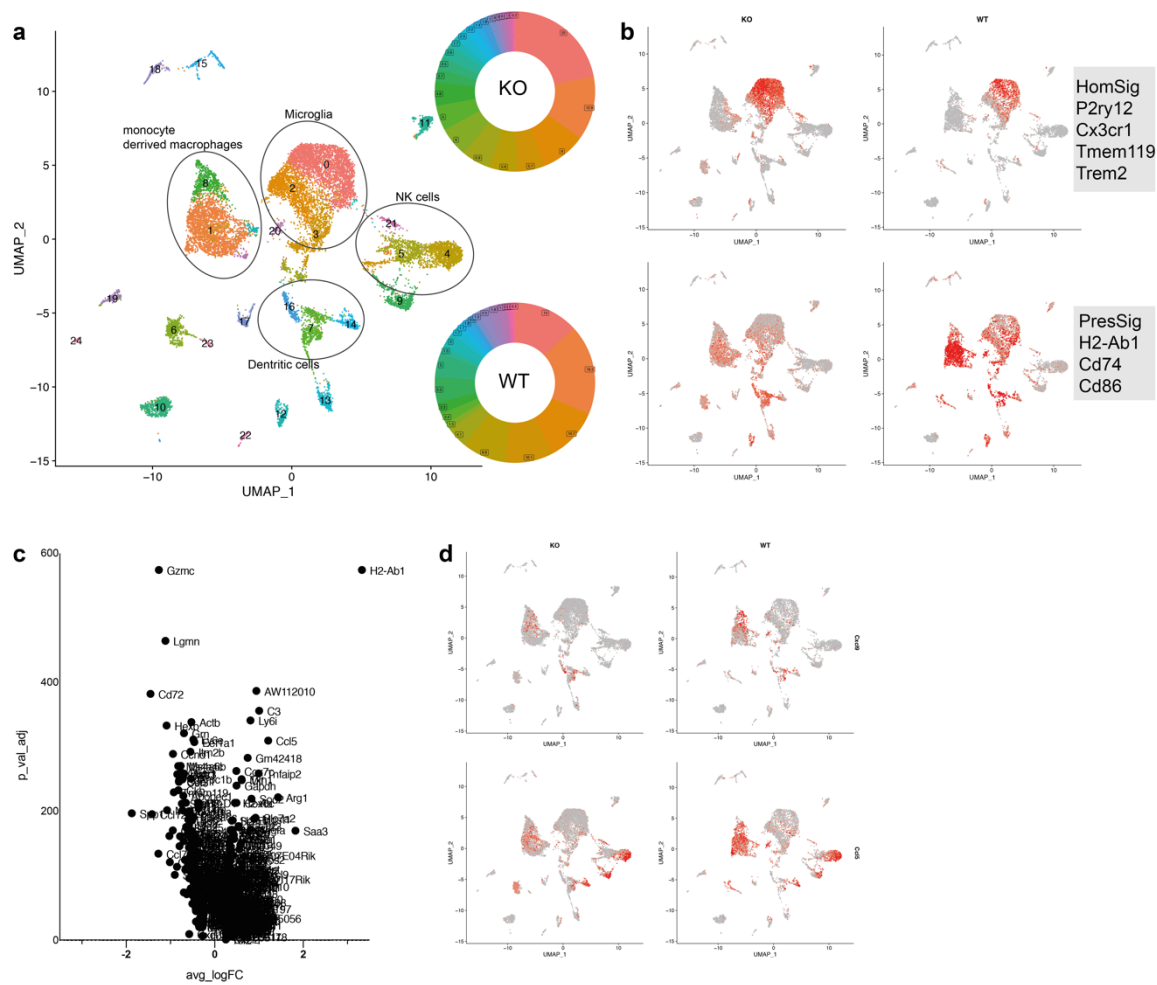


Figure 24: MHC class II knockout leads to an altered abundance and activation state of tumor-associated myeloid cells. a UMAP and cluster proportions of CD3⁺ cells recovered after single cell sequencing. b. Feature plot of combined signature genes. HomSig: Homeostatic signature, PresSig: Antigen-presenting signature c. Differential gene expression of cluster 1 using the MAST algorithm, positive values are overexpressed in MHCII WT mice. c. Feature plot of expression values of Cxcl9 and Ccl5 for MHCII KO and WT mice.

3.2.9 Myeloid MHC class II expression shapes CD4⁺ T cell and bystander CD8⁺ T cell phenotype

In-depth transcriptomic analysis of tumor infiltrating T cells revealed profound differences in the T cell compartment. Using graph-based clustering, 12 different clusters with distinct gene expression patterns were identified (Figure 25a, b). Of note, apart from classical T cells clusters like naïve and activated, proliferating and regulatory T cells, we could also identify S1pr1 as indicator for trafficking T cells, as well as Th17 and $\gamma\delta$ T cells identified by their $\gamma\delta$ TCR V regions (Figure 25b, c). As already validated before, the MHC class II knockout led to a strong decrease of activated T cells in the tumor microenvironment, demonstrated by a decrease of 50% of Lag3⁺ and Cxcr6⁺ CD4⁺ T cells (Figure 25a, c). Of note, there was no difference in the abundance of S1pr1-expressing T cells, identifying recently infiltrated T cells. This leads to the assumption that the increased chemokine expression on myeloid cells (Figure 24c) does not necessarily lead to a differential infiltration of T cells into the tumor.

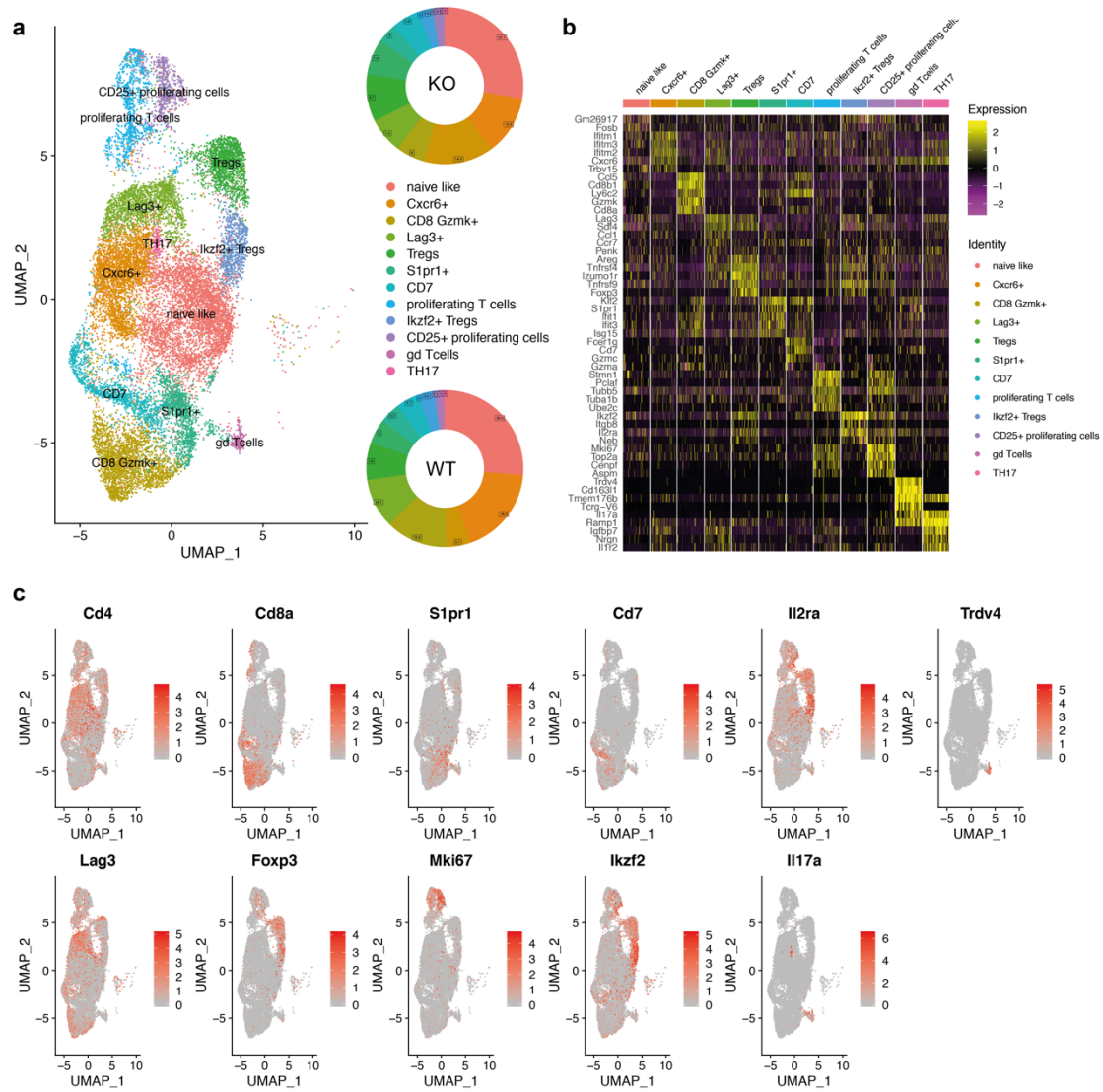


Figure 25: Depletion of MHC class II abrogates the presence of activated CD4⁺ T cells in the tumor microenvironment. a UMAP and cluster proportions of CD3⁺ T cells recovered after single cell sequencing and analyzed using the Seurat R package. Clusters were annotated using canonical marker expression. b. Heatmap showing the top 5 differentially expressed genes for each cluster. c. Feature plots for top differentially expressed genes defining cell clusters in a.

3.2.10 Myeloid MHCII expression shapes tumor-reactive CD8⁺ T cell phenotype

As we have observed abrogation in tumor control even for tumors expressing strong MHC class I epitopes recognized by CD8⁺ T cells, we analyzed tumor-reactive CD8⁺ tetramer positive T cells from SIINFEKL expressing GL261 tumors. Six clusters of tumor-reactive T cells were detected with an enrichment for cluster 0 in MHCII WT and cluster 1 in MHCII KO mice. (Figure 26a, b). Comparison between MHCII WT and KO mice revealed that tumor-reactive CD8⁺ T cells are characterized by an increased expression of exhaustion markers like CD39 (Entpd1)^{169,170}, PD-1 (Pdc1), Lag3 and Tigit^{171,172}. Of note, the terminal exhaustion marker Tim-3 (Havcr2)⁸¹ and the recently discovered transcription factor Tox, which was described to promote T cell exhaustion¹⁷³, were upregulated in the MHCII KO mice (Figure 26c, e). In contrast, looking at different activation markers, only granzyme A expression was downregulated in MHCII KO mice (Figure 26d, e). Differential gene expression analysis also showed the expression for Tpt1 and Tmsb10 to be upregulated in MHCII WT mice, the former being relevant for T cell homeostasis and proliferation¹⁷⁴, the latter being described as a proliferation marker¹⁷⁵ (Figure 26e). Applying an exhaustion signature, composed of Pd-1, Tigit, Tim3, Lag3, Ctla-4, Tox and 4-1BB to all different clusters showed an upregulation in all MHCII KO T cells and increased expression in MHCII KO enriched clusters (1 and 7) (Figure 26f, g). Strikingly, Tcf1 (Tcf7), which has recently been described to mark progenitor exhausted T cells that can be reinvigorated by immune checkpoint inhibition, was only present in MHCII WT mice (Figure 26h). Upregulation of PD-1 and decreased Ki67 expression was verified on protein level using flow cytometry (Figure 26i). These observations suggest that MHC class II on myeloid cells is required for preventing CD8⁺ T cell exhaustion.

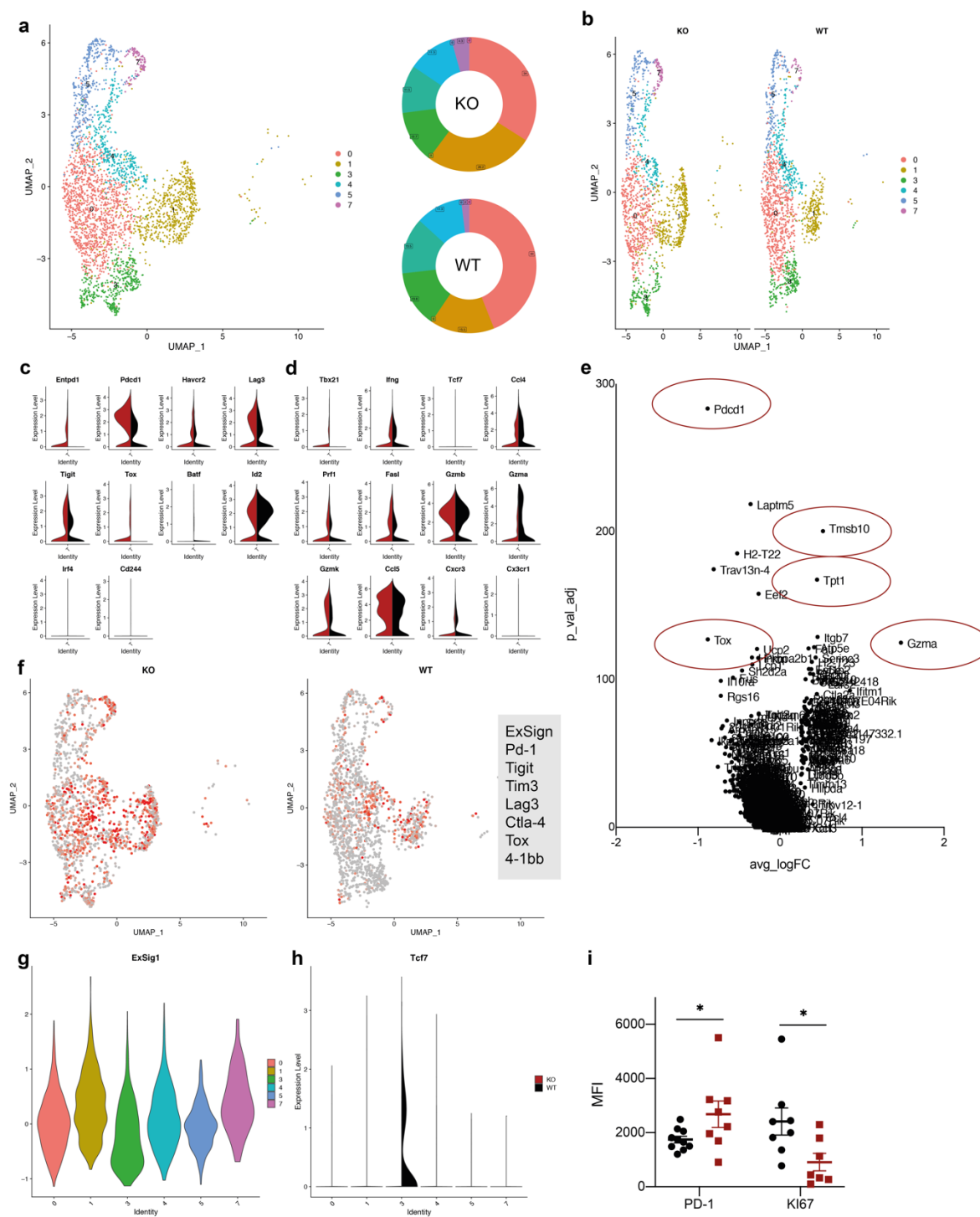


Figure 26 Depletion of MHC class II leads to an exhausted phenotype in tumor-reactive CD8⁺ T cells. a UMAP and cluster proportions of CD3⁺ tetramer⁺ T cells recovered after single cell sequencing and analyzed using the Seurat R package. b. UMAP of single cells splitted by genotype. c. Violin plots of exhaustion marker expression in all tetramer positive T cells. d. Violin plots of activation marker expression in all tetramer positive T cells. e. Differential gene expression of all tetramer positive T cells using the MAST algorithm, positive values are overexpressed in MHCII WT mice. f. Feature plots of a combined exhaustion marker signature. g. Violin plot per cluster of the exhaustion signature defined in f. h. Violin plot for Tcf7 per cluster. i. Median fluorescence intensity of tumor infiltrating tetramer positive CD8⁺ T cells in MHCII WT and KO mice. Data are represented as mean \pm SEM. Statistical significance was determined by a two-tailed student's t test and corrected for multiple testing using the Holm-Šidák method.

3.2.11 Depletion of MHC class II leads to an exhausted CD8⁺ T cell phenotype and diminishes cytotoxic capacity

Given that a myeloid-specific MHC class II knockout leads to a decrease in CD4⁺ T cell activation, we hypothesized that activated CD4⁺ T cells are required to maintain a functional tumor-reactive CD8⁺ T cell population. Therefore, co-culture assays were performed, in which CD8⁺ T cells were antigen-specifically primed with peptide-loaded APCs in the presence or absence of activated CD4⁺ T cells and cytokine production was measured after a resting phase in co-culture experiments. As expected, CD8⁺ T cells primed with activated CD4⁺ T cells showed an increased Granzyme B production compared to being primed with non-activated CD4⁺ T cells (Figure 27a, b). Of note, activating the CD4⁺ T cells in the same well as the CD8⁺ T cells increased Granzyme B expression compared to pre-activating the CD4⁺ T cells before adding them to the CD8⁺ T cells. This suggests that APCs are required to transmit a helping signal from CD4⁺ T cells to CD8⁺ T cells. Adding the supernatant of activated CD4⁺ T cells to CD8⁺ cells did not result in any increase in Granzyme B expression (Figure 27c). Moreover, tumor-infiltrating CD8⁺ T cells sorted from GL261 SIINFEKL tumors showed a 2-fold reduced *ex vivo* killing capacity against GL261 SIINFEKL tumor cells when they were isolated from MHCII KO mice (Figure 27d). Granzyme B expression was also slightly but not significantly reduced (Figure 27e).

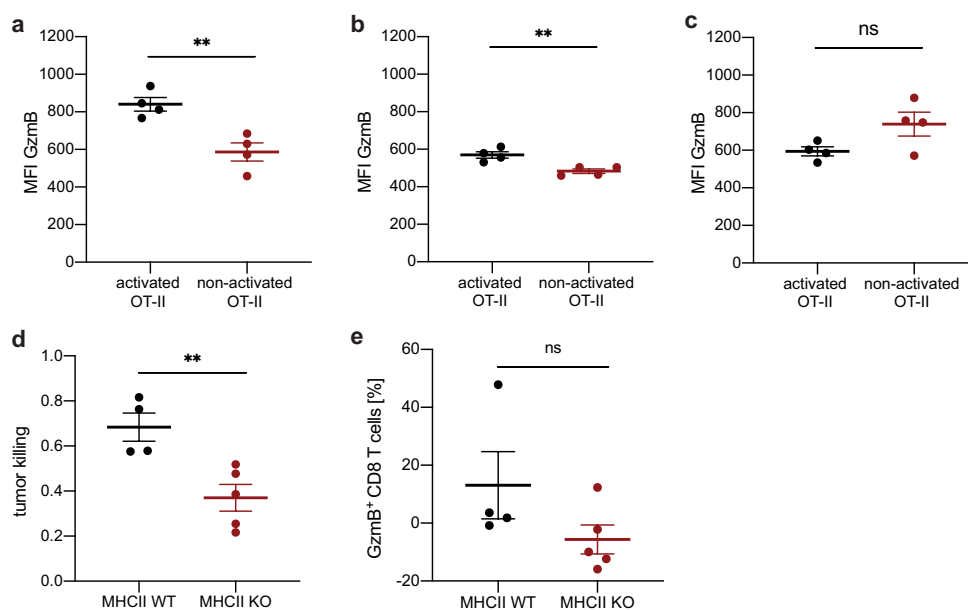


Figure 27: Activated CD4⁺ T cells are required for the formation of functional CD8⁺ T cells. a-c: OT-I CD8⁺ T cells were primed with BMDMs loaded with SIINFEKL peptide in the presence of OT-II CD4⁺ T cells for 48 h. Granzyme B expression was determined after 3 days resting phase after co-culture with GL261 SIINFEKL tumor cells. a. Additionally to SIINFEKL, the OT-II activating peptide OVA(329-337) was added to activate the CD4⁺ T cells. b. OT-II T cells were pre-activated with OVA(329-337) for 2 days before adding them to the OT-I T cells. c. Supernatant from activated OT-II T cells from b was added to the OT-I T cells. d. living CD45⁺, CD3⁺, CD8⁺ T cells were sorted from GL261 SIINFEKL tumors from MHCII KO or WT mice and co-cultured with GL261 SIINFEKL cells for 20 hours. Tumor cell killing was determined via flow cytometric counting of living tumor cells. e. Percent Granzyme B expressing T cells from d. Data are represented as mean \pm SEM. Statistical significance was determined by a two-tailed student's t test.

3.2.12 Late depletion of myeloid MHC class II leads to delayed tumor immune escape

In order to validate whether CD4⁺ T cell help is required only in an early stage of tumor-reactive CD8⁺ T cell activation to prevent exhaustion, late depletion of MHC class II was compared with the previously performed early depletion. Interestingly, depleting MHC class II 11 days after tumor inoculation instead of depleting MHC class II before tumor inoculation did not have an effect on tumor growth in MHCII KO compared to MHCII WT mice (Figure 28 a). Consequently, late MHC class II depletion did not result in any upregulation of the exhaustion marker PD-1 or downregulation of the exhaustion marker Ki67 on tumor-reactive T cells (Figure 28 b, c). This result indicates that MHC class II expression is only needed at an early time point of CD8⁺ T cell activation in order to prevent exhaustion.

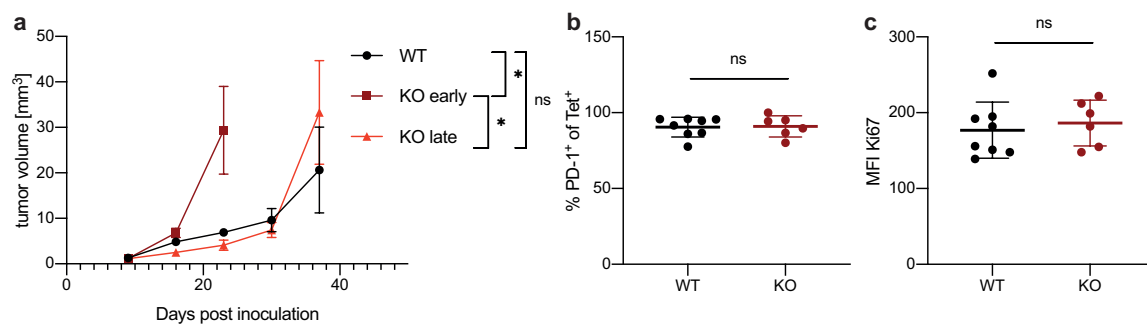


Figure 28: Late depletion of MHC class II does not lead to an exhausted CD8⁺ T cell phenotype. a. Tamoxifen was continuously applied from day -4 (KO early) or day 10 (KO late) on. Tumor volume measured by MRI, statistical significance on day 23 and day 37 was determined by one-way ANOVA with Tukey's multiple comparisons test. b, c: percentage of PD-1 expressing or median fluorescence intensity of CD45⁺, CD3⁺, CD8⁺ tetramer⁺ T cells. Statistical significance was determined by a two-tailed student's t test. a, b, c. Data are represented as mean ± SEM.

4 Discussion

4.1 Identification and therapeutic usage of CIC as a glioma specific antigen

Due to their low mutational load^{52,53}, identification of tumor-specific antigens in brain tumors is still challenging and requires a careful assessment of both the mutational profile as well as the protein levels and epitope presentation capacity on MHC class I and II^{176,177}. Increasing the number of targetable antigens can be achieved by extending the screened epitopes to glioma-associated and cancer-testis antigens that are not specific but highly expressed in tumor tissue¹⁷⁸. However, due to the lack of specificity to the tumor cells, raising an immune response against these targets harbors the risk of off-target toxicity. Nonetheless, clinical trials have shown response and safety in patients vaccinated with tumor-associated antigens¹⁷⁹. Glioma-associated antigens have also been shown to induce T cell responses in GBM patients in several clinical trials without inducing off-target toxicity^{180,181}. In contrast, neoantigens arise from *de novo* mutations and are mostly not shared between individuals¹⁸². Clinical trials in the melanoma setting have shown feasibility of targeting patient-individual neoantigens using vaccination strategies¹⁸³. Recently, two clinical trials also showed durable T cell driven immune responses in GBM against individual neoantigens^{180,184}.

In contrast, targeting shared driver mutations offers the specificity for tumor tissues as well as an off-the-shelf potential¹⁸⁵. In preclinical studies, several driver mutations have shown to be immunogenic and can lead to tumor regression, e.g. IDH1R132H, H3.3K27M and EGVRvIII^{59,152,166,186,187}. EGVRvIII has shown to induce specific antibody responses in GBM patients. However, EGVRvIII vaccination combined with radiochemotherapy failed to show prolongation of overall survival,^{188,189} potentially due to the loss of EGVRvIII in 60% of all recurrent GBMs¹⁹⁰. For the driver mutations in IDH1 and H3.3, for which the loss of mutation is very unlikely, clinical trials using peptide vaccination are currently ongoing¹⁹¹. Following up on this, 70% of 1p19q-co-deleted oligodendrogliomas harbor loss of function mutations in the capicua transcriptional repressor (CIC) gene¹⁹²⁻¹⁹⁴. The mutation at position 215 that was investigated in this thesis is prevalent in 5-10% of all oligodendrogliomas. CIC was shown to act as a tumor suppressor gene and low expression levels or loss of function in 1p19q co-deleted is correlated with poorer prognosis^{195,196}. This driver-mutation-like characterization renders CIC-derived neo-epitopes a suitable target for mutation-specific immunotherapy. In this thesis, it could be shown that point mutations at position 215 can induce DRB1.01-restricted immune responses in HLA-humanized A2.DR1 mice. Interestingly, both IDH1 and H3.3 point mutations have also been shown to raise MHC class II-restricted neoepitopes^{161,166}.

As described, targeting tumoral neoantigens is mostly achieved by vaccination with peptides, tumor lysate or, recently, RNA¹⁹⁷. However, with the discovery of T cell receptors targeting these antigens

and the development of new cloning and delivery strategies, transgenic T cell therapy has received increasing interest in targeting tumor-specific neoantigens. The identification of human tumor-specific TCRs without prior knowledge of the epitope, however, remains challenging. In mice, TCR discovery has been achieved by enriching for distinct T cell populations present in the tumor¹⁹⁸. In humans, PD-1 expression has been associated with tumor reactivity¹⁹⁹. Single cell sequencing technologies will further facilitate direct matching of T cell phenotype with TCR clonality and TCR sequences will be readily available. For known antigens, like CICR215W, Ali *et al.* have shown that neoantigen-reactive TCRs can be obtained from healthy donors²⁰⁰. This method might also be applied for CICR215W.

4.2 Using T cell receptor-transgenic T cells for the treatment of glioma

In this thesis, it was shown that transgenic T cell therapy can lead to a deceleration of tumor growth in a very aggressive brain tumor model. Cellular therapies have received emerging interest in recent years with more and more clinical trials being conducted^{201,202}. However, to date, approved T cell therapies are limited to CAR T cell therapies for non-solid tumors²⁰³. Interestingly, evaluation of CNS fluids of patients receiving CD19 CAR T cell therapy showed that systemically administered CAR T cells were able to traffic to the CNS²⁰⁴. Several phase I clinical trials are investigating CAR T cell therapy in brain tumors against EGFRvIII, HER2 and IL13R α 2²⁰⁵. However, in contrast to T cell receptor transgenic T cells, CAR T cells are limited to surface receptors that are often tumor associated but not tumor-specific, which harbors a high risk of neurotoxicity^{121,206}. In fact, CD19 CAR T cell therapy leads to neurotoxic effects in approximately 20-30% of all patients^{205,207}. In gliomas, preclinical studies and case reports of single patients have shown efficacy in murine and human brain tumors¹²⁸⁻¹³⁰. The preclinical studies could not observe any neurological symptoms due to neurotoxicity. However, in contrast to the therapeutic setting used in this thesis, preclinical studies were only conducted in immunodeficient NSG mice using human tumor cell lines and human neoantigens, making conclusions in this regard difficult. As this thesis used a fully immunocompetent mouse model and a fully murine protein overexpressing cell line, it is reasonable to conclude that targeting mutant CIC does not lead to neurotoxicity. Furthermore, in this thesis, a syngeneic tumor model was developed, resembling the generally low mutational load of brain tumors and making it advantageous to syngeneic, chemically-induced hypermutated brain tumor mouse models like GL261¹⁰⁷. Its aggressive growth makes it a suitable model for comparable aggressive human tumors such as GBM, as well. Nonetheless, cell lines are a very artificial model and tumor injection itself is an immunologic event disrupting the blood brain barrier. De novo generation of brain tumors for treatment cohorts is a suitable alternative to cell lines. For several

entities, methods have been developed to *de novo* induce brain tumors in immunocompetent mice^{156,208–211}. In particular, models overexpressing genetic drivers like H3.3K27M and C11orf95-RELA fusions could be used for immunotherapeutic studies^{210,212}.

TCR transgenic T cell therapy trials targeting cancer-testis antigens have shown clinical responses against solid tumors like melanoma^{90,213,214}. However, clinical studies investigating TCR transgenic therapy in a brain tumor setting are lacking so far. Identification of TCRs recognizing glioma-associated antigens will probably open the possibility to investigate the therapeutic relevance of adoptive transfer of TCR transgenic T cells. Chheda *et al.* have provided the first study identifying a TCR against the shared driver mutation H3.3K27M¹⁸⁷. Their method of identifying high affinity TCRs from healthy donor PBMCs could also be applicable for the CICR215W mutation. However, as described above, Chheda *et al.* identified an MHC class I restricted neopeptide tested in immunodeficient mice which is not applicable for MHC class II restricted antigens like CICR215W. In summary, this thesis provides a translational platform for the identification of neoantigen recognizing TCRs and the preclinical testing in a fully immunocompetent MHC-humanized mouse model.

4.3 Enhancing T cell therapy for glioma

As shown in this thesis adoptive T cell transfer of TCR transgenic T cells still has its limitations and only a limited preclinical effect on tumor growth has been observed. In contrast to other studies²¹⁵, preclinical effects of an MHC class II epitope were investigated. CD4⁺ T cell-mediated immune responses are believed to not directly lead to an anti-tumor effect that is observed for CD8⁺ T cells that directly lyse tumor cells but are believed to act through a rather indirect mechanism of cytokine release and cytolytic T cell activation²¹⁶. Therefore, in contrast to studies using immunodeficient mice^{128,129}, a fully immunocompetent mouse model is necessary to study CD4⁺ T cell immune responses. Preclinical mouse models have shown durable responses to ICB in an CD4⁺ T cell-dependent manner^{42,107}. Combining adoptive transfer with systemic ICB has shown clinical and preclinical anti-tumor synergisms^{217–219}. In this thesis, reinvigoration with ICB has been used to enhance T cell responses of the adoptively transferred T cells. However, a systemic treatment of ICB is believed to also target endogenous tumor-reactive T cells, which rely on a high mutational load and high antigen presentation capacity. Application of ICB could enhance efficacy of CICR215W reactive T cell adoptive transfer by inducing an endogenous CD8⁺ T cell response that could be augmented by transferred CD4⁺ T cells.

T cell therapies are usually accompanied by high dose IL2 and lymphodepletion to establish a peripheral niche which is suitable for T cell proliferation and persistence^{116,220}. However, as in this

thesis, a local administration was performed and as only neglectable numbers of transferred T cells in the lymphatic periphery were detected, we refrained from using additional stimuli that would mostly target peripheral T cells.

As described, the A2.DR1 glioma tumor model only harbors very few mutations, reassembling the mutational landscape of brain tumors^{52,53}. This fact may lead to the assumption that only few neoepitopes are generated that can lead to relevant cytolytic anti-tumor activity. Additionally, the observation that the cell line is MHC class II negative further decreases relevant antigen presentation in the tumor microenvironment. Increasing the intratumoral antigen presentation in the TME could be achieved by inducing unspecific cell death²²¹. Radiation has shown to induce immunogenic cell death leading to the release of MHC class I and II restricted antigens^{222–224}. The synergistic therapeutic effect of the combination of ICB with irradiation is also partly explained by this phenomenon^{225,226}. Adoptive T cell transfer of cytolytic CD8⁺ T cells has also been shown to benefit from irradiation²²⁷. Therefore, adoptive transfer of T cells targeting MHC class II epitopes would certainly benefit from combination with local therapeutic irradiation.

4.4 Relevant cell type for MHC class II antigen presentation

For many years, MHC class I restricted antigens recognized by CD8⁺ T cells have been thought to be the main driver of antigen-specific immune responses. However, recently, it could be shown in preclinical melanoma models that MHC class II restricted neoantigens can be the main driver of T cell mediated tumor regression²²⁸. The exact mechanisms and relevant cell compartments for MHC class II restricted antigen presentation are still largely unknown. In this thesis, it could be shown that the MHC class II presentation on tumor infiltrating macrophages is a relevant part in glioma immune responses. Tumor-associated macrophages are usually seen as immunosuppressive, especially in the context of brain tumors where they accumulate in high grade tumors^{31,39}. Furthermore, macrophages are a major source of immunosuppressive factors like PD-L1, IL10 and TGF β in the tumor microenvironment^{50,106}. However, the antigen presenting capacity of macrophages has recently been appreciated²²⁹. Triggering antigen presentation by macrophages via Toll-like receptors (TLR) agonists has been shown to overcome tumor resistance to immunotherapy and adoptive transfer²³⁰. These and our results question the recent efforts of therapeutic depletion of tumor-infiltrating macrophages using CSF1R inhibitors²³¹.

As described above, in brain tumors, macrophages are derived by two distinct lineages. Several studies report conflicting data concerning which cell type represents the majority of myeloid cells^{232,233}. In the present thesis it could be shown that the relevant antigen-presenting cell type consists of monocyte-derived macrophages rather than tissue-resident microglia. MHC class II

depletion on tumor-associated microglia did not lead to any differences in response to ICB or in abundance or activation of tumor infiltrating CD4⁺ or CD8⁺ T cells. This is in line with studies in experimental autoimmune encephalomyelitis (EAE) where it was shown that MHC class II on microglia is dispensable for disease onset²³⁴. Other studies have shown microglia to represent the effector arm. However, these effects have been observed irrespective of antigen-presentation in immunodeficient mice²³³.

The relevant localization of MHC class II antigen presentation still needs to be defined. Several studies have shown that there is lymphatic drainage from the brain^{16,25,26}. A recent study reported tumor-reactive T cells in the deep cervical lymph nodes in the GL261 tumor model²⁷. However, using the model antigen OVA, we did not detect any tumor-reactive T cells in the periphery, neither CD4⁺ nor CD8⁺ T cells, which leads to the conclusion that in our model system, the relevant epitope presentation and T cell proliferation takes place in the tumor microenvironment, which is also strengthened by the observation that CD4⁺ T cells show Ki67 expression in the tumor microenvironment and that proliferation is diminished by the MHC class II knockout. This question can be further addressed by using a functional antagonist of the S1P1 receptor that blocks egress of T cells from the lymphoid organs²³⁵. Applying this antagonist before induction of the MHC class II knockout would enable us to examine tumor site located T cell proliferation.

4.5 CD4 is help required for CD8⁺ T cell response

In this thesis it could be shown that the depletion of myeloid leads to an abrogation of CD8⁺ T cell responses and an increased exhaustion phenotype.

Several studies have shown before that CD4⁺ T cell help is required for a functional CD8⁺ T cell response^{236–240}. In one study, depleting CD4⁺ T cells leads to a lack of IL21 and to the absence of CD8⁺ T cell populations relevant for lymphocytic choriome-ningitis virus (LCMV) clearance and anti-tumor immunity²⁴⁰. In line with our results, Ahrends *et al.* observed a CD70 and CD27-mediated requirement for CD4⁺ T cell help to generate a functional CD8⁺ T cell population with prolonged anti-tumor effects²³⁹. Tumor-reactive T cells primed in the absence of CD4⁺ help showed upregulation of co-inhibitory molecules like PD-1 and Lag3. Ferris *et al.* have recently shown, that a specific subset of dendritic cells (cDC1) relays CD4⁺ T cell help to cytolytic CD8⁺ T cells in subcutaneous tumors²³⁷. However, our comprehensive single cell analysis did not reveal any relevant abundance of cDC1 cells, leading to the assumption that in brain tumors, MHC class II antigen presentation and CD4 T⁺ cell activation is executed by another cell type. Another study showed differential epigenetic remodeling in CD8⁺ T cells receiving CD4 help or not in a viral setting²³⁸. It will be investigated in the future if this also holds true in a tumor microenvironment.

Recently, the necessity for tumoral MHC class II restricted neoepitopes in CD8⁺ T cell responses has been shown²³⁶. In contrast to our results where a differential abundance of CD8⁺ T cells was not observed, this study shows an abrogation of infiltration of tumor-reactive CD8⁺ T cells when tumors do not co-express MHC class II antigens. In line with other studies mentioned above, the removal of myeloid MHC class II restricted antigen presentation rather led to an exhausted and dysfunctional phenotype of tumor-reactive CD8⁺ T cells. This effect was irrespective of tumoral MHC or tumoral neoepitope expression. Thus, it is tempting to speculate that not a tumoral MHC class II neoantigen is required, but rather an active CD4-myeloid-CD8 crosstalk irrespective of the MHC class II restricted antigen. This question can be addressed by local transfer of *ex vivo* activated CD4⁺ T cells into the tumor site.

The exact mechanisms that drive CD8⁺ T cell exhaustion is not yet fully understood. Using the MHCII KO system, we observed all typical characteristics of T cell exhaustion in the tumor-reactive CD8⁺ T cell population, including diminished *ex vivo* killing capacity and upregulation of co-inhibitory molecules like PD-1, Tim3 and Lag3. Interestingly, the terminal exhaustion marker Tox was also upregulated. Of note, the study describing the relevance of Tox in T cells exhaustion used a tumor model, solely driven by a single CD8 epitope⁷⁹. Although not conclusive, our results offer potential mechanisms that drive T cell exhaustion in the absence of CD4⁺ T cell help. Jansen *et al.* have shown that intratumoral niches that maintain stem-like tumor-reactive T cells are regions with high MHC class II expression⁸⁴. In the myeloid compartment, we have observed a strong expression of Cxcl9 in MHCII WT mice that was completely diminished in MHCII KO mice. Several studies have shown a potent role of Cxcl9 in anti-tumor immunity and Cxcl9 expression is correlated to clinical outcome in solid tumors²⁴¹. In line with our results, House *et al.* reported that macrophage derived Cxcl9 is required for response to ICB²⁴². Chow *et al.* have shown that Cxcl9 acts as a local chemokine in the tumor microenvironment, that recruits CD8⁺ T cells to DCs but does not lead to increased infiltration into the tumor²⁴³. Intratumoral activation by antigen-presenting cells together with co-stimulatory signals could prevent T cell exhaustion in our model. Interestingly, we could not observe any changes in the co-stimulatory machinery in myeloid cells in MHCII KO mice, strengthening the hypothesis that an insufficient trafficking to antigen-presenting cells leads to CD8⁺ T cell dysfunction. Furthermore, we observed decreased abundance of CD40 ligand expressing CD4⁺ T cells in MHCII KO mice. CD40 expression on CD8⁺ T cells has been shown to play a role in the generation of memory CD8⁺ T cells independent of antigen-presenting cells²⁴⁴. CD40 ligand on activated CD4⁺ T cells could therefore directly bind to CD40 on tumor-reactive T cells and impede exhaustion. This hypothesis will be further investigated by applying CD40 antibodies to rescue the effect of MHC class II depletion.

4.6 Conclusion and implication for future therapies

In summary, this thesis describes the relevance of an MHC class II and therefore CD4⁺ T cell-driven immune response. We have shown that the activation of CD4⁺ T cells prevents the exhaustion of CD8⁺ T cells in an early phase of anti-tumor immunity. This leads to several assumptions that should be taken in consideration for future therapies.

First, exploiting CD4⁺ T cell epitopes harbor the potential of being a versatile target for immunotherapy. As shown in the first part of this thesis, targeting MHC class II restricted neoepitopes originating from driver mutations can lead to anti-tumor responses. Second, adoptive transfer of transgenic tumor-reactive T cells would benefit from a spatially close CD4⁺ T cell response, either already established or reinvigorated by ICB in the tumor microenvironment or co-injected together with cytolytic T cells. In CAR T cell studies, co-injecting CD4⁺ and CD8⁺ T cells has been demonstrated to be superior to injecting CD8⁺ T cells alone²⁴⁵. Our results also indicate this necessity for *ex vivo* activation steps, routinely performed for DNA-construct delivery into T cells.

Furthermore, the relevance of intratumoral MHC class II antigen presentation has been demonstrated. Total MHC class II expression in publically available patient datasets, however, is associated with decreased survival but also correlates with tumor grade. Due to the lack of single cell resolution, these datasets can not distinguish between tumoral and myeloid MHC class II²⁴⁶. The results of this thesis suggest that increasing MHC class II presentation in the TME could lead to accelerated immune responses. This is especially relevant for tumors that have been shown to downregulate myeloid cell antigen presentation like IDH1 mutated tumors²⁴⁷ (Friedrich *et al.*, accepted).

5 Literature

1. Ferlay, J., Parkin, D. M. & Steliarova-Foucher, E. Estimates of cancer incidence and mortality in Europe in 2008. *Eur. J. Cancer* (2010) doi:10.1016/j.ejca.2009.12.014.
2. Ostrom, Q. T. *et al.* CBTRUS statistical report: Primary brain and central nervous system tumors diagnosed in the United States in 2007–2011. *Neuro. Oncol.* (2014) doi:10.1093/neuonc/nou223.
3. Louis, D. N. *et al.* *The 2016 WHO classification of tumors of the central nervous system. Acta Neuropathol* (2016).
4. Capper, D. *et al.* DNA methylation-based classification of central nervous system tumours. *Nature* (2018) doi:10.1038/nature26000.
5. Reifenberger, G., Wirsching, H. G., Knobbe-Thomsen, C. B. & Weller, M. Advances in the molecular genetics of gliomas-implications for classification and therapy. *Nature Reviews Clinical Oncology* (2017) doi:10.1038/nrclinonc.2016.204.
6. Gilbert, M. R. *et al.* Dose-dense temozolomide for newly diagnosed glioblastoma: A randomized phase III clinical trial. *J. Clin. Oncol.* (2013) doi:10.1200/JCO.2013.49.6968.
7. Weller, M. *et al.* EANO guidelines on the diagnosis and treatment of diffuse gliomas of adulthood. *Nat. Rev. Clin. Oncol.* (2020) doi:10.1038/s41571-020-00447-z.
8. Wen, P. Y. *et al.* Glioblastoma in adults: A Society for Neuro-Oncology (SNO) and European Society of Neuro-Oncology (EANO) consensus review on current management and future directions. *Neuro-Oncology* (2020) doi:10.1093/neuonc/noaa106.
9. Tirosh, I. & Suvà, M. L. Tackling the Many Facets of Glioblastoma Heterogeneity. *Cell Stem Cell* (2020) doi:10.1016/j.stem.2020.02.005.
10. Neftel, C. *et al.* An Integrative Model of Cellular States, Plasticity, and Genetics for Glioblastoma. *Cell* (2019) doi:10.1016/j.cell.2019.06.024.
11. Patel, A. P. *et al.* Single-cell RNA-seq highlights intratumoral heterogeneity in primary glioblastoma. *Science* (80-.). (2014) doi:10.1126/science.1254257.
12. Frattini, V. *et al.* The integrated landscape of driver genomic alterations in glioblastoma. *Nat. Genet.* (2013) doi:10.1038/ng.2734.
13. Celiku, O., Gilbert, M. R. & Lavi, O. Computational modeling demonstrates that glioblastoma cells can survive spatial environmental challenges through exploratory adaptation. *Nat. Commun.* (2019) doi:10.1038/s41467-019-13726-w.
14. Engelhardt, B., Vajkoczy, P. & Weller, R. O. The movers and shapers in immune privilege of the CNS. *Nature Immunology* (2017) doi:10.1038/ni.3666.
15. Carson, M. J., Doose, J. M., Melchior, B., Schmid, C. D. & Ploix, C. C. CNS immune privilege: Hiding in plain sight. *Immunological Reviews* (2006) doi:10.1111/j.1600-

- 065X.2006.00441.x.
16. Louveau, A., Harris, T. H. & Kipnis, J. Revisiting the Mechanisms of CNS Immune Privilege. *Trends in Immunology* (2015) doi:10.1016/j.it.2015.08.006.
 17. Wang, L. *et al.* Decitabine Enhances Lymphocyte Migration and Function and Synergizes with CTLA-4 Blockade in a Murine Ovarian Cancer Model. *Cancer Immunol Res* **3**, 1030–1041 (2015).
 18. MEDAWAR, P. B. Immunity to homologous grafted skin; the fate of skin homografts. *Br. J. Exp. Pathol.* (1948).
 19. Brabb, T. *et al.* In situ tolerance within the central nervous system as a mechanism for preventing autoimmunity. *J. Exp. Med.* (2000) doi:10.1084/jem.192.6.871.
 20. Brabb, T. *et al.* Triggers of Autoimmune Disease in a Murine TCR-Transgenic Model for Multiple Sclerosis. *J. Immunol.* (1997).
 21. Bechmann, I. *et al.* Immune surveillance of mouse brain perivascular spaces by blood-borne macrophages. *Eur. J. Neurosci.* (2001) doi:10.1046/j.0953-816X.2001.01793.x.
 22. Na, S. Y. *et al.* Naïve CD8 T-cells initiate spontaneous autoimmunity to a sequestered model antigen of the central nervous system. *Brain* (2008) doi:10.1093/brain/awn148.
 23. Ifergan, I. *et al.* Central nervous system recruitment of effector memory CD8+ T lymphocytes during neuroinflammation is dependent on $\alpha 4$ integrin. in *Brain* (2011). doi:10.1093/brain/awr268.
 24. Boztug, K. *et al.* Leukocyte Infiltration, But Not Neurodegeneration, in the CNS of Transgenic Mice with Astrocyte Production of the CXC Chemokine Ligand 10. *J. Immunol.* (2002) doi:10.4049/jimmunol.169.3.1505.
 25. Louveau, A. *et al.* Structural and functional features of central nervous system lymphatic vessels. *Nature* (2015) doi:10.1038/nature14432.
 26. Aspelund, A. *et al.* A dural lymphatic vascular system that drains brain interstitial fluid and macromolecules. *J. Exp. Med.* (2015) doi:10.1084/jem.20142290.
 27. Song, E. *et al.* VEGF-C-driven lymphatic drainage enables immunosurveillance of brain tumours. *Nature* (2020) doi:10.1038/s41586-019-1912-x.
 28. Hu, X. *et al.* Meningeal lymphatic vessels regulate brain tumor drainage and immunity. *Cell Res.* (2020) doi:10.1038/s41422-020-0287-8.
 29. Quail, D. F. & Joyce, J. A. The Microenvironmental Landscape of Brain Tumors. *Cancer Cell* (2017) doi:10.1016/j.ccell.2017.02.009.
 30. Klemm, F. & Joyce, J. A. Microenvironmental regulation of therapeutic response in cancer. *Trends in Cell Biology* (2015) doi:10.1016/j.tcb.2014.11.006.
 31. Hambardzumyan, D., Gutmann, D. H. & Kettenmann, H. The role of microglia and

- macrophages in glioma maintenance and progression. *Nature Neuroscience* (2015) doi:10.1038/nn.4185.
32. Simmons, G. W. *et al.* Neurofibromatosis-1 heterozygosity increases microglia in a spatially and temporally restricted pattern relevant to mouse optic glioma formation and growth. *J. Neuropathol. Exp. Neurol.* (2011) doi:10.1097/NEN.0b013e3182032d37.
 33. Graeber, M. B., Scheithauer, B. W. & Kreutzberg, G. W. Microglia in brain tumors. *GLIA* (2002) doi:10.1002/glia.10147.
 34. Chen, Z. *et al.* Cellular and molecular identity of tumor-associated macrophages in glioblastoma. *Cancer Res.* (2017) doi:10.1158/0008-5472.CAN-16-2310.
 35. Gomez Perdiguero, E. *et al.* Tissue-resident macrophages originate from yolk-sac-derived erythro-myeloid progenitors. *Nature* (2015) doi:10.1038/nature13989.
 36. Ginhoux, F. *et al.* Fate mapping analysis reveals that adult microglia derive from primitive macrophages. *Science (80-.).* (2010) doi:10.1126/science.1194637.
 37. Shi, C. & Pamer, E. G. Monocyte recruitment during infection and inflammation. *Nature Reviews Immunology* (2011) doi:10.1038/nri3070.
 38. Bennett, M. L. *et al.* New tools for studying microglia in the mouse and human CNS. *Proc. Natl. Acad. Sci. U. S. A.* (2016) doi:10.1073/pnas.1525528113.
 39. Komohara, Y., Ohnishi, K., Kuratsu, J. & Takeya, M. Possible involvement of the M2 anti-inflammatory macrophage phenotype in growth of human gliomas. *J. Pathol.* (2008) doi:10.1002/path.2370.
 40. Hambardzumyan, D., Gutmann, D. H. & Kettenmann, H. The role of microglia and macrophages in glioma maintenance and progression. **19**, (2016).
 41. Brat, D. J. *et al.* Comprehensive, Integrative Genomic Analysis of Diffuse Lower-Grade Gliomas. *N. Engl. J. Med.* **372**, 2481–2498 (2015).
 42. Aslan, K. *et al.* Heterogeneity of response to immune checkpoint blockade in hypermutated experimental gliomas. *Nat. Commun.* (2020) doi:10.1038/s41467-020-14642-0.
 43. Piao, Y. *et al.* Glioblastoma resistance to anti-VEGF therapy is associated with myeloid cell infiltration, stem cell accumulation, and a mesenchymal phenotype. *Neuro. Oncol.* (2012) doi:10.1093/neuonc/nos158.
 44. Sevenich, L. *et al.* Analysis of tumour- and stroma-supplied proteolytic networks reveals a brain-metastasis-promoting role for cathepsin S. *Nat. Cell Biol.* (2014) doi:10.1038/ncb3011.
 45. Pyonteck, S. M. *et al.* CSF-1R inhibition alters macrophage polarization and blocks glioma progression. *Nat. Med.* (2013) doi:10.1038/nm.3337.
 46. Quail, D. F. *et al.* The tumor microenvironment underlies acquired resistance to CSF-1R inhibition in gliomas. *Science (80-.).* (2016) doi:10.1126/science.aad3018.

47. Wculek, S. K. *et al.* Dendritic cells in cancer immunology and immunotherapy. *Nature Reviews Immunology* (2020) doi:10.1038/s41577-019-0210-z.
48. Chen, Q. *et al.* Carcinoma-astrocyte gap junctions promote brain metastasis by cGAMP transfer. *Nature* (2016) doi:10.1038/nature18268.
49. Osswald, M. *et al.* Brain tumour cells interconnect to a functional and resistant network. *Nature* (2015) doi:10.1038/nature16071.
50. Henrik Heiland, D. *et al.* Tumor-associated reactive astrocytes aid the evolution of immunosuppressive environment in glioblastoma. *Nat. Commun.* (2019) doi:10.1038/s41467-019-10493-6.
51. Farber, D. L. Form and function for T cells in health and disease. *Nat. Rev. Immunol.* (2020) doi:10.1038/s41577-019-0267-8.
52. Hodges, T. R. *et al.* Mutational burden, immune checkpoint expression, and mismatch repair in glioma: Implications for immune checkpoint immunotherapy. *Neuro. Oncol.* (2017) doi:10.1093/neuonc/nox026.
53. Brennan, C. W. *et al.* The somatic genomic landscape of glioblastoma. *Cell* (2013) doi:10.1016/j.cell.2013.09.034.
54. Woroniecka, K. I., Rhodin, K. E., Chongsathidkiet, P., Keith, K. A. & Fecci, P. E. T-Cell dysfunction in glioblastoma: Applying a new framework. *Clinical Cancer Research* (2018) doi:10.1158/1078-0432.CCR-18-0047.
55. K., W. *et al.* T cell exhaustion in patients and mice with GBM. *Neuro. Oncol.* (2016).
56. Bunse, L. *et al.* Suppression of antitumor T cell immunity by the oncometabolite (R)-2-hydroxyglutarate. *Nat. Med.* (2018) doi:10.1038/s41591-018-0095-6.
57. Uyttenhove, C. *et al.* Evidence for a tumoral immune resistance mechanism based on tryptophan degradation by indoleamine 2,3-dioxygenase. *Nat. Med.* (2003) doi:10.1038/nm934.
58. Alizadeh, D. *et al.* Induction of anti-glioma natural killer cell response following multiple low-dose intracerebral CpG therapy. *Clin. Cancer Res.* (2010) doi:10.1158/1078-0432.CCR-09-3087.
59. Cantini, G., Pisati, F., Pessina, S., Finocchiaro, G. & Pellegatta, S. Immunotherapy against the radial glia marker GLAST effectively triggers specific antitumor effectors without autoimmunity. *Oncoimmunology* (2012) doi:10.4161/onci.20637.
60. Gross, C. C. *et al.* Regulatory functions of natural killer cells in multiple sclerosis. *Frontiers in Immunology* (2016) doi:10.3389/fimmu.2016.00606.
61. Zhang, B., Yamamura, T., Kondo, T., Fujiwara, M. & Tabira, T. Regulation of experimental autoimmune encephalomyelitis by natural killer (NK) cells. *J. Exp. Med.* (1997).

62. Crome, S. Q. *et al.* A distinct innate lymphoid cell population regulates tumor-associated T cells. *Nat. Med.* (2017) doi:10.1038/nm.4278.
63. Gao, Y. *et al.* Tumor immunoevasion by the conversion of effector NK cells into type 1 innate lymphoid cells. *Nat. Immunol.* (2017) doi:10.1038/ni.3800.
64. Waldman, A. D., Fritz, J. M. & Lenardo, M. J. A guide to cancer immunotherapy: from T cell basic science to clinical practice. *Nature Reviews Immunology* (2020) doi:10.1038/s41577-020-0306-5.
65. Pardoll, D. M. The blockade of immune checkpoints in cancer immunotherapy. *Nat Rev Cancer* **12**, 252–264 (2012).
66. Rosenberg, S. A., Yang, J. C. & Restifo, N. P. Cancer immunotherapy: Moving beyond current vaccines. *Nature Medicine* (2004) doi:10.1038/nm1100.
67. Klein, G., Sjögren, H. O., Klein, E. & Hellstrom, K. E. Demonstration of Resistance against Methylcholanthrene-induced Sarcomas in the Primary Autochthonous Host. *Cancer Res.* (1960) doi:10.1097/00006534-196201000-00064.
68. Foley, E. J. Antigenic Properties of Methylcholanthrene-induced Tumors in Mice of the Strain of Origin. *Cancer Res.* (1953).
69. Oiseth, S. J. & Aziz, M. S. Cancer immunotherapy: a brief review of the history, possibilities, and challenges ahead. *J. Cancer Metastasis Treat.* (2017) doi:10.20517/2394-4722.2017.41.
70. Halliday, G. M., Patel, A., Hunt, M. J., Tefany, F. J. & Barnetson, R. S. C. Spontaneous regression of human melanoma/nonmelanoma skin cancer: Association with infiltrating CD4+ T cells. *World J. Surg.* (1995) doi:10.1007/BF00299157.
71. Vesely, M. D. & Schreiber, R. D. Cancer immunoediting: Antigens, mechanisms, and implications to cancer immunotherapy. *Ann. N. Y. Acad. Sci.* (2013) doi:10.1111/nyas.12105.
72. Matsushita, H. *et al.* Cancer exome analysis reveals a T-cell-dependent mechanism of cancer immunoediting. *Nature* (2012) doi:10.1038/nature10755.
73. Wherry, E. J. & Kurachi, M. Molecular and cellular insights into T cell exhaustion. *Nature Reviews Immunology* (2015) doi:10.1038/nri3862.
74. Schietinger, A. & Greenberg, P. D. Tolerance and exhaustion: Defining mechanisms of T cell dysfunction. *Trends in Immunology* (2014) doi:10.1016/j.it.2013.10.001.
75. Schietinger, A. *et al.* Tumor-Specific T Cell Dysfunction Is a Dynamic Antigen-Driven Differentiation Program Initiated Early during Tumorigenesis. *Immunity* (2016) doi:10.1016/j.immuni.2016.07.011.
76. Philip, M. *et al.* Chromatin states define tumour-specific T cell dysfunction and reprogramming. *Nature* (2017) doi:10.1038/nature22367.

77. Jadhav, R. R. *et al.* Epigenetic signature of PD-1+ TCF1+ CD8 T cells that act as resource cells during chronic viral infection and respond to PD-1 blockade. *Proc. Natl. Acad. Sci. U. S. A.* (2019) doi:10.1073/pnas.1903520116.
78. Khan, O. *et al.* TOX transcriptionally and epigenetically programs CD8+ T cell exhaustion. *Nature* (2019) doi:10.1038/s41586-019-1325-x.
79. Scott, A. C. *et al.* TOX is a critical regulator of tumour-specific T cell differentiation. *Nature* (2019) doi:10.1038/s41586-019-1324-y.
80. F., A. *et al.* TOX reinforces the phenotype and longevity of exhausted T cells in chronic viral infection. *Nature* (2019).
81. Miller, B. C. *et al.* Subsets of exhausted CD8+ T cells differentially mediate tumor control and respond to checkpoint blockade. *Nat. Immunol.* (2019) doi:10.1038/s41590-019-0312-6.
82. Siddiqui, I. *et al.* Intratumoral Tcf1 + PD-1 + CD8 + T Cells with Stem-like Properties Promote Tumor Control in Response to Vaccination and Checkpoint Blockade Immunotherapy. *Immunity* (2019) doi:10.1016/j.immuni.2018.12.021.
83. Kurtulus, S. *et al.* Checkpoint Blockade Immunotherapy Induces Dynamic Changes in PD-1 – CD8 + Tumor-Infiltrating T Cells. *Immunity* (2019) doi:10.1016/j.immuni.2018.11.014.
84. Jansen, C. S. *et al.* An intra-tumoral niche maintains and differentiates stem-like CD8 T cells. *Nature* (2019) doi:10.1038/s41586-019-1836-5.
85. Woroniecka, K. *et al.* T-cell exhaustion signatures vary with tumor type and are severe in glioblastoma. *Clin. Cancer Res.* (2018) doi:10.1158/1078-0432.CCR-17-1846.
86. Sharma, P. & Allison, J. P. Immune checkpoint targeting in cancer therapy: Toward combination strategies with curative potential. *Cell* **161**, 205–214 (2015).
87. Topalian, S. L., Drake, C. G. & Pardoll, D. M. Immune checkpoint blockade: A common denominator approach to cancer therapy. *Cancer Cell* vol. 27 451–461 (2015).
88. Paschen, A. & Schadendorf, D. The era of checkpoint inhibition: Lessons learned from melanoma. in *Recent Results in Cancer Research* (2020). doi:10.1007/978-3-030-23765-3_6.
89. Maio, M. *et al.* Five-year survival rates for treatment-naïve patients with advanced melanoma who received ipilimumab plus dacarbazine in a phase III trial. *J. Clin. Oncol.* (2015) doi:10.1200/JCO.2014.56.6018.
90. Robbins, P. F. *et al.* Tumor regression in patients with metastatic synovial cell sarcoma and melanoma using genetically engineered lymphocytes reactive with NY-ESO-1. *J. Clin. Oncol.* (2011) doi:10.1200/JCO.2010.32.2537.
91. Xin Yu, J., Hubbard-Lucey, V. M. & Tang, J. Immuno-oncology drug development goes global. *Nature Reviews Drug Discovery* (2019) doi:10.1038/d41573-019-00167-9.
92. Havel, J. J., Chowell, D. & Chan, T. A. The evolving landscape of biomarkers for checkpoint

- inhibitor immunotherapy. *Nature Reviews Cancer* (2019) doi:10.1038/s41568-019-0116-x.
93. Gong, J., Chehrazi-Raffle, A., Reddi, S. & Salgia, R. Development of PD-1 and PD-L1 inhibitors as a form of cancer immunotherapy: A comprehensive review of registration trials and future considerations. *Journal for ImmunoTherapy of Cancer* (2018) doi:10.1186/s40425-018-0316-z.
 94. Van Allen, E. M. *et al.* Genomic correlates of response to CTLA-4 blockade in metastatic melanoma. *Science* (80-.). **350**, 207–211 (2015).
 95. Brown, S. D. *et al.* Neo-antigens predicted by tumor genome meta-analysis correlate with increased patient survival. *Genome Res.* **24**, 743–750 (2014).
 96. Schumacher, T. N. & Schreiber, R. D. Neoantigens in cancer immunotherapy. *Science* (80-.). **348**, 69–74 (2015).
 97. Gajewski, T. F., Schreiber, H. & Fu, Y. X. Innate and adaptive immune cells in the tumor microenvironment. *Nature Immunology* (2013) doi:10.1038/ni.2703.
 98. Sampson, J. H., Gunn, M. D., Fecci, P. E. & Ashley, D. M. Brain immunology and immunotherapy in brain tumours. *Nature Reviews Cancer* (2020) doi:10.1038/s41568-019-0224-7.
 99. Brandes, A. A. *et al.* A Phase II randomized study of galunisertib monotherapy or galunisertib plus lomustine compared with lomustine monotherapy in patients with recurrent glioblastoma. *Neuro. Oncol.* (2016) doi:10.1093/neuonc/now009.
 100. Long, G. V. *et al.* Epcadostat plus pembrolizumab versus placebo plus pembrolizumab in patients with unresectable or metastatic melanoma (ECHO-301/KEYNOTE-252): a phase 3, randomised, double-blind study. *Lancet Oncol.* (2019) doi:10.1016/S1470-2045(19)30274-8.
 101. Rohle, D. *et al.* An inhibitor of mutant IDH1 delays growth and promotes differentiation of glioma cells. *Science* (80-.). (2013) doi:10.1126/science.1236062.
 102. Popovici-Muller, J. *et al.* Discovery of AG-120 (Ivosidenib): A First-in-Class Mutant IDH1 Inhibitor for the Treatment of IDH1 Mutant Cancers. *ACS Med. Chem. Lett.* (2018) doi:10.1021/acsmchemlett.7b00421.
 103. Kadiyala, P. *et al.* Inhibition of 2-Hydroxyglutarate Elicits Metabolic-reprogramming and Mutant IDH1 Glioma Immunity in Mice. *J. Clin. Invest.* (2020) doi:10.1172/jci139542.
 104. CSF1R Inhibitor Prevents Glioblastoma Recurrence. *Cancer Discov.* (2020) doi:10.1158/2159-8290.cd-nb2020-078.
 105. Butowski, N. *et al.* Orally administered colony stimulating factor 1 receptor inhibitor PLX3397 in recurrent glioblastoma: An Ivy Foundation Early Phase Clinical Trials Consortium phase II study. *Neuro. Oncol.* (2016) doi:10.1093/neuonc/nov245.

106. Aslan, K. *et al.* Heterogeneity of response to immune checkpoint blockade in hypermutated experimental gliomas. *Nat. Commun.* (2020) doi:10.1038/s41467-020-14642-0.
107. Reardon, D. A. *et al.* Glioblastoma eradication following immune checkpoint blockade in an orthotopic, immunocompetent model. *Cancer Immunol. Res.* (2016) doi:10.1158/2326-6066.CIR-15-0151.
108. Reardon, D. A. *et al.* OS10.3 Randomized Phase 3 Study Evaluating the Efficacy and Safety of Nivolumab vs Bevacizumab in Patients With Recurrent Glioblastoma: CheckMate 143. *Neuro. Oncol.* (2017) doi:10.1093/neuonc/nox036.071.
109. Reardon, D. A. *et al.* Effect of Nivolumab vs Bevacizumab in Patients with Recurrent Glioblastoma: The CheckMate 143 Phase 3 Randomized Clinical Trial. *JAMA Oncol.* (2020) doi:10.1001/jamaoncol.2020.1024.
110. Cloughesy, T. F. *et al.* Neoadjuvant anti-PD-1 immunotherapy promotes a survival benefit with intratumoral and systemic immune responses in recurrent glioblastoma. *Nat. Med.* (2019) doi:10.1038/s41591-018-0337-7.
111. Schalper, K. A. *et al.* Neoadjuvant nivolumab modifies the tumor immune microenvironment in resectable glioblastoma. *Nature Medicine* (2019) doi:10.1038/s41591-018-0339-5.
112. Zhao, J. *et al.* Immune and genomic correlates of response to anti-PD-1 immunotherapy in glioblastoma. *Nat. Med.* (2019) doi:10.1038/s41591-019-0349-y.
113. Rosenberg, S. A. *et al.* A Progress Report on the Treatment of 157 Patients with Advanced Cancer Using Lymphokine-Activated Killer Cells and Interleukin-2 or High-Dose Interleukin-2 Alone. *N. Engl. J. Med.* (1987) doi:10.1056/nejm198704093161501.
114. Topalian, S. L. *et al.* Immunotherapy of patients with advanced cancer using tumor-infiltrating lymphocytes and recombinant interleukin-2: A pilot study. *J. Clin. Oncol.* (1988) doi:10.1200/JCO.1988.6.5.839.
115. Rosenberg, S. A. *et al.* Use of Tumor-Infiltrating Lymphocytes and Interleukin-2 in the Immunotherapy of Patients with Metastatic Melanoma. *N. Engl. J. Med.* (1988) doi:10.1056/nejm198812223192527.
116. Rohaan, M. W., Wilgenhof, S. & Haanen, J. B. A. G. Adoptive cellular therapies: the current landscape. *Virchows Archiv* (2019) doi:10.1007/s00428-018-2484-0.
117. Mehta, G. U. *et al.* Outcomes of Adoptive Cell Transfer with Tumor-infiltrating Lymphocytes for Metastatic Melanoma Patients with and Without Brain Metastases. *J. Immunother.* (2018) doi:10.1097/CJI.0000000000000223.
118. Dillman, R. O. *et al.* Intracavitary placement of autologous lymphokine-activated killer (LAK) cells after resection of recurrent glioblastoma. *J. Immunother.* (2004)

- doi:10.1097/00002371-200409000-00009.
119. Dillman, R. O. *et al.* Intralesional lymphokine-activated killer cells as adjuvant therapy for primary glioblastoma. *J. Immunother.* (2009) doi:10.1097/CJI.0b013e3181b2910f.
 120. Liu, Z. *et al.* Tumor-infiltrating lymphocytes (TILs) from patients with glioma. *Oncoimmunology* (2017) doi:10.1080/2162402X.2016.1252894.
 121. Rafiq, S., Hackett, C. S. & Brentjens, R. J. Engineering strategies to overcome the current roadblocks in CAR T cell therapy. *Nature Reviews Clinical Oncology* (2020) doi:10.1038/s41571-019-0297-y.
 122. June, C. H., O'Connor, R. S., Kawalekar, O. U., Ghassemi, S. & Milone, M. C. CAR T cell immunotherapy for human cancer. *Science* (2018) doi:10.1126/science.aar6711.
 123. Morgan, R. A. *et al.* Recognition of glioma stem cells by genetically modified T cells targeting EGFRvIII and development of adoptive cell therapy for glioma. *Hum. Gene Ther.* (2012) doi:10.1089/hum.2012.041.
 124. Brown, C. E. *et al.* Stem-like tumor-initiating cells isolated from IL13R α 2 expressing gliomas are targeted and killed by IL13-zetakine-redirected T cells. *Clin. Cancer Res.* (2012) doi:10.1158/1078-0432.CCR-11-1669.
 125. Mount, C. W. *et al.* Potent antitumor efficacy of anti-GD2 CAR T cells in H3-K27M+ diffuse midline gliomas letter. *Nat. Med.* (2018) doi:10.1038/s41591-018-0006-x.
 126. Wang, D. *et al.* Chlorotoxin-directed CAR T cells for specific and effective targeting of glioblastoma. *Sci. Transl. Med.* (2020) doi:10.1126/scitranslmed.aaw2672.
 127. Majzner, R. G. *et al.* CAR T cells targeting B7-H3, a pan-cancer antigen, demonstrate potent preclinical activity against pediatric solid tumors and brain tumors. *Clin. Cancer Res.* (2019) doi:10.1158/1078-0432.CCR-18-0432.
 128. Theruvath, J. *et al.* Locoregionally administered B7-H3-targeted CAR T cells for treatment of atypical teratoid/rhabdoid tumors. *Nat. Med.* (2020) doi:10.1038/s41591-020-0821-8.
 129. Donovan, L. K. *et al.* Locoregional delivery of CAR T cells to the cerebrospinal fluid for treatment of metastatic medulloblastoma and ependymoma. *Nat. Med.* (2020) doi:10.1038/s41591-020-0827-2.
 130. Brown, C. E. *et al.* Regression of Glioblastoma after Chimeric Antigen Receptor T-Cell Therapy. *N. Engl. J. Med.* (2016) doi:10.1056/nejmoa1610497.
 131. Anguille, S., Smits, E. L., Lion, E., Van Tendeloo, V. F. & Berneman, Z. N. Clinical use of dendritic cells for cancer therapy. *The Lancet Oncology* (2014) doi:10.1016/S1470-2045(13)70585-0.
 132. Heimberger, A. B. *et al.* Bone marrow-derived dendritic cells pulsed with tumor homogenate induce immunity against syngeneic intracerebral glioma. *J. Neuroimmunol.* (2000)

- doi:10.1016/S0165-5728(99)00172-1.
133. Grauer, O. M. *et al.* Elimination of regulatory T cells is essential for an effective vaccination with tumor lysate-pulsed dendritic cells in a murine glioma model. *Int. J. Cancer* (2008) doi:10.1002/ijc.23284.
 134. Pellegatta, S. *et al.* Dendritic cells pulsed with glioma lysates induce immunity against syngeneic intracranial gliomas and increase survival of tumor-bearing mice. *Neurol. Res.* (2006) doi:10.1179/016164106X116809.
 135. Mitchell, D. A. *et al.* Tetanus toxoid and CCL3 improve dendritic cell vaccines in mice and glioblastoma patients. *Nature* (2015) doi:10.1038/nature14320.
 136. Prins, R. M. *et al.* Gene expression profile correlates with T-cell infiltration and relative survival in glioblastoma patients vaccinated with dendritic cell immunotherapy. *Clin. Cancer Res.* (2011) doi:10.1158/1078-0432.CCR-10-2563.
 137. Huszthy, P. C. *et al.* In vivo models of primary brain tumors: Pitfalls and perspectives. *Neuro-Oncology* (2012) doi:10.1093/neuonc/nos135.
 138. Rall, D. P. Studies on the Chemotherapy of Experimental Brain Tumors: Development of an Experimental Model. *Cancer Res.* (1970).
 139. Szatmári, T. *et al.* Detailed characterization of the mouse glioma 261 tumor model for experimental glioblastoma therapy. *Cancer Sci.* (2006) doi:10.1111/j.1349-7006.2006.00208.x.
 140. Murphy, K. A. *et al.* CD8 + T Cell–Independent Tumor Regression Induced by Fc-OX40L and Therapeutic Vaccination in a Mouse Model of Glioma . *J. Immunol.* (2014) doi:10.4049/jimmunol.1301633.
 141. Tomek, P. *et al.* Imprinted and ancient gene: A potential mediator of cancer cell survival during tryptophan deprivation. *Cell Commun. Signal.* (2018) doi:10.1186/s12964-018-0301-7.
 142. Oh, T. *et al.* Immunocompetent murine models for the study of glioblastoma immunotherapy. *Journal of Translational Medicine* (2014) doi:10.1186/1479-5876-12-107.
 143. Hidalgo, M. *et al.* Patient-derived Xenograft models: An emerging platform for translational cancer research. *Cancer Discov.* (2014) doi:10.1158/2159-8290.CD-14-0001.
 144. Braekeveldt, N. *et al.* Neuroblastoma patient-derived orthotopic xenografts retain metastatic patterns and geno- and phenotypes of patient tumours. *Int. J. Cancer* (2015) doi:10.1002/ijc.29217.
 145. Zeng, W. *et al.* Patient-derived xenografts of different grade gliomas retain the heterogeneous histological and genetic features of human gliomas. *Cancer Cell Int.* (2020) doi:10.1186/s12935-019-1086-5.
 146. William, D. *et al.* Optimized creation of glioblastoma patient derived xenografts for use in

- preclinical studies. *J. Transl. Med.* (2017) doi:10.1186/s12967-017-1128-5.
147. Patrizii, M., Bartucci, M., Pine, S. R. & Sabaawy, H. E. Utility of glioblastoma patient-derived orthotopic xenografts in drug discovery and personalized therapy. *Front. Oncol.* (2018) doi:10.3389/fonc.2018.00023.
 148. Tentler, J. J. *et al.* Patient-derived tumour xenografts as models for oncology drug development. *Nature Reviews Clinical Oncology* (2012) doi:10.1038/nrclinonc.2012.61.
 149. Bao, S. *et al.* Glioma stem cells promote radioresistance by preferential activation of the DNA damage response. *Nature* (2006) doi:10.1038/nature05236.
 150. Singh, S. K. *et al.* Identification of human brain tumour initiating cells. *Nature* (2004) doi:10.1038/nature03128.
 151. Pajot, A. *et al.* A mouse model of human adaptive immune functions: HLA-A2.1-/HLA-DR1-transgenic H-2 class I-/class II-knockout mice. *Eur. J. Immunol.* (2004) doi:10.1002/eji.200425463.
 152. Schumacher, T. *et al.* A vaccine targeting mutant IDH1 induces antitumour immunity. *Nature* **512**, 324–327 (2014).
 153. Ochs, K. *et al.* K27M-mutant histone-3 as a novel target for glioma immunotherapy. *Oncoimmunology* (2017) doi:10.1080/2162402X.2017.1328340.
 154. Platt, R. J. *et al.* CRISPR-Cas9 knockin mice for genome editing and cancer modeling. *Cell* (2014) doi:10.1016/j.cell.2014.09.014.
 155. Ventura, A. & Dow, L. E. Modeling Cancer in the CRISPR Era. *Annual Review of Cancer Biology* (2018) doi:10.1146/annurev-cancerbio-030617-050455.
 156. Zuckermann, M. *et al.* Somatic CRISPR/Cas9-mediated tumour suppressor disruption enables versatile brain tumour modelling. *Nat. Commun.* (2015) doi:10.1038/ncomms8391.
 157. Gengenbacher, N., Singhal, M. & Augustin, H. G. Preclinical mouse solid tumour models: Status quo, challenges and perspectives. *Nature Reviews Cancer* (2017) doi:10.1038/nrc.2017.92.
 158. Shultz, L. D. *et al.* Human Lymphoid and Myeloid Cell Development in NOD/LtSz- scid IL2R γ null Mice Engrafted with Mobilized Human Hemopoietic Stem Cells. *J. Immunol.* (2005) doi:10.4049/jimmunol.174.10.6477.
 159. Zuckermann, M. *et al.* Somatic CRISPR/Cas9-mediated tumour suppressor disruption enables versatile brain tumour modelling. *Nat. Commun.* **6**, 1–9 (2015).
 160. Schrörs, B. *et al.* Multi-Omics Characterization of the 4T1 Murine Mammary Gland Tumor Model. *Front. Oncol.* (2020) doi:10.3389/fonc.2020.01195.
 161. Schumacher, T. *et al.* A vaccine targeting mutant IDH1 induces antitumour immunity. *Nature* (2014) doi:10.1038/nature13387.

162. Stuart, T. *et al.* Comprehensive Integration of Single-Cell Data. *Cell* (2019) doi:10.1016/j.cell.2019.05.031.
163. Finak, G. *et al.* MAST: A flexible statistical framework for assessing transcriptional changes and characterizing heterogeneity in single-cell RNA sequencing data. *Genome Biol.* (2015) doi:10.1186/s13059-015-0844-5.
164. Suzuki, H. *et al.* Mutational landscape and clonal architecture in grade II and III gliomas. *Nat. Genet.* (2015) doi:10.1038/ng.3273.
165. Draaisma, K. *et al.* PI3 kinase mutations and mutational load as poor prognostic markers in diffuse glioma patients. *Acta Neuropathol. Commun.* (2015) doi:10.1186/s40478-015-0265-4.
166. Ochs, K. *et al.* K27M-mutant histone-3 as a novel target for glioma immunotherapy. *Oncoimmunology* **6**, (2017).
167. Vora, P. *et al.* The Rational Development of CD133-Targeting Immunotherapies for Glioblastoma. *Cell Stem Cell* (2020) doi:10.1016/j.stem.2020.04.008.
168. Sankowski, R. *et al.* Mapping microglia states in the human brain through the integration of high-dimensional techniques. *Nat. Neurosci.* (2019) doi:10.1038/s41593-019-0532-y.
169. Canale, F. P. *et al.* CD39 expression defines cell exhaustion in tumor-infiltrating CD8+ T cells. *Cancer Res.* (2018) doi:10.1158/0008-5472.CAN-16-2684.
170. Gupta, P. K. *et al.* CD39 Expression Identifies Terminally Exhausted CD8+ T Cells. *PLoS Pathog.* (2015) doi:10.1371/journal.ppat.1005177.
171. Jiang, Y., Li, Y. & Zhu, B. T-cell exhaustion in the tumor microenvironment. *Cell Death and Disease* (2015) doi:10.1038/cddis.2015.162.
172. Anderson, A. C., Joller, N. & Kuchroo, V. K. Lag-3, Tim-3, and TIGIT: Co-inhibitory Receptors with Specialized Functions in Immune Regulation. *Immunity* (2016) doi:10.1016/j.immuni.2016.05.001.
173. Bordon, Y. TOX for tired T cells. *Nature Reviews Immunology* (2019) doi:10.1038/s41577-019-0193-9.
174. Wu, P.-S. *et al.* Critical Roles of Translationally Controlled Tumor Protein in the Homeostasis and TCR-Mediated Proliferation of Peripheral T Cells. *J. Immunol.* (2009) doi:10.4049/jimmunol.0900668.
175. Zhang, X. *et al.* Thymosin beta 10 is a key regulator of tumorigenesis and metastasis and a novel serum marker in breast cancer. *Breast Cancer Res.* (2017) doi:10.1186/s13058-016-0785-2.
176. Dutoit, V. *et al.* Exploiting the glioblastoma peptidome to discover novel tumour-associated antigens for immunotherapy. *Brain* (2012) doi:10.1093/brain/aws042.
177. Platten, M. & Offringa, R. Cancer immunotherapy: Exploiting neoepitopes. *Cell Res.* (2015)

- doi:10.1038/cr.2015.66.
178. Gjerstorff, M. F., Andersen, M. H. & Ditzel, H. J. Oncogenic cancer/testis antigens: Prime candidates for immunotherapy. *Oncotarget* (2015) doi:10.18632/oncotarget.4694.
 179. Sahin, U. *et al.* An RNA vaccine drives immunity in checkpoint-inhibitor-treated melanoma. *Nature* (2020) doi:10.1038/s41586-020-2537-9.
 180. Hilf, N. *et al.* Actively personalized vaccination trial for newly diagnosed glioblastoma. *Nature* (2019) doi:10.1038/s41586-018-0810-y.
 181. Rampling, R. *et al.* A cancer research UK first time in human phase i trial of IMA950 (novel multi-peptide therapeutic vaccine) in patients with newly diagnosed glioblastoma. in *Clinical Cancer Research* (2016). doi:10.1158/1078-0432.CCR-16-0506.
 182. Yarchoan, M., Johnson, B. A., Lutz, E. R., Laheru, D. A. & Jaffee, E. M. Targeting neoantigens to augment antitumour immunity. *Nature Reviews Cancer* (2017) doi:10.1038/nrc.2016.154.
 183. Sahin, U. *et al.* Personalized RNA mutanome vaccines mobilize poly-specific therapeutic immunity against cancer. *Nature* (2017) doi:10.1038/nature23003.
 184. Keskin, D. B. *et al.* Neoantigen vaccine generates intratumoral T cell responses in phase Ib glioblastoma trial. *Nature* (2019) doi:10.1038/s41586-018-0792-9.
 185. Zhao, W., Wu, J., Chen, S. & Zhou, Z. Shared neoantigens: Ideal targets for off-the-shelf cancer immunotherapy. *Pharmacogenomics* (2020) doi:10.2217/pgs-2019-0184.
 186. Congdon, K. L. *et al.* Epidermal growth factor receptor and variant III targeted immunotherapy. *Neuro-Oncology* (2014) doi:10.1093/neuonc/nou236.
 187. Chheda, Z. S. *et al.* Novel and shared neoantigen derived from histone 3 variant H3.3K27M mutation for glioma T cell therapy. *J. Exp. Med.* (2018) doi:10.1084/jem.20171046.
 188. Sampson, J. H. *et al.* An epidermal growth factor receptor variant III-targeted vaccine is safe and immunogenic in patients with glioblastoma multiforme. *Mol. Cancer Ther.* (2009) doi:10.1158/1535-7163.MCT-09-0124.
 189. Weller, M. *et al.* Rindopepimut with temozolomide for patients with newly diagnosed, EGFRvIII-expressing glioblastoma (ACT IV): a randomised, double-blind, international phase 3 trial. *Lancet Oncol.* (2017) doi:10.1016/S1470-2045(17)30517-X.
 190. Sampson, J. H. *et al.* Immunologic escape after prolonged progression-free survival with epidermal growth factor receptor variant III peptide vaccination in patients with newly diagnosed glioblastoma. *J. Clin. Oncol.* (2010) doi:10.1200/JCO.2010.28.6963.
 191. Platten, M. *et al.* A mutation-specific peptide vaccine targeting IDH1R132H in patients with newly diagnosed malignant astrocytomas: A first-in-man multicenter phase I clinical trial of the German Neurooncology Working Group (NOA-16). *J. Clin. Oncol.* (2018)

- doi:10.1200/jco.2018.36.15_suppl.2001.
192. Yip, S. *et al.* Concurrent CIC mutations, IDH mutations, and 1p/19q loss distinguish oligodendrogliomas from other cancers. *J. Pathol.* (2012) doi:10.1002/path.2995.
 193. Bettgowda, C. *et al.* Mutations in CIC and FUBP1 Contribute to Human Oligodendroglioma. *Science (80-.).* **333**, 1453–1455 (2011).
 194. Sahm, F. *et al.* CIC and FUBP1 mutations in oligodendrogliomas, oligoastrocytomas and astrocytomas. *Acta Neuropathol.* (2012) doi:10.1007/s00401-012-0993-5.
 195. Yang, R. *et al.* Cic loss promotes gliomagenesis via aberrant neural stem cell proliferation and differentiation. *Cancer Res.* (2017) doi:10.1158/0008-5472.CAN-17-1018.
 196. Bunda, S. *et al.* CIC protein instability contributes to tumorigenesis in glioblastoma. *Nat. Commun.* (2019) doi:10.1038/s41467-018-08087-9.
 197. Hollingsworth, R. E. & Jansen, K. Turning the corner on therapeutic cancer vaccines. *npj Vaccines* (2019) doi:10.1038/s41541-019-0103-y.
 198. Gee, M. H. *et al.* Antigen Identification for Orphan T Cell Receptors Expressed on Tumor-Infiltrating Lymphocytes. *Cell* (2018) doi:10.1016/j.cell.2017.11.043.
 199. Thommen, D. S. *et al.* A transcriptionally and functionally distinct pd-1 + cd8 + t cell pool with predictive potential in non-small-cell lung cancer treated with pd-1 blockade. *Nat. Med.* (2018) doi:10.1038/s41591-018-0057-z.
 200. Ali, M. *et al.* Induction of neoantigen-reactive T cells from healthy donors. *Nat. Protoc.* (2019) doi:10.1038/s41596-019-0170-6.
 201. Yu, J. X., Upadhaya, S., Tataka, R., Barkalow, F. & Hubbard-Lucey, V. M. Cancer cell therapies: the clinical trial landscape. *Nature reviews. Drug discovery* (2020) doi:10.1038/d41573-020-00099-9.
 202. Guedan, S., Ruella, M. & June, C. H. Emerging Cellular Therapies for Cancer. *Annu. Rev. Immunol.* (2019) doi:10.1146/annurev-immunol-042718-041407.
 203. Zheng, P. P., Kros, J. M. & Li, J. Approved CAR T cell therapies: ice bucket challenges on glaring safety risks and long-term impacts. *Drug Discovery Today* (2018) doi:10.1016/j.drudis.2018.02.012.
 204. Lee, D. W. *et al.* T cells expressing CD19 chimeric antigen receptors for acute lymphoblastic leukaemia in children and young adults: A phase 1 dose-escalation trial. *Lancet* (2015) doi:10.1016/S0140-6736(14)61403-3.
 205. Akhavan, D. *et al.* CAR T cells for brain tumors: Lessons learned and road ahead. *Immunological Reviews* (2019) doi:10.1111/imr.12773.
 206. Neelapu, S. S. *et al.* Chimeric antigen receptor T-cell therapy-assessment and management of toxicities. *Nature Reviews Clinical Oncology* (2018) doi:10.1038/nrclinonc.2017.148.

207. Gust, J. *et al.* Endothelial activation and blood–brain barrier disruption in neurotoxicity after adoptive immunotherapy with CD19 CAR-T cells. *Cancer Discov.* (2017) doi:10.1158/2159-8290.CD-17-0698.
208. Feng, W., Liu, H. K. & Kawauchi, D. CRISPR-engineered genome editing for the next generation neurological disease modeling. *Progress in Neuro-Psychopharmacology and Biological Psychiatry* (2018) doi:10.1016/j.pnpbp.2017.05.019.
209. Pajtler, K. W. *et al.* YAP1 subgroup supratentorial ependymoma requires TEAD and nuclear factor I-mediated transcriptional programmes for tumorigenesis. *Nat. Commun.* (2019) doi:10.1038/s41467-019-11884-5.
210. Pathania, M. *et al.* H3.3 K27M Cooperates with Trp53 Loss and PDGFRA Gain in Mouse Embryonic Neural Progenitor Cells to Induce Invasive High-Grade Gliomas. *Cancer Cell* (2017) doi:10.1016/j.ccell.2017.09.014.
211. Cordero, F. J. *et al.* Histone H3.3K27M represses p16 to accelerate gliomagenesis in a murine model of DIPG. *Mol. Cancer Res.* (2017) doi:10.1158/1541-7786.MCR-16-0389.
212. Ozawa, T. *et al.* A De Novo Mouse Model of C11orf95-RELA Fusion-Driven Ependymoma Identifies Driver Functions in Addition to NF- κ B. *Cell Rep.* (2018) doi:10.1016/j.celrep.2018.04.099.
213. Rapoport, A. P. *et al.* NY-ESO-1-specific TCR-engineered T cells mediate sustained antigen-specific antitumor effects in myeloma. *Nat. Med.* (2015) doi:10.1038/nm.3910.
214. Morgan, R. A. *et al.* Cancer regression in patients after transfer of genetically engineered lymphocytes. *Science (80-.).* (2006) doi:10.1126/science.1129003.
215. Abad, J. D. *et al.* T-cell receptor gene therapy of established tumors in a murine melanoma model. *J. Immunother.* (2008) doi:10.1097/CJI.0b013e31815c193f.
216. Borst, J., Ahrends, T., Båbala, N., Melief, C. J. M. & Kastenmüller, W. CD4+ T cell help in cancer immunology and immunotherapy. *Nature Reviews Immunology* (2018) doi:10.1038/s41577-018-0044-0.
217. Kverneland, A. H. *et al.* Adoptive cell therapy in combination with checkpoint inhibitors in ovarian cancer. *Oncotarget* **11**, 2092–2105 (2020).
218. Shi, L. Z. *et al.* Blockade of CTLA-4 and PD-1 enhances adoptive t-cell therapy efficacy in an ICOS-mediated manner. *Cancer Immunol. Res.* (2019) doi:10.1158/2326-6066.CIR-18-0873.
219. John, L. B. *et al.* Anti-PD-1 antibody therapy potently enhances the eradication of established tumors by gene-modified T cells. *Clin. Cancer Res.* (2013) doi:10.1158/1078-0432.CCR-13-0458.
220. Dudley, M. E. *et al.* Adoptive cell transfer therapy following non-myeloablative but

- lymphodepleting chemotherapy for the treatment of patients with refractory metastatic melanoma. *J. Clin. Oncol.* (2005) doi:10.1200/JCO.2005.00.240.
221. Wu, Q. *et al.* Modulating both tumor cell death and innate immunity is essential for improving radiation therapy effectiveness. *Frontiers in Immunology* (2017) doi:10.3389/fimmu.2017.00613.
 222. Gameiro, S. R. *et al.* Radiation-induced immunogenic modulation of tumor enhances antigen processing and calreticulin exposure, resulting in enhanced T-cell killign. *Oncotarget* (2014) doi:10.18632/oncotarget.1719.
 223. Perez, C. A., Fu, A., Onishko, H., Hallahan, D. E. & Geng, L. Radiation induces an antitumour immune response to mouse melanoma. *Int. J. Radiat. Biol.* (2009) doi:10.3109/09553000903242099.
 224. Reits, E. A. *et al.* Radiation modulates the peptide repertoire, enhances MHC class I expression, and induces successful antitumor immunotherapy. *J. Exp. Med.* (2006) doi:10.1084/jem.20052494.
 225. Demaria, S. *et al.* Immune-mediated inhibition of metastases after treatment with local radiation and CTLA-4 blockade in a mouse model of breast cancer. *Clin. Cancer Res.* (2005).
 226. Kalbasi, A., June, C. H., Haas, N. & Vapiwala, N. Radiation and immunotherapy: A synergistic combination. *Journal of Clinical Investigation* (2013) doi:10.1172/JCI69219.
 227. Chakraborty, M. *et al.* Irradiation of Tumor Cells Up-Regulates Fas and Enhances CTL Lytic Activity and CTL Adoptive Immunotherapy. *J. Immunol.* (2003) doi:10.4049/jimmunol.170.12.6338.
 228. Kreiter, S. *et al.* Mutant MHC class II epitopes drive therapeutic immune responses to cancer. *Nature* **520**, 692–696 (2015).
 229. Muntjewerff, E. M., Meesters, L. D. & van den Bogaart, G. Antigen Cross-Presentation by Macrophages. *Frontiers in Immunology* (2020) doi:10.3389/fimmu.2020.01276.
 230. Muraoka, D. *et al.* Antigen delivery targeted to tumor-associated macrophages overcomes tumor immune resistance. *J. Clin. Invest.* (2019) doi:10.1172/JCI97642.
 231. Coniglio, S. J. *et al.* Microglial stimulation of glioblastoma invasion involves epidermal growth factor receptor (EGFR) and colony stimulating factor 1 receptor (CSF-1R) signaling. *Mol. Med.* (2012) doi:10.2119/molmed.2011.00217.
 232. Yu, K. *et al.* A nonmyeloablative chimeric mouse model accurately defines microglia and macrophage contribution in glioma. *Neuropathol. Appl. Neurobiol.* (2019) doi:10.1111/nan.12489.
 233. Hutter, G. *et al.* Microglia are effector cells of CD47-SIRP α antiphagocytic axis disruption against glioblastoma. *Proc. Natl. Acad. Sci. U. S. A.* (2019) doi:10.1073/pnas.1721434116.

234. Wolf, Y. *et al.* Microglial MHC class II is dispensable for experimental autoimmune encephalomyelitis and cuprizone-induced demyelination. *Eur. J. Immunol.* **48**, 1308–1318 (2018).
235. Matloubian, M. *et al.* Lymphocyte egress from thymus and peripheral lymphoid organs is dependent on S1P receptor 1. *Nature* (2004) doi:10.1038/nature02284.
236. Alspach, E. *et al.* MHC-II neoantigens shape tumour immunity and response to immunotherapy. *Nature* (2019) doi:10.1038/s41586-019-1671-8.
237. Ferris, S. T. *et al.* cDC1 prime and are licensed by CD4⁺ T cells to induce anti-tumour immunity. *Nature* (2020) doi:10.1038/s41586-020-2611-3.
238. Ahrends, T. *et al.* CD4⁺ T cell help creates memory CD8⁺ T cells with innate and help-independent recall capacities. *Nat. Commun.* (2019) doi:10.1038/s41467-019-13438-1.
239. Ahrends, T. *et al.* CD4⁺ T Cell Help Confers a Cytotoxic T Cell Effector Program Including Coinhibitory Receptor Downregulation and Increased Tissue Invasiveness. *Immunity* (2017) doi:10.1016/j.immuni.2017.10.009.
240. Zander, R. *et al.* CD4⁺ T Cell Help Is Required for the Formation of a Cytolytic CD8⁺ T Cell Subset that Protects against Chronic Infection and Cancer. *Immunity* (2019) doi:10.1016/j.immuni.2019.10.009.
241. Dangaj, D. *et al.* Cooperation between Constitutive and Inducible Chemokines Enables T Cell Engraftment and Immune Attack in Solid Tumors. *Cancer Cell* (2019) doi:10.1016/j.ccell.2019.05.004.
242. House, I. G. *et al.* Macrophage-derived CXCL9 and CXCL10 are required for antitumor immune responses following immune checkpoint blockade. *Clin. Cancer Res.* (2020) doi:10.1158/1078-0432.CCR-19-1868.
243. Chow, M. T. *et al.* Intratumoral Activity of the CXCR3 Chemokine System Is Required for the Efficacy of Anti-PD-1 Therapy. *Immunity* (2019) doi:10.1016/j.immuni.2019.04.010.
244. Bourgeois, C., Rocha, B. & Tanchot, C. A role for CD40 expression on CD8⁺ T cells in the generation of CD8⁺ T cell memory. *Science* (80-.). (2002) doi:10.1126/science.1072615.
245. Sommermeyer, D. *et al.* Chimeric antigen receptor-modified T cells derived from defined CD8⁺ and CD4⁺ subsets confer superior antitumor reactivity in vivo. *Leukemia* (2016) doi:10.1038/leu.2015.247.
246. Fan, X. *et al.* Expression of HLA-DR genes in gliomas: Correlation with clinicopathological features and prognosis. *Chinese Neurosurg. J.* (2017) doi:10.1186/s41016-017-0090-7.
247. Friebe, E. *et al.* Single-Cell Mapping of Human Brain Cancer Reveals Tumor-Specific Instruction of Tissue-Invading Leukocytes. *Cell* (2020) doi:10.1016/j.cell.2020.04.055.